DISTRUBUTION AGREEMENT

Distribution Agreement

In presenting this thesis or dissertation as a partial fulfillment of the requirements for an advanced degree from Emory University, I hereby grant to Emory University and its agents the non-exclusive license to archive, make accessible, and display my thesis or dissertation in whole or in part in all forms of media, now or hereafter known, including display on the world wide web. I understand that I may select some access restrictions as part of the online submission of this thesis or dissertation. I retain all ownership rights to the copyright of the thesis or dissertation. I also retain the right to use in future works (such as articles or books) all or part of this thesis or dissertation.

Signature:

_____ _____

Rachel Cliburn Branco Date

APPROVAL SHEET

Vesicular monoamine transporter 2: a modulator of outcomes associated with posttraumatic stress disorder

By

Rachel Cliburn Branco
Neuroscience

_____

Gary Miller, PhD
Advisor

_____

Tanja Jovanovic, PhD
Committee Member

_____

Shannon Gourley, PhD
Committee Member

_____

David Weinshenker, PhD
Committee Member

_____

Ellen Hess, PhD
Committee Member

Accepted:

_____

Lisa A. Tedesco, PhD
Dean of the James T. Laney School of Graduate Studies

_____

Date

Vesicular monoamine transporter 2: a modulator of outcomes associated with posttraumatic stress disorder

By

Rachel Cliburn Branco
B.S., Baylor University 2012
M.S. University of Maastricht, 2013

Advisor: Gary W. Miller, Ph.D.

An abstract of a dissertation
submitted to the Faculty of the
James T. Laney School of Graduate Studies of Emory University
in partial fulfillment of the requirements for the degree of
Doctor of Philosophy

Graduate Division of Biological and Biomedical Sciences
Neuroscience training program
2018

Abstract

Vesicular monoamine transporter 2: a modulator of
outcomes associated with posttraumatic stress disorder
By Rachel Cliburn Branco

Vesicular monoamine transporter 2 (VMAT2, *SLC18A2*) is a transmembrane transporter protein that packages monoamine neurotransmitters into vesicles in preparation for release from the presynaptic neuron. In this way, VMAT2 is a critical modulator of monoaminergic neurotransmission in the central nervous system. Our laboratory has generated a suite of tools to study VMAT2 function. We have generated transgenic strains of mice that express either 5% of wild type (VMAT2-LO mice) or 200% of wild type levels (VMAT2-HI mice) of VMAT2 protein. We developed a novel antibody to the VMAT2 protein and demonstrate that the antibody specifically recognizes VMAT2 and localizes to synaptic vesicles. We show the distribution of VMAT2 in monoaminergic regions of mouse brain, notably the midbrain, striatum, olfactory tubercle, dopaminergic paraventricular nuclei, tuberomammillary nucleus, raphe nucleus, and locus coeruleus. VMAT2 protein is also expressed in areas critical to the expression of fear behavior, the hippocampus and amygdala. Furthermore, immunohistochemical analysis confirmed that variation in VMAT2 gene dose results in variation in VMAT2 protein expression in these areas. We performed radioactive uptake to measure vesicular storage capacity, high performance liquid chromatography to measure monoamine metabolite content, and fast-scan cyclic voltammetry to measure stimulated dopamine release. We found that VMAT2-LO mice have reduced monoaminergic vesicular storage capacity in both the striatum and frontal cortex, show a pattern of reduced monoamine metabolites, and greatly reduced capacity to release dopamine upon stimulation. VMAT2-HI animals showed improved storage capacity, a pattern of increased monoamine metabolites, increased capacity to release dopamine upon stimulation, and altered dopamine release patterns following pharmacological blockade of the dopamine transporter. Since variation in *SLC18A2*, the gene that encodes VMAT2, confers risk for the development of PTSD, we used the VMAT2-transgenic mice to probe whether VMAT2 causally impacts fear behavior. VMAT2-LO mice showed increased cued and contextual fear expression, altered fear extinction, inability to discriminate threat from safety cues, and altered startle response compared to wild-type mice. Alternately, VMAT2-HI did not show changes in respect to wild-type mice in these behavioral assays. To test whether VMAT2 protein amount plays a causal role in deleterious non-fear symptoms associated with PTSD, we tested transgenic mice that represent a continuum of VMAT2 gene dose in a variety of sensory, affective, social, and appetitive assays. We found that VMAT2-LO mice tend to show a high-anxiety phenotype, but no deficits in sensory or social function. By contrast, VMAT2-HI mice are similar to wild-type mice in most assays, with some evidence of a reduced anxiety phenotype. These behavioral characterizations of VMAT2 transgenic mice may help characterize subsets of highly heterogeneous psychiatric disorders in humans. Together, these data corroborate and enrich the human genetic data showing that reduced VMAT2 expression impacts monoamine function and fear behavior. Since presynaptic monoamine function mediates PTSD-like outcomes in our mouse model, targeting this system may be an exciting strategy for future pharmacotherapies for disorders like PTSD.

Vesicular monoamine transporter 2: a modulator of outcomes associated with posttraumatic stress disorder

By

Rachel Cliburn Branco
B.S., Baylor University 2012
M.S. University of Maastricht, 2013

Advisor: Gary W. Miller, Ph.D.

A dissertation submitted to the Faculty of the
James T. Laney School of Graduate Studies of Emory University
in partial fulfillment of the requirements for the degree of
Doctor of Philosophy

Graduate Division of Biological and Biomedical Sciences
Neuroscience training program
2018

Acknowledgements

I would like to thank my advisor, Dr. Gary Miller, for his excellent mentorship during my time in his laboratory. He has been a continual source of optimism and enthusiasm regarding my research, and has continually challenged me to work diligently and think creatively. In my first meeting with Gary, he tasked me with finding a way to test whether mice are happy—a formidable task even for an experienced behaviorist. This original project was the seed for the results described in this dissertation. I have appreciated how Dr. Miller has encouraged independence while guiding growth. It is also nice that he let me go to Paris for science expeditions on three separate occasions.

I would also like to thank Dr. W. Michael Caudle, Dr. Malu Tansey, Dr. Nael McCarty, Dr. Jason Schroeder and my committee members: Drs. Ellen Hess, Tanja Jovanovic, Shannon Gourley, and David Weinshenker. I appreciate their thoughtful feedback on my research, technical support, and encouragement for me to grow as a critical thinker. I also thank Gary Longstreet and Adrienne Schwartz for their valuable administrative support – it makes learning to be a scientist that much more enjoyable.

Thank you also to my labmates, who made daily life in lab a true pleasure: Kelly, Thommy, Kristen, Shawn, Carlie, Min, Josh, Aimée, Merry, Vrinda, Rohan, Emily, and William. I truly looked forward to spending time with each of you. We work hard in the laboratory, but it was the friendships, support, and laughter that made time pass quickly during long experiments. I will be an early investor into the creation of a sitcom about what happens in a basic science laboratory, based on our time together.

Finally, I must thank my supportive friends and family. Thank you to my Mom and Dad, who have always been so encouraging and enthusiastic of my academic pursuits.

Thank you for giving me the intellectual curiosity to pursue this endeavor. Thank you Dad, in particular, for reading every single thing I've ever written. To my Atlanta-area friends: because of you, Atlanta has become such a welcoming and joyful home. Thank you to Fred, my beloved cat who cheered me up almost every day of graduate school. Justin—you have enthusiastically celebrated my successes, empathetically listened to my frustrations, and kept me company weekends and nights in lab more than any significant other rightly should. Thank you for being my biggest cheerleader.

Table of Contents

List of Figures

I. Chapter 1. Introduction: Posttraumatic stress disorder, vesicular function, and the evidence for VMAT2 as a potential mediator of fear behavior

BACKGROUND

Section I: Posttraumatic stress disorder – a debilitating disease in human populations

Posttraumatic stress disorder (PTSD) occurs in a subset of people that experience a traumatic event, such as tragedy in a combat zone, interpersonal or sexual violence, a natural disaster, or a disastrous accident. The lifetime prevalence of PTSD is about 7%, depending on the number of soldiers sent to combat zones and other world events (Kessler *et al*, 2005).

PTSD has gone by a variety of names throughout the centuries. In *The Iliad,* Homer describes soldiers that 'go berserk' at short notice and that feel 'already dead', symptoms that we now, with less poetic license, call hyper-arousal and numbness (Shay, 1991). In the United States, military personnel have used a variety of colloquial terms to describe soldiers with symptoms of PTSD: it was "soldier's heart" for jitteriness in the Civil War, "shell shock" for those in the first World War, and "combat fatigue" in the second (Andreasen, 2010). The American medical field started to develop parallel terms starting in the beginning of the 20th century: combat personnel with poor psychiatric outcomes were first thought to have developed a "psycho-neuroses" surrounding their trauma, later termed a "stress response syndrome" in the first iteration of the Diagnostic and Statistics Manual (DSM) in the 1950's (American Psychiatric Association, 1952). Our modern term for the disorder was enshrined in the third iteration of the DSM. DSM-III operationalized the features of the disorder: exposure to a uniquely distressing event that results in a persistent cluster of symptoms including re-experiencing, avoidance, and hyper-arousal. This newly-

official diagnosis was met with resistance: the Department of Veterans Affairs argued that wars did not contribute to the psychological troubles of veterans, stating "It has never been demonstrated that the diagnosis PTSD is relevant to the mission of the Veterans Administration" (van der Kolk and Najavits, 2013). Though PTSD is a particular burden to individuals re-entering civilian life following combat experience (Hoge *et al*, 2004), it is by no means limited to service members that experience combat. Within the last three decades of clinical practice and research, the popular understanding of PTSD as a soldier's condition has been widened to include those who experience non-combat trauma, such as sexual violence, intrapersonal violence, natural disasters, or traumatic accidents.

DSM criteria. The most recognized symptoms of this psychiatric disorder, such as re-experiencing the trauma and increased arousal, are associated with dysregulated fear responses. While PTSD is primarily characterized by these aberrant fear responses, other co-occurring symptoms include depression, social anxiety, social withdrawal, and cognitive changes (Kessler *et al*, 1995; Pietrzak *et al*, 2011; Spinhoven *et al*, 2014). These changes to cognition and mood symptoms can profoundly impact the daily function and quality of life of people who suffer from PTSD. According to the DSM-5, people with PTSD meet the following symptom criteria, which persist for more than a month and cause significant distress and problems functioning in other areas of life (American Psychiatric Association, 2013):

1.) Intrusive thoughts, including flashbacks, memories of the trauma, distressing dreams, or feelings of 're-living' the traumatic experience.

2.) Avoidance, including avoiding the people, places, activities, or situations that are associated with the distressing memory. Other avoidance symptoms include resistance to talking or thinking about traumatic events or the personal feelings surrounding the trauma.
3.) Negative thoughts and feelings, including a persistent feeling of fear, horror, guilt, shame, anger, lack of enjoyment in other activities, and social detachment.
4.) Hyperarousal, including sudden outbursts, irritability, recklessness, being easily startled, inability to sleep or concentrate.

PTSD heterogeneity. Like many mental disorders, PTSD is not a uniform disorder – indeed, clinicians have observed multiple subtypes of PTSD (American Psychiatric Association, 2013). The timing, severity, and subset of PTSD symptoms can vary according to a variety of factors, including gender, type of trauma, or timing of trauma (Andrews *et al*, 2007; Choi *et al*, 2017; Garza and Jovanovic, 2017; Guina *et al*, 2018). For example, trauma arising from combat experience is associated with the psychological and physical symptoms of hyperarousal, while sexual trauma experience is more closely associated with avoidance symptoms and negative affect (Guina *et al*, 2018). Furthermore, the conditional probability of developing PTSD if exposed to a trauma depends on a number of factors. Women are more vulnerable to the development of PTSD if they are exposed to a trauma, likely due to the interaction of hormone systems and the biological response to stressful events (Briscione *et al*, 2017; Glover *et al*, 2013). This heterogeneity in the etiology and predominant symptoms of PTSD suggests that there are diverse genetic or biological underpinnings of PTSD risk, and these risk factors interact with life

experience to give rise to the diagnosis and symptoms of PTSD in a unique way for subsets of patients.

PTSD and other psychiatric disorders. People who have PTSD are more likely to have other psychiatric disorders such as depression, bipolar disorder, insomnia, and addiction, and are twice as likely to die by suicide (Araújo *et al*, 2014; Bajor *et al*, 2013; Bernal *et al*, 2007; El-Solh *et al*, 2018; Kessler *et al*, 1995; Post *et al*, 2016; Sareen *et al*, 2007). In 50% of cases, a patient with PTSD also is diagnosed with another psychiatric disorder (Pietrzak *et al*, 2011). Interestingly, with the exception of anxiety disorders, these comorbid psychiatric conditions are usually not present before the development of PTSD, but develop concurrently with PTSD symptoms following a trauma (Kessler *et al*, 2017).

Historically, it was thought that people with PTSD are more likely to abuse psychoactive drugs as a means to cope with the anxiety and anhedonia common to the disorder. This "self-medication hypothesis" is supported by evidence that individuals with PTSD but without substance use disorder (SUD) display heightened startle responses, while those with SUD alone or comorbid PTSD/SUD did not have heightened fear-potentiated startle responses (Davis *et al*, 2013). While this may be partly true, recent evidence has suggested that there is a common risk factor for the development of *both* disorders. The veteran population of the U.S. is at particular risk for comorbid PTSD and substance use disorders. In a study of hospitalized veterans with PTSD, 70% had a concurrent substance-use disorder, with alcohol being the most commonly abused substance (Kulka *et al*, 1988). This relationship between PTSD and alcohol use disorders (AUD) is well supported in epidemiologic studies (Blanco *et al*, 2013; Debell *et al*, 2014;

Jacobsen *et al*, 2001; Kessler *et al*, 1995; Shorter *et al*, 2015; Wilk *et al*, 2010). In fact, a PTSD diagnosis confers a three-fold increased risk of developing an AUD (Kessler *et al*, 1997), likely because self-medication can reduce the intrusive hypervigilance associated with PTSD (Davis *et al*, 2013). Not only is comorbid PTSD/AUD very common, but the comorbid condition changes prognosis and treatment options. The symptoms of PTSD and AUD are more severe in individuals with a dual diagnosis, including increased suicidal ideation and suicide attempts (Rojas *et al*, 2014), earlier onset of AUD symptoms (Driessen *et al*, 2008), prolonged course of the illness (Bremner *et al*, 1996), and poorer recovery outcomes (Ipser *et al*, 2015; Schäfer and Najavits, 2007; Shorter *et al*, 2015).

Section II. Biological correlates of PTSD

Because PTSD is a psychiatric disorder with variable clinical presentations, biological correlates that can predict PTSD risk or expression have been important to the study of the disease. These biological correlates include preexisting factors that correspond to increased vulnerability, like genes and endocrine factors.

Genetic risk factors for PTSD. Transgenerational and twins studies indicate that genetics play a role in the etiology of PTSD (Koenen *et al*, 2003; Xian *et al*, 2000; Yehuda *et al*, 1998). As is common in complex behavioral disorders, there is no single gene directly responsible for all PTSD diagnoses. There are a host of genetic risk factors that play a role in mediating the risk for the development of PTSD if exposed to a trauma. These genetic risk factors are largely either related to the hypothalamic-pituitary-adrenal (HPA) axis or

to monoamine metabolism. The most prominent and well-verified gene connecting HPA axis function to PTSD diagnosis is the *FKBP5* gene, which regulates glucocorticoid receptor sensitivity (Binder, 2009; Carvalho *et al*, 2017). There are also a variety of genetic risk factors that fall under the umbrella of monoamine metabolism. A single nucleotide polymorphism in the *COMT* gene that replaces valine (Val) by methionine (Met) increases risk of psychiatric disorders, including PTSD (Boscarino *et al*, 2011; Kolassa *et al*, 2010; Lachman *et al*, 1996). The *COMT* gene encodes the protein catechol-o-methyl transferase, an enzyme that degrades monoamines in the extracellular space following release from the presynaptic terminal. Importantly, the gene that encodes the vesicular monoamine transporter 2 is also implicated in PTSD risk. In a recent candidate gene study of two large independent samples, the gene *SLC18A2* was identified as a risk haplotype for the development of PTSD (Solovieff *et al*, 2014). *SLC18A2* encodes the vesicular monoamine transporter 2 (VMAT2), a protein responsible for packaging monoamines neurotransmitter molecules into neuronal vesicles.

Hypothalamic-pituitary-adrenal axis activity. Typically, the hypothalamus, a small brain region just ventral of the thalamus, responds to a stress event by releasing corticotropin-releasing hormone (CRH), which acts on the pituitary, a neuroendocrine gland. The pituitary, in turn, releases adrenocorticotropic hormone (ACTH), which acts on receptors in the adrenal cortex, an endocrine gland that sits just above the kidneys in humans. In response to an increase in ACTH, the adrenal cortex releases cortisol into the bloodstream. Cortisol acts throughout the body to respond to stress: it increases readily-usable energy by increasing blood-glucose concentration, suppresses the immune system,

acts as a diuretic. Cortisol also inhibits production of CRH and ACTH, creating a negative feedback loop. Though cortisol follows diurnal patterns of release, it falls within a predictable range in most people. Patients with PTSD exhibit enhanced negative feedback, lower cortisol levels overall, and flattened diurnal cycling of cortisol (Wingenfeld *et al*, 2015; Yehuda *et al*, 2006, 2007; Zaba *et al*, 2015).

Section III. Current PTSD treatments

Psychotherapeutic approaches for the treatment of PTSD. There are multiple existing psychotherapeutic treatments for the symptoms of PTSD, which can be broadly divided into exposure and non-exposure therapies. Of the non-exposure therapies, cognitive behavioral therapy is among the most effective (Steenkamp *et al*, 2017; Yang *et al*, 2018). Cognitive behavioral therapy is a strategy wherein a trained therapist works with a patient to revisit the avoidance and cognitive distortion symptoms associated with the trauma, and can include aspects of exposure to events surrounding the trauma. Stress inoculation therapy teaches people with PTSD strategies of coping with the anxiety associated with the disorder. This strategy includes muscle relaxation training, use of biofeedback, and training in positive self-talk. Other non-exposure strategies for the treatment of PTSD include group therapy, therapy for issues peripheral to the trauma itself (such as interpersonal or emotional therapies), or use of an emotional support animal (Jovanovic *et al*, 2017). Alternately, exposure therapies such as prolonged exposure (PE) are based on the idea of extinction learning (Foa *et al*, 2005). Often, cues related to the original trauma will cause symptoms of stress and hyperarousal in people suffering from

PTSD. PE exposes people with PTSD to cues related to their original trauma in a gradual, therapeutic way (Cooper *et al*, 2017). Virtual reality has been an exciting recent advancement in exposure therapy that allows a controlled increase in exposure to trauma-related cues (Peskin *et al*, 2018).

Pharmacologic approaches for the treatment of PTSD. Though psychotherapies have been shown to be more effective in the long term reduction of PTSD symptoms (Lee *et al*, 2016), pharmacological treatments of PTSD are more widely available and more widely used compared to psychotherapies, especially among veterans (Bernardy *et al*, 2012). In a study of Veterans Affairs treatment of PTSD, only 3-6% of qualifying patients received evidence-based psychotherapies (Watts *et al*, 2014). It's unclear if this dearth of effective treatment is due to longstanding institutional culture, the relative ease with which a clinician can write a prescription compared to the time commitment of therapy, or the cost to the patient. In any case, effective pharmacological tools are important to the widespread treatment of PTSD.

Several drugs have been shown to be effective in treating symptoms of PTSD either as a monotherapy or in conjunction with psychotherapy (American Psychiatric Association, 2013). Selective serotonin reuptake inhibitors (SSRIs) are a class of compounds that block the plasmalemmenal serotonin transporter, increasing the amount of time serotonin spends in the synaptic space and allowing for increased activation of serotonergic receptors. Currently, sertraline and paroxetine—both SSRIs—are the only FDA-approved pharmacological treatments for PTSD. There has been some interest in the use of selective norepinephrine uptake inhibitors either alone or in conjunction with SSRIs

to treat PTSD (Hoskins *et al*, 2015). Though SSRI treatment of PTSD does show a consistent improvement over placebo, overall effect sizes are small and this class of drugs is less effective in the treatment of dissociative symptoms (Cipriani *et al*, 2017; Martenyi *et al*, 2002). A class of drugs that is similar to SSRI's have also been tested for efficacy in the treatment of PTSD. These are the 'serotonin/norepinephrine reuptake inhibitors (SNRIs), which, as the name suggests, blocks the clearance of both serotonin and norepinephrine from the extracellular space, allowing these two monoaminergic neurotransmitters to act on receptors for a prolonged time. Currently, venlafaxine (trade name Effexor XR) is an SNRI that is approved to treat anxiety and panic disorder, common conditions in individuals with PTSD. SNRIs have been found to be equivalently effective as SSRI monotherapy in reducing PTSD symptoms—that is to say, not as effective as talk based therapies (Lee *et al*, 2016; Susskind *et al*, 2012). Furthermore, compounds that act on noradrenergic receptors have been tested to treat symptoms of PTSD. In a recent study of the efficacy of the α_1-adrenoreceptor antagonist prazosin, treatment did not alleviate the anxiety or nightmares in an adult veteran population with PTSD (Raskind *et al*, 2018), but has been effective in reducing nightmares in children with PTSD symptoms (Keeshin *et al*, 2017). Methylenedioxymethamphetamine (MDMA) is gaining traction as a potential pharmacotherapeutic tool for the treatment of PTSD, and is in phase two of clinical trials (Mithoefer *et al*, 2011; Thal and Lommen, 2018). MDMA is an amphetamine derivative that exerts its prosocial effects by acting on serotonin 2_A receptors (Pitts *et al*, 2017). Interestingly, the R(-) enantiomer of MDMA shows the therapeutic pro-social effects of the drug without the neurotoxic side effects observed in the racemic mixture (Curry *et al*,

2018). MDMA is not considered a candidate for monotherapy but as an adjunctive therapy that can enhance learning during psychotherapy sessions (Young *et al*, 2015).

Section IV. How to study PTSD? Tools and models

Behavioral models in humans with PTSD. Like most psychiatric disorders, PTSD cannot be diagnosed with a biopsy or a blood test. In the absence of a 'definitive' assay for PTSD, diagnosis depends on the expertise of a trained clinician. Even with clinical expertise, however, psychiatric diagnosis depends on patient self-report or, in some cases, the reports of friends and family members of the affected individual. In an experimental setting, there are a variety of tools available to study the presence and/or severity of PTSD symptomology in humans. Research of PTSD in humans relies on easily measurable, noninvasive behavioral phenotypes (Jovanovic *et al*, 2017).

These behavioral phenotypes are often related to the physiological hyper-arousal symptoms of PTSD. In an early method for screening for PTSD, a person would verbally describe a traumatic event. Researchers would play back a recording of the description of the trauma while measuring heart rate and skin conductance. People with PTSD tend to have a higher heart rate and skin conductance during the trauma replay compared to people without PTSD (Pitman *et al*, 1987). Though this technique has poor selectivity and specificity, it is still a relatively reliable way of assessing the presence of the disorder (Bauer *et al*, 2013; Keane *et al*, 1998). Another avenue of behavioral testing also takes advantage of the hyper-arousal symptoms of PTSD by measuring the fear-potentiated startle response to an unpleasant stimulus, like a loud noise or a puff of air to the neck

(Grillon *et al*, 1996). The degree of startle is measured via electromyography that measures the magnitude of eyeblink muscle contraction. Lastly, Pavlovian conditioning provides a way to measure response to learned fear (Pittig *et al*, 2018; Wolpe and Plaud, 1997). In a Pavlovian fear conditioning paradigm, an aversive stimulus such as a loud noise (the unconditioned stimulus, or "US") produces an unconditioned response ("UR"), such as a fearful reaction. The aversive stimulus is paired with a neutral stimulus (conditioned stimulus, "CS"), such as an image of a shape, for multiple presentations. In this way, the neutral stimulus becomes associated with the unconditioned response (now called the conditioned response, "CR"). Typically, a separate neutral cue, or a non-reinforced conditioned stimulus (CS-), is used to indicate that no unpleasant stimulus is going to happen, and this neutral cue is termed a 'safety signal'. People with PTSD tend to show elevated heart rate, skin conductance, and startle responses to both a danger cue (CS+) and a safety signal (CS-) (Jovanovic and Norrholm, 2011; Orr *et al*, 2000; Peri *et al*, 2000).

Endophenotypes of PTSD in humans. Endophenotypes are any quantitative, biological trait that reflects the function of biological system (Lee Gregory *et al*, 2015). Endophenotypes are intermediaries between innate biological risk and clinical presentation and can provide more information about the etiology or potential treatment of PTSD. In many cases, polymorphisms of a gene of interest will affect the structure or function of a biological process, which will in turn affect clinical outcome. In this way, endophenotypes are not as 'small scale' as changes in a gene or a protein, but not as heterogenous as a DSM-defined psychiatric disorder. In the study of PTSD, endophenotypes have fallen into two categories: brain network activity and HPA-axis reactivity. Brian network activity

measures the blood oxygen-level dependent signal of interconnected brain regions involved in the observed dysfunction of PTSD, including executive function, threat detection, emotional regulation, and contextual processing. A series of recent papers have implicated fMRI activity in the ventral medial prefrontal cortex during a response inhibition task as an endophenotype for PTSD (Jovanovic *et al*, 2013; Milad *et al*, 2009; van Rooij *et al*, 2016).

Another method of assessing PTSD in humans is to measure the function of the hypothalamic-pituitary-adrenal (HPA). Dexamethasone suppression tests (DST) are a way to assay HPA function by measuring the extent that the HPA axis inhibits cortisol production in response to administration of an exogenous synthetic cortisol. Individuals recently exposed to trauma, with and without PTSD, show an enhanced suppression of cortisol in this DST test (Yehuda *et al*, 1995). There are other methods of using peripheral collection of cortisol to assay HPA axis activity, such as 24-hour urine collection or saliva samples soon after waking up. However, these tests have not yet demonstrated selectivity or specificity for PTSD over trauma-exposed individuals or individuals with other psychiatric disorders.

Trauma questionnaires. A number of questionnaire tools have been useful in assessing an individual's experience with trauma. These include questionnaires tailored to ask about experiences in childhood (Childhood Trauma Questionnaire, "CTQ") and adulthood (Traumatic Events Inventory, "TEI") (Bernstein *et al*, 1994; Gillespie *et al*, 2009; Scher *et al*, 2001). Though these questionnaires inherently rely on a self-reported experience, they have been helpful in determining extent and type of trauma that can be

used as a continuous variable in research about specific PTSD symptomology (van Rooij *et al*, 2016). The current 'gold standard' for PTSD is the Clinican Administered PTSD Scale (CAPS) which asses both symptom severity and presence of the disorder (Blake *et al*, 1995).

Behavioral tests in rodent models of PTSD. The architecture of fear biology is highly conserved in mammals, so animal models serve as a useful tool for studying fear behavior in humans (Flandreau and Toth, 2017). Fear conditioning paradigms capitalize on this shared circuitry and can be used in rodents and humans to model fear-related symptoms of PTSD (Jovanovic *et al*, 2005; Jovanovic and Ressler, 2010). Fear conditioning provides an experimental paradigm to model formation of fear memories during a traumatic event. Indeed, rodent shock paradigms have given rise to most of our modern understanding of fear circuitry and regulation (Davis, 1992). This paradigm is commonly used in mice to test the contribution of a gene, drug, or other manipulation to PTSD-like behaviors (Flandreau and Toth, 2017).

This relatively simple and reproducible paradigm allows for examination of constructs associated with PTSD, including deficient extinction, fear generalization, and exaggerated threat/salience detection (Morey *et al*, 2015a; Norrholm *et al*, 2011, 2015a). In rodent models, there are four common concepts that are probed via foot shock freezing models: fear conditioning, fear inhibition, fear generalization, and fear extinction (Briscione *et al*, 2014). Pavlovian fear conditioning in rodents mirrors the protocol in humans, with adaptations to suit the change in species. In this paradigm, an aversive stimulus (often a mild, unescapable electric shock) is paired with a neutral stimulus (often

an auditory tone), such that the rodent exhibits fearful behavior in response to the neutral stimulus alone. In mice, the behavioral response to fear is freezing. So, one can objectively measure the fear response by measuring amount of time spent freezing. In a fear inhibition paradigm, freezing is measured in response to a 'safety signal,' a neutral cue that indicates that no aversive stimulus is forthcoming. Fear generalization paradigms test behavioral responses to cues that are similar but not identical to the original fear-paired cue. For example, a mouse may be trained to associate a 8 kHz tone to a foot shock, and then are tested for freezing responses to 6, 7, 9, and 10 kHz tones. The resultant data shows the threshold for how different a cue can be from the original fear memory and still elicit behavioral fear responses. Fear extinction is a measure of new learning: the cue that previously was paired with an aversive stimuli is now presented multiple times without the US. Over time, the rodent learns that the cue no longer predicts an aversive stimulus, and exhibits progressively less fear behavior in response to the cue. This is laboratory analog to exposure therapy for PTSD in humans.

Section V. The monoamine systems

Monoamines as neuromodulators. The brain monoamine system contains three major neurotransmitter systems, each with their own unique profile. Dopamine is primarily produced in neurons in the midbrain, which contains the substantia nigra and the ventral tegmental area (Ciliax *et al*, 1995). The dopamine pathway projecting from the substantia nigra to the dorsal striatum is critical to movement, and it is this nigrostriatal pathway that degenerates in Parkinson's disease (Hornykiewicz, 1970, 1998). The dopamine neurons

from the ventral tegmental area project to the nucleus accumbens, as well as diffusely throughout the frontal cortex. This mesocorticolimbic pathway drives appetitive responses. Increased signaling in this pathway is the final common denominator for drugs of abuse, and becomes pathological in addiction, including addiction to alcohol (Di Chiara and Imperato, 1988; Diana, 2011; Wise, 1980, 1987). Most of the norepinephrine found in the brain is produced in the locus coeruleus. Norepinephrine is distributed broadly throughout cerebral cortex, hippocampus, thalamus, basal nucleus of the stria terminalis, and amygdala (Ordway *et al*, 2007). Norepinephrine modulates arousal, including alertness, attention, and physiological responses to stress (Mitchell and Weinshenker, 2010). Serotonergic neurons project from the raphe nucleus diffusely to hippocampus, amygdala, thalamus, and cerebral cortex. Serotonin's complex receptor pharmacology underscores its varied role in appetitive responses and affective behavior (Berger *et al*, 2009; Mohammad-Zadeh *et al*, 2008; Sirek and Sirek, 1970).

Monoamines and PTSD symptomology. Genetic variation in multiple monoaminergic systems has been implicated in risk for PTSD (Naß and Efferth, 2017). All three major central monoamine systems—dopamine, norepinephrine, and serotonin—interact with each other, and individually to contribute to PTSD outcomes. The relationship between these neurotransmitters and the expression and maintenance of fear symptomology is complex. Patients with PTSD have altered basal levels of catecholamines, and exhibit altered peripheral noradrenergic responses to stressful stimuli (Highland *et al*, 2015; Wingenfeld *et al*, 2015). In general, norepinephrine is a neuromodulator which increase alertness and attention, directing physiological resources

to the most salient stimuli in the environment. In this sense, an overabundance of norepinephrine is associated with hypervigilance and sleep disturbances. Indeed, norepinephrine is crucial to the expression of startle and other panic-related behaviors (Kao *et al*, 2015; O'Donnell *et al*, 2004). Like dopamine, norepinephrine plays a role in the synaptic plasticity necessary for memory reconsolidation following a stressful or traumatic event (Fitzgerald *et al*, 2015; Giustino and Maren, 2018; Lee *et al*, 2017; Lee and Kim, 2016; Otis *et al*, 2015). However, also like dopamine, the timing, location, and frequency of norepinephrine efflux seems to be critical for the behavioral outcome, as in some cases extracellular norepinephrine concentration actually has an anxiolytic effect (Estrada *et al*, 2016; Montoya *et al*, 2016). Serotoninergic transmission in the amygdala facilitates expression of fear (Johnson *et al*, 2015), yet inhibiting the reuptake of serotonin is a mainstay of pharmacological treatment for PTSD (Kelmendi *et al*, 2016) and this synaptic serotonin is necessary for pharmacologically-mediated acceleration of fear extinction learning (Young *et al*, 2017). VMAT2 itself, which packages dopamine, norepinephrine, and serotonin, can be responsive to stimuli, as a single prolonged stress in a rodent model can reduce VMAT2 protein level in amygdala and hippocampus (Lin *et al*, 2016).

Amygdala and hippocampus. The amygdala and hippocampus are two structures within the limbic system that are critical to the expression and maintenance of fear behavior. Evolutionarily, fear responses are extremely advantageous: the ability to respond appropriately to a dangerous situation promotes survival. Because of this, fear responses are robust and highly conserved (Flandreau and Toth, 2017). The amygdala is a highly connected region of the ventral striatum that underlies multiple functions (Janak and Tye,

2015). Decades of research point in particular to the heterogeneous basolateral nucleus of the amygdala as a critical contributor to the formation and retrieval of fear-associated memories (Fox and Shackman, 2017; Krabbe *et al*, 2018; Orsini and Maren, 2012; Fanselow and LeDoux, 1999). There is a particularly fascinating example of an amygdala pathology that results in unusual fear-related behavioral deficits: Urbach-Wiethe disease is an extremely rare genetic condition that can result in bilateral calcification of the blood vessels in the amygdala, eventually leading to tissue death. In some cases, people with this condition show personal lack of fear and selective impairment in the recognition of fear in others (Koen *et al*, 2016; Meletti *et al*, 2014) Similarly, the hippocampus is important to fear memories. In particular, the hippocampus contributes to the association of an emotional response (i.e. fear) to contextual cues (Moita *et al*, 2003; Xiao *et al*, 2018). Dopamine, serotonin, and norepinephrine are all released in a diffuse manner in both rodent and human amygdala (Smith and Porrino, 2008) and hippocampus (Dale *et al*, 2016; Rosen *et al*, 2015; Weitemier and McHugh, 2017).

Section VI. VMAT2 – Master of monoamine packaging

What it does. Synaptic vesicles mediate the release of neurotransmitters at synaptic terminals throughout the brain. Vesicular monoamine transporter 2 (VMAT2; *SLC18A2*) is a synaptic vesicle transport protein found primarily in the central nervous system with two primary purposes related to neurotransmission and neuronal cell health (Caudle *et al*, 2008; Erickson *et al*, 1992; Guillot and Miller, 2009; Peter *et al*, 1995a; Takahashi *et al*, 1997). First, VMAT2 packages monoamines (dopamine, serotonin, norepinephrine,

epinephrine, and histamine) into vesicles for the release from synaptic terminals. VMAT2 transports these neurotransmitter molecules by coupling with an H^+-ATPase antiporter to maintain an electrochemical gradient and exchanging two protons for one monoamine molecule (Eiden *et al*, 2004). VMAT2 also sequesters dopamine into synaptic vesicles, thereby reducing cytosolic dopamine concentrations, oxidative stress, and the subsequent destruction of dopamine neurons (Alter *et al*, 2013; Goldstein *et al*, 2013; Liu *et al*, 1992; Lohr *et al*, 2014). In the brain, VMAT2 is present in both small vesicles and dense core vesicles in neural regions with high monoaminergic activity (Caudle *et al*, 2008; Nirenberg *et al*, 1995). In order to look at the effects of presynaptic monoamine function as a whole, we use genetically altered mice that have varying levels of VMAT2. Since VMAT2 packages each of these neurotransmitters in preparation for release (Alter *et al*, 2016; Cliburn *et al*, 2016; Lohr *et al*, 2014), modulating VMAT2 is a way to adjust the 'gain' of these systems.

Human link to PTSD outcomes. Even though exposure to severe trauma is relatively common, only a small proportion of those exposed to trauma will go on to develop PTSD (Breslau *et al*, 1999; Keane *et al*, 2009; Kessler *et al*, 1995; Shiromani *et al*, 2009). Though it is known that both genetic and social factors mediate risk for PTSD (Binder *et al*, 2008; Charney, 2004; Li *et al*, 2016; Ozer *et al*, 2003), it is still not fully understood why only a certain number of people who experience a traumatic event will develop PTSD. In a recent candidate gene analysis of more than 3,000 single nucleotide polymorphisms across more than 300 genes, the gene *SLC18A2* was identified as a risk haplotype for PTSD diagnosis in a cohort of 2,538 European women and replicated in an independent cohort of 748 male

and female African Americans (Solovieff *et al*, 2014). In a post-mortem analysis of brains collected from people with and without PTSD, expression of the protein VMAT2 was reduced in the brains of PTSD patients (Bharadwaj *et al*, 2016). Furthermore, the psychiatric disorders that often present concurrently with PTSD have been independently associated with VMAT2 dysfunction (Eiden and Weihe, 2011; Schwartz *et al*, 2003; Zubieta *et al*, 2001; Zucker *et al*, 2002). Taken together, these findings indicate that VMAT2 dysfunction may be an underlying cause for a variety of associated psychiatric disorders, including PTSD. For these reasons, the function of VMAT2 merits further analysis as it relates to PTSD and psychiatric risk.

Section VI. Our model: VMAT2 transgenic mice

A continuum of VMAT2 function. To answer questions regarding the causal relationship of VMAT2 protein amount a variety of biochemical and behavioral outcomes, our laboratory has developed and characterized strains of transgenic mice that provide a continuum of presynaptic monoaminergic tone within the central nervous system. Specifically, these mice express differing amounts of VMAT2: 95% reduced (VMAT2-LO) (Caudle *et al*, 2007; Taylor *et al*, 2009), normal (VMAT2-WT), or 200% elevated levels (VMAT2-HI) (Lohr *et al*, 2014, 2016).

Generation of the VMAT2-transgenic mice. VMAT2-LO mice were generated by backcrossing the original mixed-background VMAT2-deficient strain (Caudle *et al*, 2008; Taylor *et al*, 2014) to Charles River C57BL/6 mice for four generations using a marker-

assisted selection (i.e. “speed congenic”) approach (Lohr *et al*, 2016). VMAT2-HI mice were generated using a bacterial artificial chromosome-mediated transgene to insert three additional copies of the murine *Slc18a2* (VMAT2) gene, including its endogenous promotor and regulatory elements (Lohr *et al*, 2014). These founders were then backcrossed to the same generation of a Charles River C57BL/6 mice.

Identical genetic background enables behavioral comparisons. We have bred VMAT2-HI and -LO lines to be on identical genetic backgrounds (C57BL/6J). In our studies of these mice, the wild-type littermates of VMAT2-LO mice and the wild-type littermates of VMAT2-HI mice show no difference in neurochemical or behavioral outcomes. This indicates that VMAT2 gene dose is driving the observed differences in neurochemistry and behavior among VMAT2-LO, -WT, and -HI mice. This continuum of VMAT2 expression is an ideal tool for testing whether the functional reduction of VMAT2 is a causal factor in producing an aberrant fear phenotype.

Characterization of VMAT2-transgenic mice – What do we already know? Transgenic mice under- or over-expressing VMAT2 provide a unique tool to study the effect of VMAT2 on mouse behavior and neurological functioning. Past studies of VMAT2-transgenic animals have focused on the dopamine system. A complete knockout of VMAT2 results in pups dying within a few days of birth (Wang *et al*, 1997). However, mice expressing 5% of the normal levels of VMAT2 survive into adulthood. These VMAT2-deficient mice (VMAT2-LO) have reduced vesicular uptake of dopamine, an age-dependent reduction in striatal dopamine, increased dopamine-related oxidative toxicity as

indicated by an increased DOPAC/DA ratio, increased tyrosine hydroxylase activity, progressive decline in dopamine transporter immunoreactivity, and a progressive loss of dopamine terminals and cell bodies in the substantia nigra pars compacta (Caudle *et al*, 2007). In this way, aged VMAT2-LO mice serve as a mouse model of Parkinson's Disease (PD) and recapitulate both motor and non-motor symptoms of PD including decreased locomotor activity, age-dependent deficits in social and non-social olfactory acuity, sleep disturbances. and gastrointestinal dysfunction (Caudle *et al*, 2007; Taylor *et al*, 2009). In contrast, VMAT2-overexpressing mice, known as VMAT2-HI mice, have approximately a three-fold increase in VMAT2 mRNA, a three-fold increase in VMAT2 in striatal homogenate, a three-fold increase in VMAT2 in vesicle fractions, increased vesicular volume, increased dopamine uptake, increased extracellular dopamine, and an increased protection against the detrimental of effects dopaminergic neurotoxins on dopamine neurons compared to their wild-type (VMAT2-WT) littermates (Lohr et al., 2014).

RATIONALE & HYPOTHESIS

Rationale. Our continuum of VMAT2-transgenic mice is an exciting and promising novel model for the study of PTSD for a number of reasons:

1.) *Genetic susceptibility reflected from human data.* Our lab uses mice that display either increased (VMAT2-HI) or greatly reduced (VMAT2-LO) VMAT2 protein expression. Furthermore, we have carefully bred both VMAT2-LO and -HI mouse lines to be on identical genetic backgrounds, such that the only

genetic difference between mouse lines is the gene-dose of VMAT2. This continuum creates a powerful tool to investigate the role of genetic variation of VMAT2 on complex behavior. The continuum will also allow us to probe the susceptibilities suggested from human genetic studies using a mouse model. Thus, this model has construct validity, since it reflects the genetic risk factors of humans.

2.) *Sensitivity to both resilience and susceptibility*. In current PTSD research, assays are most often sensitive only to deleterious perturbations, rather than gain in function. In this way, we have created a model that captures both the *susceptibility* suggested from human data of reduced VMAT2 content, and also suggests a novel mechanism of *resiliency* via increased VMAT2 amount in the VMAT2-HI mice. We find this to be a very exciting aspect of our model, as it allows us to probe the mechanism and potential therapeutics that contribute to resilient phenotypes.

3.) *Capture of the non-fear symptomology of PTSD.* PTSD is a heterogeneous disorder which includes altered fear processing. Some of the most disabling aspects of the disorder are its effects on social, affective, and appetitive responses.

4.) *Usefulness for understanding underlying neurological circuits of PTSD.* Another advantage of this model is that it allows us to probe the mechanism of

behaviors associated with PTSD in these mice. VMAT2 has a well-characterized expression pattern in the brain and well-defined roles within the monoaminergic circuits of the brain. In this way, these results allow for future parsing of brain regions and neurotransmitter systems that are critical for the expression of susceptible or resilient fear phenotypes.

5.) *Immediate translational relevance.* Our continuum of VMAT2 transgenic mice provides a template on which we can test therapies to promote resilience to developing PTSD. These findings highlight the future potential for gene therapy in humans that could target VMAT2 to address fear- and affect- related pathology.

Hypothesis. **VMAT2 protein expression in the brain is inversely correlated to PTSD-associated outcomes** such that animals with reduced VMAT2 will show reduced monoaminergic function and a PTSD-like behavioral phenotype whereas animals with increased VMAT2 expression will show enhanced monoaminergic function and improved outcomes on tests of PTSD-like behavior**.** I will explore this hypothesis in the following four chapters. Each chapter will address progressive questions relating to VMAT2 and PTSD-associated outcomes:

Chapter 2: VMAT2 localization. In this chapter, I will use a newly developed immunochemical tool to determine whether VMAT2 protein is expressed in areas pertinent to fear or non-fear symptomology of PTSD, and whether the VMAT2 protein amount varies by VMAT2 genotype.

Chapter 3: Functional consequences of altered VMAT2 protein amount. In this chapter, I will test whether the change in VMAT2 protein amount results in changes in monoamine vesicular storage, release, and content.

Chapter 4: VMAT2 mediation of fear-related behaviors. In this chapter, I will use VMAT2 transgenic mice to test whether changes in VMAT2 amount causally affects expression of fear behavior.

Chapter 5: VMAT2 mediation of non-fear PTSD symptomology. In this chapter, I will use VMAT2 transgenic mice to test whether changes in VMAT2 amount causally produces aberrant sensory, affective, social, or appetitive behaviors.

II. Chapter 2. Immunological analysis of the expression of VMAT2 in VMAT2 transgenic mice

A version of this chapter was published as a manuscript:

Rachel A. Cliburn, Amy R. Dunn, Kristen A. Stout, Carlie A. Hoffman, Kelly M. Lohr, Alison I. Bernstein, Emily J. Winokur, James Burkett, Yvonne Schmitz, W. Michael Caudle, Gary W. Miller. (2016) Journal of Chemical Neuroanatomy, Vol 83-84, pages 82-90. PMID: 27836486

ABSTRACT

Vesicular monoamine transporter 2 (VMAT2, *SLC18A2*) is a transmembrane transporter protein that packages dopamine, serotonin, norepinephrine, epinephrine, and histamine into vesicles in preparation for neurotransmitter release from the presynaptic neuron. VMAT2 function and related vesicle dynamics have been linked to susceptibility to oxidative stress, exogenous toxicants, and Parkinson's disease. To address a recent depletion of commonly used antibodies to VMAT2, we generated and characterized novel rabbit polyclonal antibody generated against a 19 amino acid epitope corresponding to an antigenic sequence within the C-terminal tail of mouse VMAT2. We used genetic models of altered VMAT2 expression to demonstrate that the antibody specifically recognizes VMAT2 and localizes to synaptic vesicles. Furthermore, immunohistochemical labeling using this VMAT2 antibody produces immunoreactivity that is consistent with expected VMAT2 regional distribution. We show the distribution of VMAT2 in monoaminergic brain regions of mouse brain, notably the midbrain, striatum, olfactory tubercle, dopaminergic paraventricular nuclei, tuberomammillary nucleus, raphe nucleus, and locus coeruleus. Furthermore, VMAT2 protein is expressed in areas critical to the expression of fear behavior, the hippocampus and amygdala. Normal neurotransmitter vesicle dynamics are critical for proper health and functioning of the nervous system, and this VMAT2 antibody will be a key tool in studying neurodegenerative and neuropsychiatric conditions characterized by vesicular dysfunction.

INTRODUCTION

The vesicular monoamine transporter 2 (VMAT2, *SLC18A2*) is a twelve-transmembrane glycoprotein within the TEXAN (Toxin EXtrduing ANtiporter) family of transporters (Eiden *et al*, 2004). VMAT2 resides on the membrane of secretory vesicles in monoaminergic neurons of the nervous system and in a variety of secretory cells in the gastrointestinal, endocrine, hematopoietic, and immune systems, and is often co-expressed in the periphery with its non-neuronal isoform, VMAT1 (Anlauf et al., 2006, 2004, 2003; Erickson et al., 1992; Erickson et al., 1996; Henry et al., 1994; Peter et al., 1995a; Schuldiner et al., 1995; Tillinger et al., 2010; Weihe et al., 1994). VMAT2 utilizes an electrochemical gradient maintained by a vesicular H^+-ATPase to transport one monoamine molecule (dopamine, serotonin, norepinephrine, or histamine) into the highly acidic vesicular lumen in exchange for the efflux of two protons (Chaudhry et al., 2008; Eiden et al., 2004; Erickson et al., 1995; Wimalasena, 2011). The function of VMAT2 is multifold: it prepares neurotransmitters for presynaptic release (Erickson *et al*, 1992; Henry *et al*, 1994) and prevents oxidative damage by sequestering deleterious cytosolic monoamines into the vesicle (Alter *et al*, 2013; Sulzer and Zecca, 2000).

VMAT2 regulates neurotransmitter dynamics and neuronal health (Fon *et al*, 1997; Wang *et al*, 1997). Disrupted monoamine vesicle dynamics characterize a variety of neurodegenerative and neuropsychiatric disorders, such as dystonia, Huntington's disease, depression, attention deficit hyperactivity disorder, schizophrenia, and addiction (Creese *et al*, 1996; Eisenberg *et al*, 1988; Freis, 1954; Hornykiewicz, 1998; Klawans *et al*, 1972; Ritz *et al*, 1988; Song *et al*, 2012). In the case of Parkinson's Disease (PD), presynaptic

monoamine vesicle function is substantially disrupted, and this dysfunction is hypothesized to contribute to neuronal vulnerability in PD pathogenesis (Pifl *et al*, 2014). *In vitro*, excess cytosolic dopamine causes intracellular damage via formation of reactive oxygen species in cell cultures (Zhang *et al*, 2000). *In vivo,* a mouse model created by our laboratory with 95% decreased VMAT2 expression (VMAT2-LO) has reduced ability to sequester deleterious cytosolic dopamine into vesicles and display a number of age-dependent motor and non-motor symptoms associated with PD (Caudle et al., 2008, 2007; Taylor et al., 2011, 2014). Alternately, our laboratory's mouse model with two-fold VMAT2 protein overexpression (VMAT2-HI) has increased ability to sequester dopamine into vesicles and is protected against dopaminergic degeneration (Lohr *et al*, 2014, 2015).

The continuum of VMAT2 gene expression represented by the VMAT2-LO, wild type, and -HI mice is helpful for confirming the usefulness and specificity of a VMAT2 antibody. Here, we show the use of our polyclonal VMAT2 antibody in a variety of immunochemical assays. The antibody successfully binds to and labels VMAT2, showing specific protein expression in regions that correspond to monoamine production and release (Ciliax *et al*, 1995; Fujiwara *et al*, 1999; Mazzoni *et al*, 1991; Zhou *et al*, 1996).

Due to stock depletion, the source of a previously-used effective antibody to VMAT2 is no longer currently available. Following this stock depletion, we were unable to identify a suitable commercially-available antibody that met the needs of our laboratory. Though other laboratories have had success with commercially available VMAT2 antibodies (Iritani *et al*, 2010; Shin *et al*, 2012; Temple *et al*, 2016; Zhang *et al*, 2015), we were unsuccessful in using these antibodies to achieve the specificity and selectivity needed for a battery of immunochemical assays. To address this deficit, we have designed

a polyclonal rabbit VMAT2 antibody against a peptide in the C-terminal region of mouse VMAT2. Since creating this antibody, our laboratory has received multiple requests for its use, indicating a need for an effective, well-validated VMAT2 antibody. This antibody will be an important tool in the study of presynaptic monoamine handling in relation to neurotransmission and neurodegeneration. Here, we use our newly-developed antibody to describe the precise cellular and regional distribution of VMAT2 within the mouse brain.

MATERIALS & METHODS

VMAT2 antibody production. The C-terminal region of mouse VMAT2 (TQNNVQPYPVGDDEESESD) was conjugated to maleimide activated mcKLH (Thermo Scientific) and sent to Bethyl Laboratories (Montgomery, TX, USA) and Covance Custom Immunology Services (Princeton, NJ, USA) to be injected into two rabbits from each company. Initially, animals were immunized with 500 μg conjugated protein per animal and boosted with 250 μg after 2, 4, and 6 weeks and 125 μg every four weeks thereafter. Sera were collected every other week for 6-12 months and sent back to our laboratory. We optimized the immunochemical use of antisera using VMAT2-WT and -LO brains and VMAT2-transfected HEK cells. Bleeds from one rabbit from Covalence Custom Immunology Services yielded polyclonal anti-VMAT2 serum that passed screening in our immunochemical applications.

Mice. VMAT2-LO mice were generated by backcrossing the original mixed-background VMAT2-deficient strain (Caudle *et al*, 2008; Taylor *et al*, 2014) to Charles

River C57BL/6 for four generations using a marker-assisted selection (i.e. "speed congenic") approach (Lohr *et al*, 2016). VMAT2-HI mice were generated as previously described (Lohr *et al*, 2014). Briefly, we used a bacterial artificial chromosome-mediated transgene to insert three additional copies of the murine *SLC18A2* (VMAT2) gene, including its endogenous promotor and regulatory elements. These founders were then backcrossed to a Charles River C57BL/6 background. Thus, VMAT2-LO, -WT, and -HI mice share an identical genetic background. Mice received food and water *ad libitum* on a 12:12 light cycle. All procedures were conducted in accordance with the National Institutes of Health Guide for Care and Use of Laboratory Animals and were approved by the Institutional Animal Care and Use Committee at Emory University.

Immunoprecipitation. Immunoprecipitation was performed using the Pierce co-immunoprecipitation kit (Thermo Scientific) according to manufacturer's protocols. Briefly, the VMAT2 antibody was cross-linked to agarose beads. Crude synaptosomal preparations were achieved through differential centrifugation. Samples were centrifuged at 1150 x g for 5 minutes, then the resulting supernatant was centrifuged at 18400 x g for 60 minutes. The resulting pellet was then re-suspended in homogenization buffer (320 mM sucrose, 5 mM HEPES, pH 7.4). Samples were incubated with the antibody-bound columns overnight at 4^{o}C. Bound protein complexes were eluted the following day and efficacy of immunoprecipitation was determined through immunoblot using the VMAT2 antibody.

Differential fractionation. For use in immunoblot assays, mouse brains were differentially fractionated using one of three preparations: a crude synaptosomal

preparation containing the whole isolated presynaptic terminal, a membrane-associated fraction containing the presynaptic plasma membrane, and the cytosolic vesicle fraction containing cytosol and vesicles. To produce the crude synaptosomal preparation, brains were homogenized in ice-cold homogenization buffer (320 mM sucrose, 5 mM HEPES, pH 7.4) and protease inhibitors (1:1000) using an immersion homogenizer (Tissue Tearor) for approximately 15 seconds. This homogenate was spun at 1000 x *g* for 10 minutes and the resultant supernatant was centrifuged at 20,000 x *g* for 20 minutes. To generate the membrane-associated fraction, the crude synaptosomes were osmotically lysed in pure water, then neutralized by addition of HEPES and potassium tartrate (final concentration: 25 mM and 100 mM, respectively). The lysed synaptosomes were centrifuged at 20,000 x *g* for 20 minutes. The pellet was suspended in assay buffer (25 mM HEPES, 100 mM potassium tartrate, 100 µM EDTA, 50 µM EGA, pH 7.4). To generate the cytoplasmic vesicle fraction, the supernatant was centrifuged at 120,000 x *g* for 2 hours. This fraction was suspended in assay buffer. Protein content was determined by BCA assay.

Immunoblot. For the blots in Fig 2-1, crude synaptosomal preparations from VMAT2-LO, -WT, and -HI striata were prepared as described above. For the immunoblots shown in Fig 2-2, whole brains from VMAT2-WT and -HI animals underwent whole-brain fractionation to yield a membrane-associated fraction and cytosolic vesicle fraction as described above. Samples were *not* boiled. We used 400 mM dithriothrietol (DTT, Sigma) in NuPage LDS Sample Buffer 4X (Invitrogen) to make 4X loading buffer. We specify these parameters because boiling samples and using non-DTT containing loading buffers appears to destroy the VMAT2-specific epitope. Samples were run on a NuPage 10% bis

tris gel (Life Technologies) and transferred to a PVDF membrane. Nonspecific antibody binding was blocked with a 7.5% milk solution and the membrane was then incubated in primary antibody overnight at 4°C. Primary antibodies used were polyclonal rabbit anti-VMAT2 serum (1:10,000), rabbit anti-SV2C (1:5,000, developed in our lab, see Stout et al., 2016), mouse anti-alpha-synuclein (1:1000, BD Biosciences 610787), rat anti-dopamine transporter (1:1000, Millipore MAB369), rabbit anti-tyrosine hydroxylase (1:1000, Millipore AB152), mouse anti-Rab3 (1:2500, Transduction Laboratories R35520), mouse anti-amphiphysin (1:10,000, Transduction Laboratories A59420), mouse anti-Bramp2 (1:1000, Transduction Laboratories B67020), mouse anti-complexin 2 (1:500, Transduction Laboratories C60320), mouse anti-rabaptin-5 (1:1000, Transduction Laboratories R78620), mouse anti-rabphilin 3A (1:5,000, Transduction Laboratories R44520), mouse anti-rim (1:1000, Transduction Laboratories R69420), mouse anti-sec8 (1:1000, Transduction Laboratories R56420), mouse anti-synapsin IIa (1:5000, Transduction Laboratories S56820), rabbit anti-synaptojanin I (1:1,000, Synaptic Systems 145003), rabbit anti-syntaxin I (1:1000, Sigma Aldrich S1172), rabbit anti-scamp (1:2000, Novus Biologicals NBP1-03412), rabbit anti-SNAP25 (1:1000, Cell Signaling Technologies 3926S), rabbit anti-synaptophysin (1:1000, Millipore AB9272), mouse anti-synaptotagmin I (1:5000, Synaptic Systems 105102), mouse anti-synaptotagmin 2 (1:5000, Synaptic Systems 105123), mouse anti-actin (1:5000, Sigma Aldrich A3853), mouse anti-tubulin (1:5000, Millipore CP06). The following day, the membrane was incubated with the appropriate HRP-linked secondary antibody (1:5,000, Jackson ImmunoResearch) for one hour. For preabsorption, a PVDF membrane containing only protein from a VMAT2-LO animal was allowed to

soak in 1:10000 VMAT2 antibody for one hour. This antibody solution was then siphoned off and used as primary antibody for other western blot applications, thereby reducing resultant non-specific banding.

Immunoblot was used to quantify the amount of VMAT2 protein in VMAT2 transgenic animals. Densitometric analysis was performed and calibrated to coblotted dilutional standards of pooled striata from all control samples. Actin blots were used to ensure equal protein loading across all samples. Differences between groups were determined via one-way ANOVA with genotype (LO, WT, HI) as factor and with post-hoc Dunnett's test to determine differences between groups. We did not perform densitometry on IHC data because IHC is dependent on a horseradish peroxidase diaminobenzidine reaction, in which color density does not linearly correlate with protein amount. Furthermore, we did not quantify the IHC via stereology because while it would show the number of VMAT2-positive neurons, it would not quantify the total amount of VMAT2, since we know that the amount of VMAT2 changes on the vesicle itself (Kelly *et al*, 2014).

Cell culture and immunofluorescence. We prepared co-cultures from postnatal day 0-2 mice (C57BL/6J mice, The Jackson Laboratory) plating dissociated cells from ventral midbrain, striatum, cortex, and thalamus, each at a density of 20,000 cells/cm^2 on a monolayer of cortical rat astrocyte cultures (as described in Rayport et al., 1992). Cultures were grown for 2 weeks and fixed with 4% paraformaldehyde for 5 min at RT followed by 10 min 100% methanol at -20°C. After three 15 min rinses in PBS and a blocking step with 10% normal donkey serum in PBS/0.1% Triton-X for 30 min, dishes were incubated with primary antibodies diluted in PBS/0.1% Triton-X/2% normal donkey serum at 4°C

overnight. The primary antibodies were monoclonal rat anti-DAT (1:500, Millipore MAB369), polyclonal chicken anti-TH (1:1000, Millipore AB9702), and polyclonal rabbit anti-VMAT2 at 1:2000 dilution. Cultures were rinsed again three times for 15 min in PBS and incubated in ALEXA 594/488-conjugated secondary donkey antibodies and DyLight 350-conjugated goat anti-chicken antibody at 1:400 dilution for one hour at RT (Thermofisher), followed by three more rinses in PBS. Images were taken on an Olympus IX81 inverted microscope using 20x and 60x objectives with a Photometrics CoolSNAP HQ2 monochromatic camera controlled by Metamorph software.

Immunohistochemistry. Immunohistochemistry was performed as previously described (Caudle *et al*, 2007). Tissue was incubated at 70°C in Citra (BioGenix) antigen retrieval solution for one hour. Non-specific antibody binding was blocked with a 10% normal goat serum block for one hour at room temperature. Tissue was incubated overnight at 4°C in polyclonal rabbit anti-VMAT2 serum (1:20,000 or 1:50,000, as indicated). In general, VMAT2-LO tissue was incubated at higher primary antibody concentration in order to increase detection sensitivity in an attempt to visualize any VMAT2 immunoreactive regions. Tissue was then incubated at room temperature in biotinylated goat anti-rabbit (1:200, Jackson ImmunoResearch) secondary antibody and visualized using a 60-second 3.3'-diaminobenzidine (DAB) reaction. The reaction was terminated with a PBS rinse. All images were acquired with NeuroLucida (MicroBright-Field).

RESULTS

Normalized VMAT2 protein amount increases as gene-dose of VMAT2 increases. VMAT2-LO mice have greatly reduced VMAT2 protein amount wheras VMAT2-HI mice have increased VMAT2 protein amount ($F(2,9) = 730.4$, $p < 0.0001$, Dunnett's test LO<WT $p < 0.0001$ and HI>WT $p<0.0001$) (Fig 2-1A).

VMAT2 antibody specificity. Immunohistochemical staining revealed strong VMAT2 detection in the striatum, a dopaminergic region. Furthermore, the intensity of VMAT2 staining reflected VMAT2 gene-dose effect across the continuum of VMAT2-expressing transgenic mice. VMAT2-LO mouse striatal slices displayed an absence of immunoreactivity for VMAT2. VMAT2-WT and -HI brain slices showed strong, gene-dose dependent immunohistological staining for VMAT2 antibody in the striatum (Figure 2-1C). In immunoblot analysis of VMAT2-LO, -WT, and -HI mouse striatal homogenate, the VMAT2-specific bands appeared at approximately 70, 56, and 42 kD, and increased in protein density as gene-dose of VMAT2 increased. The full western blot showed some non-specific band patterns, which was reduced by preabsorbing the VMAT2 antibody on VMAT2-LO tissue. This preabsorption reveals that the gene-dose of VMAT2 protein is maintained across glycosylation weights of VMAT2 (Figure 2-1B). Furthermore, the antibody successfully pulled down VMAT2 in an immunoprecipitation assay that was then detected via immunoblot using the VMAT2 antibody (Figure 2-1D).

VMAT2 antibody localizes to synaptic vesicles. By comparison of immunoblots from the membrane-associated fraction and cytoplasmic vesicle fraction of brain homogenate that were probed for a variety of known synaptic vesicle proteins (synaptic

vesicle glycoprotein 2C, synaptotagmin 2, synaptophysin, synaptojanin 1, synapsis II, exocyst complex component 4, rabphilin 3, rabphilin 3A, amphiphysin, and brain form of amphiphysin 2), we confirmed that the VMAT2 antibody localizes to synaptic vesicles. VMAT2-HI mice showed differential expression of VMAT2 in the cytoplasmic vesicle fraction but no differential expression of other synaptic vesicle proteins, indicating that the genetic modification of VMAT2 protein amount did not result in alterations in the expression of these synaptic proteins (Figure 2-2).

VMAT2 expression and localization within a dopaminergic neuron. Co-cultures of dopaminergic midbrain neurons plated with cortical, thalamic, and striatal cells (14 days) were double labeled for VMAT2 and tyrosine hydroxylase (TH) or plasmalemmal dopamine transporter (DAT). VMAT2 label was found exclusively in neurons expressing TH or DAT. The VMAT2 antibody strongly labeled axonal varicosities and axons, while much weaker label was found in cell bodies and dendrites (Figure 2-3).

VMAT2 expression and localization within the dopaminergic system. As expected, VMAT2 antibody staining was reliably observed in dopaminergic cell groups and their terminal fields. In WT mouse brain, VMAT2 antibody staining was observed diffusely through the dorsal and ventral striatum, olfactory tubercle, paraventricular dopamine cell groups, and the dopaminergic midbrain (Figure 2-4). This staining was negligible in VMAT2-LO mouse tissue, and was darker in VMAT2-HI tissue. This expected differential intensity of VMAT2 antibody staining across gene-dose of VMAT2 demonstrates the specificity of the antibody to the VMAT2 protein. At higher magnification, neurons and

processes of the ventral tegmental area (VTA; cell group A10) were immunoreactive for VMAT2 (Figure 2-5A). The substantia nigra pars compacta (SNc; cell group A9) displayed a similar pattern of immunoreactivity, with robust labelling of perikarya and a meshwork of neuronal processes (Figure 2-5B). VMAT2 immunoreactivity was also observed in the terminal fields of dopaminergic midbrain neurons and was concentrated in the neuropil of the dorsal and ventral striatum. Labelling patterns in striatal dopamine terminal regions exhibited compartmental organization with some areas where VMAT2 antibody staining was absent (Figure 2-5D, E), likely due to the absence of dopamine terminal markers in the white matter tracts that run through the striatum. Furthermore, VMAT2 antibody displayed staining in paraventricular cell groups (cell groups A11-A15), including sparse perikarya puncta in the more rostral cell groups and preferential granular terminal staining in caudal cell groups along the ventricle (Figure 2-5C). These expression patterns are consistent with studies linking VMAT2 to the susceptibility of the dopamine system to dopamine toxicity (Caudle *et al*, 2007; Reveron *et al*, 2002), exogenous toxins (Guillot *et al*, 2008b; Lohr *et al*, 2015; Richardson *et al*, 2006), and PD-like pathology (Lohr *et al*, 2014; Lohr and Miller, 2014).

VMAT2 expression and localization within the serotonergic system. VMAT2 antibody stained the serotonergic raphe nucleus in WT tissue (Figure 2-6). This VMAT2 antibody staining was absent in VMAT2-LO tissue and was more robust in VMAT2-HI tissue. The differential intensity of immunochemical staining demonstrates the specificity of the VMAT2 antibody in detecting VMAT2 protein (Figure 2-6A). Higher magnification examination of VMAT2 antibody staining in WT tissue showed dense immunoreactivity

in cell bodies and a rich, diffuse meshwork of VMAT2-positive neuronal processes surrounding the dorsal raphe nucleus (Figure 2-6B).

VMAT2 expression and localization within the noradrenergic system. VMAT2 antibody is immunoreactive in the locus coeruleus in VMAT2-WT and -HI tissue, but was negligible in VMAT2-LO brain tissue (Figure 2-7A). VMAT2 antibody displayed very dense cell body staining that was regionally restricted to the triangular locus coeruleus, with a faint meshwork of neuronal processes surrounding these densely labelled cell bodies (Figure 2-7B).

VMAT2 expression and localization within the histaminergic system. Lastly, the VMAT2 antibody stained the histaminergic tuberomammillary nucleus in VMAT2-WT tissue and also exhibited slightly more robust staining in VMAT2-HI brain tissue, but this staining was absent in VMAT2-LO tissue (Figure 2-8A). This difference in staining across VMAT2-altered genotypes lends credence to the specificity of the VMAT2 antibody to VMAT2 protein. The tuberomammillary nucleus shows weak, granular, diffuse staining in WT tissue along the ventral border of the brain, with sparse VMAT2-postive cell bodies (Figure 2-8B).

VMAT2 expression and localization in the hippocampus and amygdala. The presence of VMAT2 in circuits critical to expression and maintenance of fear behavior (amygdala and hippocampus) has not been verified in adult mice. Using immunohistochemistry, we showed that VMAT2 was sparsely present in both the anterior

basolateral nucleus of the amygdala and in the dentate gyrus of the hippocampus in VMAT2-WT and -HI mouse tissue, and that VMAT2 staining was negligible in VMAT2-LO tissue (Figure 2-9)

DISCUSSION

These results indicate that our newly developed rabbit polyclonal VMAT2 antibody is specific for the mouse VMAT2 protein and is useful in immunoblot, immunohistochemical, immunocytochemical, and immunoprecipitation studies using homogenates of mouse brain tissue, mouse brain sections fixed via paraformaldehyde, and mouse primary cell culture. The continuum of gene-dose represented by the VMAT2-LO, -WT, and -HI mice—as demonstrated by decreased, normal, and elevated levels, respectively, of VMAT2 mRNA, protein, and function—serves as an excellent series of negative and positive controls for testing the polyclonal VMAT2 antibody (Caudle *et al*, 2007, 2008; Lohr *et al*, 2014).

Since the rabbit anti-VMAT2 antibody is polyclonal, the presence of non-specific bands is not surprising. In an effort to minimize non-specific staining, our laboratory attempted to affinity-purify the polyclonal antibody both in-house and through Covance. Unfortunately, affinity purification resulted in a total loss of the VMAT2-specific band. We suspect that this affinity purification strongly bound the VMAT2-specific antibodies such that no specific antibodies were eluted and thus the VMAT2-specific band was lost. However, by preabsorbing the VMAT2 antibody on VMAT2-LO tissue, the non-specific band pattern was greatly reduced. With preabsorption treatment, bands corresponding to

varyingly glycosylated VMAT2 are readily apparent, and are consistent with the previously established weights of this protein with post-translational modifications in mouse (Gainetdinov et al., 1998; Richardson et al., 2006; Wang et al., 1997).

Our VMAT2 antibody localizes to the synaptic vesicle, which is consistent with the known cellular localization of VMAT2 (Erickson *et al*, 1992; Wimalasena, 2011). In primary dopaminergic cell culture from VMAT2-WT neonates, the VMAT2-antibody colocalizes with dopaminergic markers and permeates the whole dopaminergic neuron, staining the cell body, neuronal processes, and terminal fields. These stained cell bodies and terminal regions are readily apparent via immunohistochemistry. VMAT2 antibody staining was selectively observed in monoaminergic brain regions, including those related to dopamine, serotonin, norepinephrine, and histamine. Indeed, the regional expression pattern of VMAT2 protein in VMAT2-WT and -HI mouse brain aligns with known distributions of markers for dopamine (Ciliax *et al*, 1995), serotonin (Zhou *et al*, 1996), norepinephrine (Mazzoni *et al*, 1991), and histamine (Fujiwara *et al*, 1999). This labeling is consistent with similar studies showing regional distribution in rat (Cruz-Muros et al., 2008; Erickson et al., 1995; Peter et al., 1995b; Weihe et al., 1994) and primate brain, though primate brains display increased terminal VMAT2 immunohistochemical puncta in the cortex that is not present in rodent models (Erickson et al., 1996; Miller et al., 1999). We observe VMAT2 protein expression in the same brain regions that the Allen Brain Atlas (freely available at www.brain-map.org) indicates as regions with high VMAT2 mRNA expression, notably in the hypothalamus, midbrain, and brain stem nuclei.

Importantly, VMAT2 gene-dose has been linked to either neurotoxic or neuroprotective effects within each of the monoamine neurotransmitter systems including

serotonin signaling (Alter et al., 2016), noradrenergic degeneration (Taylor *et al*, 2014), non-motor symptoms of PD (Taylor *et al*, 2009), and dopamine handling, toxicity, and dopamine-related neurodegeneration (Little *et al*, 2003; Lohr *et al*, 2015; Pifl *et al*, 2014). The significant expression of VMAT2 in dopaminergic regions such as the striatum and midbrain suggests possible sites of action for the previously reported VMAT2-mediated neuroprotection from toxic exposure to pesticides (Richardson et al., 2006), methamphetamine (Guillot *et al*, 2008b; Lohr *et al*, 2015; Takahashi *et al*, 1997), and MPTP (Liu *et al*, 1992; Lohr *et al*, 2014). The localization of VMAT2 at dopaminergic terminals and the direct mediation of quantal dopamine release by VMAT2 (Lohr et al., 2014) may also provide a mechanism for age-dependent dopaminergic neurodegeneration in VMAT2-LO mice (Caudle *et al*, 2007). Similarly, VMAT2-LO mice show neurodegeneration of the locus coeruleus (Taylor *et al*, 2014), a region that also degenerates in PD and shows immunoreactivity to our VMAT2 antibody. This observed reduction in immunoreactivity for VMAT2 in the VMAT2-LO mice is responsible for the disrupted serotonin signaling in these animals (Alter et al., 2016). These effects provide evidence that VMAT2 is broadly important in monoaminergic transmission, with higher gene-dose consistently linked to neuroprotection and lower gene-dose consistently linked to neurodegeneration and neuronal vulnerability.

Lastly, we showed that VMAT2 protein is present in areas of the brain critical to expression of learned fear, the hippocampus and the amygdala. The presence of VMAT2 in the amygdala and hippocampus had not yet been established in our VMAT2 transgenic mouse model. This lends credence to the hypothesis that VMAT2 variation may influence fear behavior.

Overall, the rabbit polyclonal VMAT2 antibody described here will be a useful tool in a variety of immunological methods. This immunochemical characterization of VMAT2 within mouse neurons and circuits will inform the study of monoaminergic vesicular dynamics and associated neurodegenerative and neuropsychiatric diseases.

FIGURES

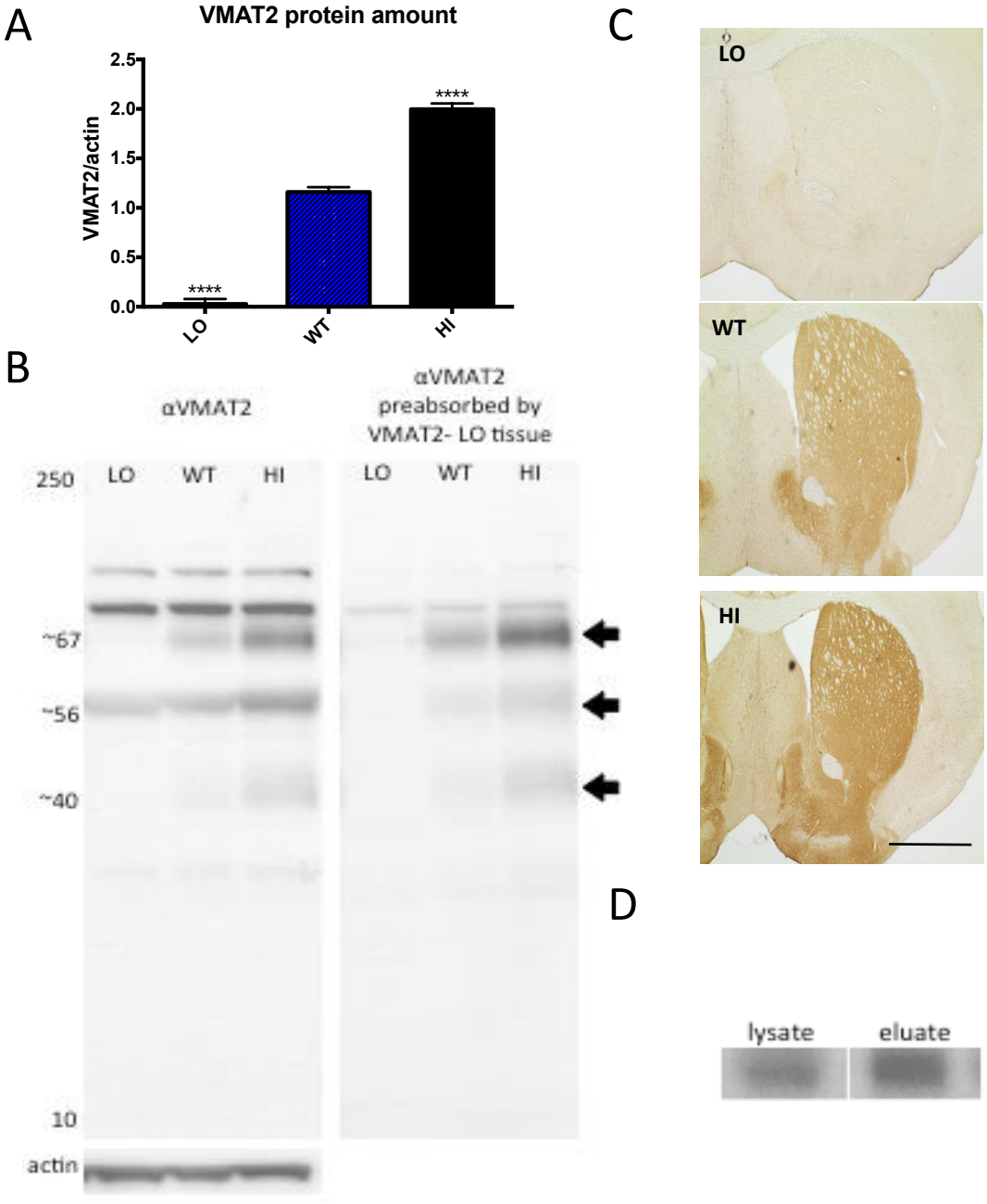
A
VMAT2 protein amount
VMAT2/actin
2.5
2.0
1.5
1.0
0.5
0.0
****
****
LO
WT
HI
B
αVMAT2
αVMAT2 preabsorbed by VMAT2- LO tissue
250
LO
WT
HI
LO
WT
HI
~67
~56
~40
10
actin
C
LO
WT
HI
D
lysate
eluate

Figure 2-1. Molecular specificity of the polyclonal VMAT2 antibody. A. VMAT2 protein amount increases as VMAT2 gene dose increases (n = 4 animals per group). B. Western blot detection of mouse VMAT2 protein in VMAT2-LO, –WT, and –HI mouse crude synaptosomal striatal homogenate. Left: anti-VMAT2 antibody used at 1:10,000. Right: the same blot was stripped and reprobed with anti-VMAT2 antibody that had been preabsorbed by VMAT2-LO tissue for one hour. VMAT2-specific bands (black arrows) appear at approximately 70, 56, and 42 kD, corresponding with varying VMAT2 glycosylation weights. Bottom: Actin loading control shows no difference in protein amount between lanes. C. Immunohistochemical staining of VMAT2 is virtually absent in VMAT2-LO brain but is expressed in the striatum of VMAT2-WT and more intensely in VMAT2-HI striatum. Scale bar 1 mm. D. Co-immunoprecipitation of VMAT2 from striatal homogenate of WT mice.

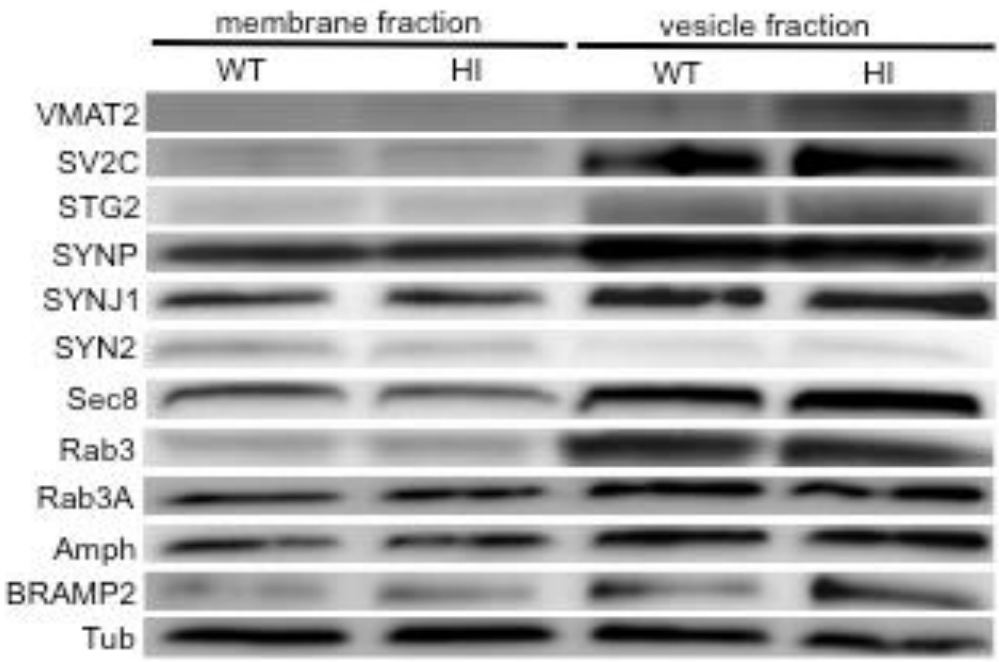

Figure 2-2. VMAT2 localizes to synaptic vesicles. Brain homogenate from WT and VMAT2-HI mice was fractionated by differential centrifugation into membrane-associated and cytoplasmic vesicle fractions. VMAT2 expression is highest in the cytoplasmic fraction, in conjunction with other synaptic vesicle proteins, including the synaptic vesicle glycoprotein 2C (SV2C), synaptotagmin 2 (STG2), synaptophysin (SYNP), synaptojanin 1 (SYNJ1), synapsin II (SYN2), exocyst complex component 4 (sec8), rabphilin 3 (rab3), rabphilin 3A (rab3A), amphiphysin (AMPH), and brain form of amphiphysin 2 (BRAMP2). Loading control: beta-tubulin.

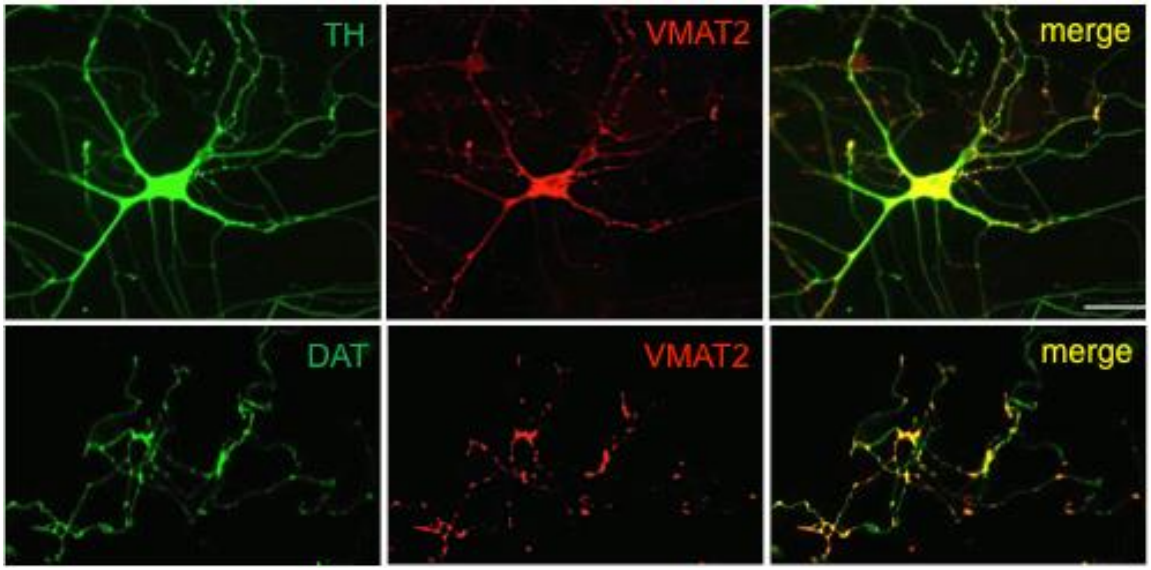

Figure 2-3. VMAT2 co-localizes with dopaminergic markers in primary culture TH+ neurons. VMAT2 is expressed in the cell body and neuronal processes of TH+ primary cell culture from VMAT2-WT neonates. Similarly, VMAT2 is co-localizes with DAT in terminal fields primary cell culture. Primary antibodies used at the following dilutions: rat anti-DAT 1:500, chicken anti-TH 1:1000, and rabbit anti-VMAT2 1:2000.

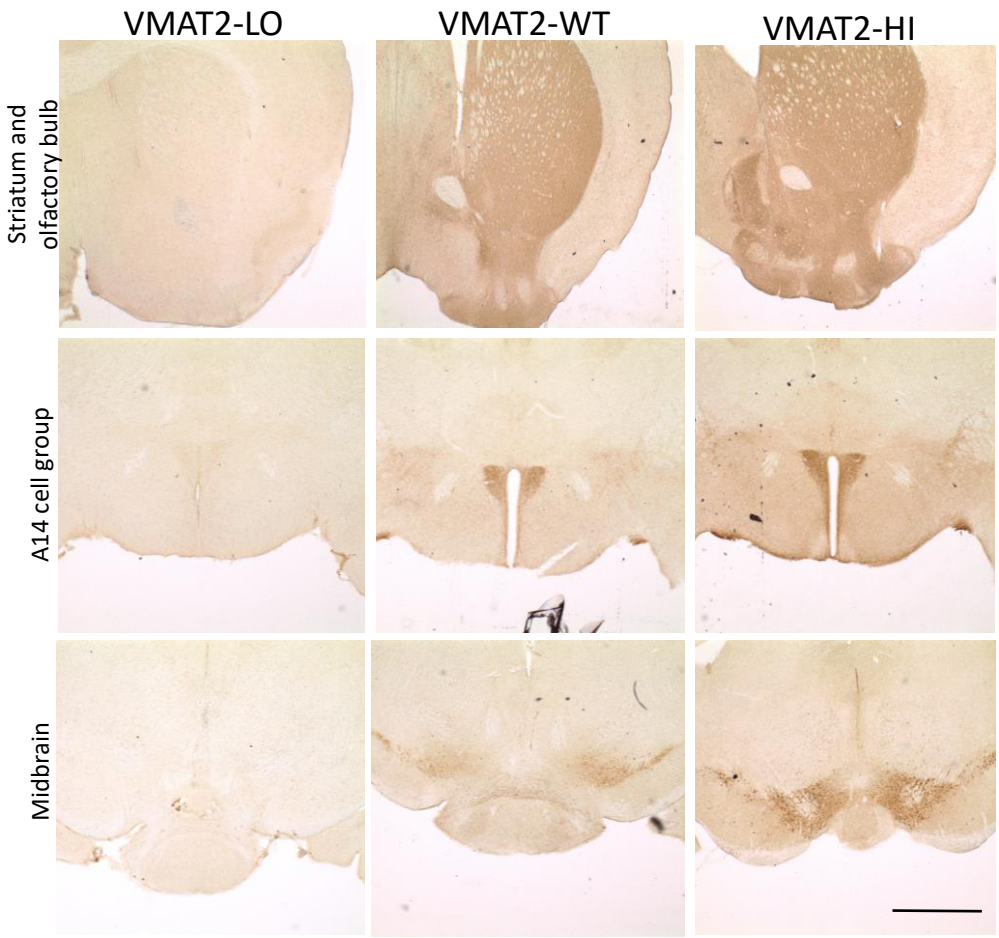

Figure 2-4. VMAT2 immunohistochemistry in dopaminergic regions of mouse brain. VMAT2-LO (A, B, C) mice show negligible VMAT2 immunohistochemical staining in dopaminergic brain regions. In both VMAT2-WT and –HI mice, VMAT2 protein is expressed in dopaminergic brain regions. Polyclonal rabbit anti-VMAT2 was used at 1:50,000 on VMAT2-WT and –HI mice, 1:20,000 for VMAT-2 LO tissue. Scale bar 1 mm.

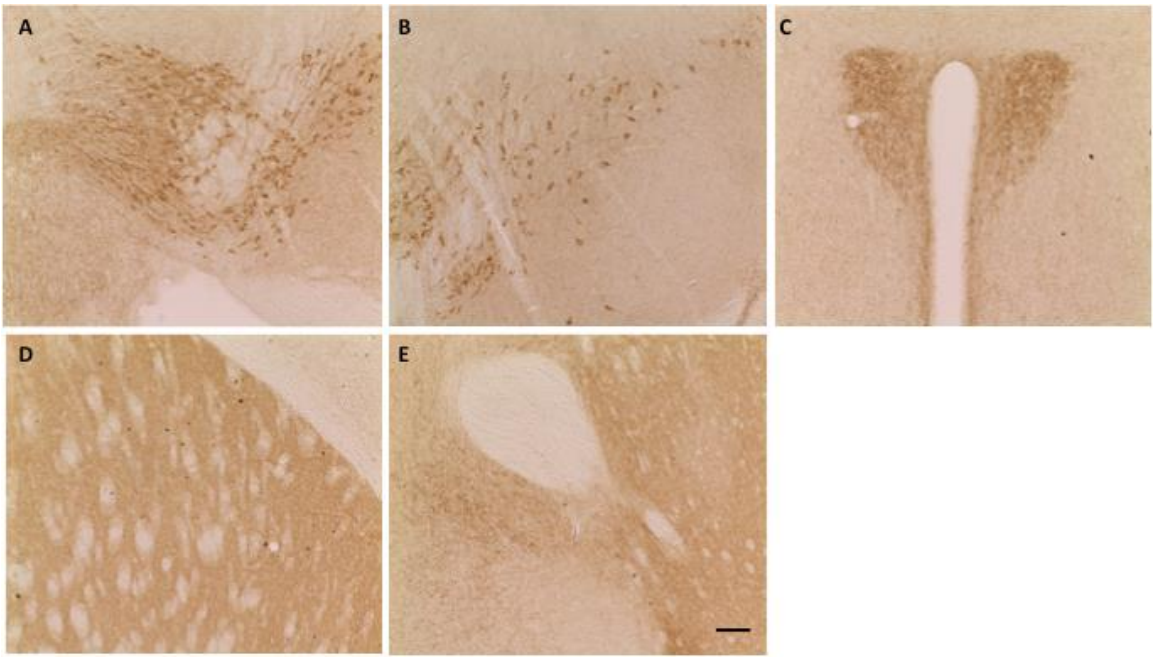

Figure 2-5. VMAT2 immunohistochemistry in dopaminergic cell groups and terminal regions in mouse brain. VMAT2 antibody binds the cell bodies of dopamine neurons in the ventral tegmental area (A), the substantia nigra pars compacta (B), the A14 nucleus (C) and dopaminergic terminal regions in the dorsolateral striatum (D) and ventral striatum (E). Polyclonal rabbit anti-VMAT2 was used at 1:50,000 on VMAT2-WT tissue. Scale bar 100 μm.

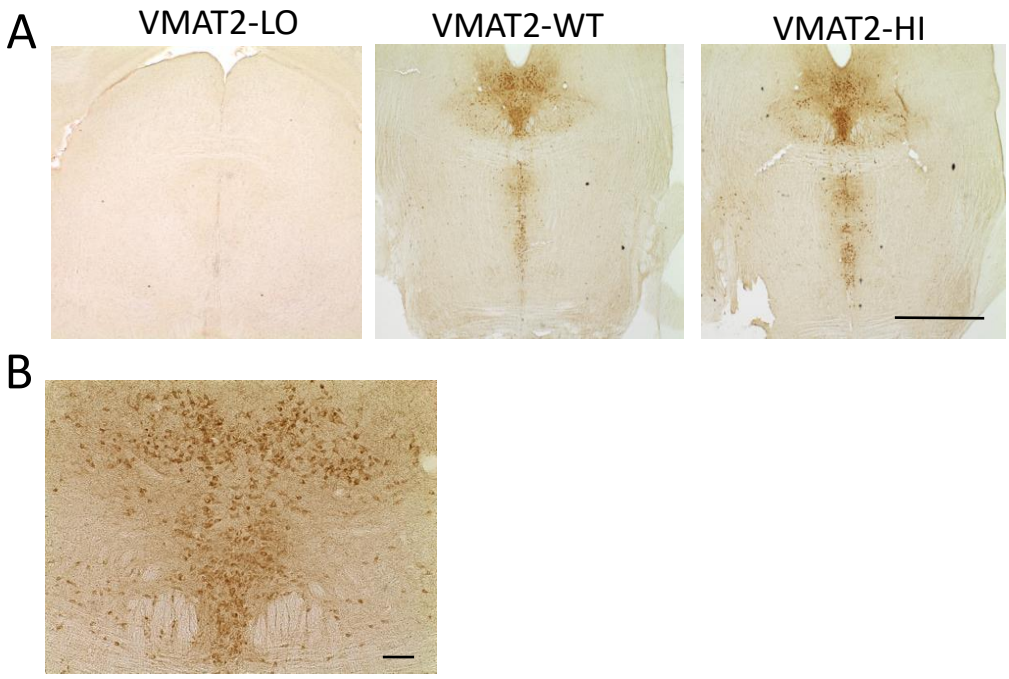

Figure 2-6. VMAT2 immunohistochemistry in a serotonergic nucleus of mouse brain. VMAT2 antibody staining is negligible in VMAT2-LO tissue. In VMAT2-WT and -HI tissue, VMAT2 antibody stains the serotonergic raphe nucleus, shown in higher magnification in WT tissue (B). Polyclonal rabbit anti-VMAT2 was used at 1:50,000 on VMAT2-WT and -HI mice, 1:20,000 for VMAT-2 LO tissue. Scale bar 1 mm in A-C, 100 µm in B.

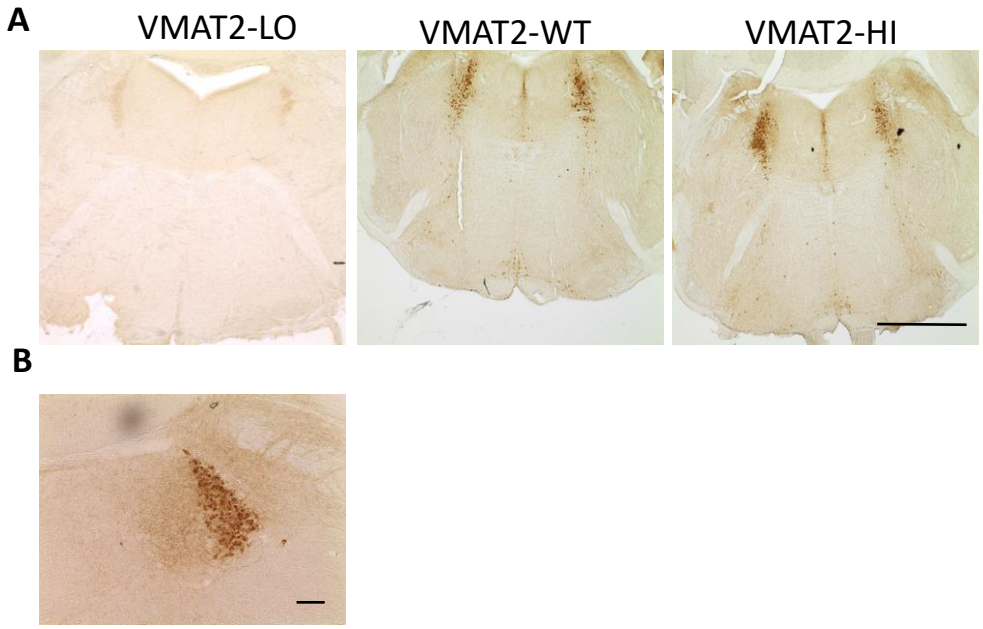

Figure 2-7. VMAT2 immunohistochemistry in a noradrenergic region of mouse brain. VMAT2-LO (A) mice show negligible VMAT2 immunohistochemical staining. both VMAT2-WT (A-H) and VMAT2-HI (I-P) mice, VMAT2 protein is expressed in the locus coreleus, as shown in higher magnification in B. Polyclonal rabbit anti-VMAT2 was used at 1:50,000 on VMAT2-WT and -HI mice, 1:20,000 for VMAT-2 LO tissue. Scale bar 1 mm in A-C, 100 µm in B.

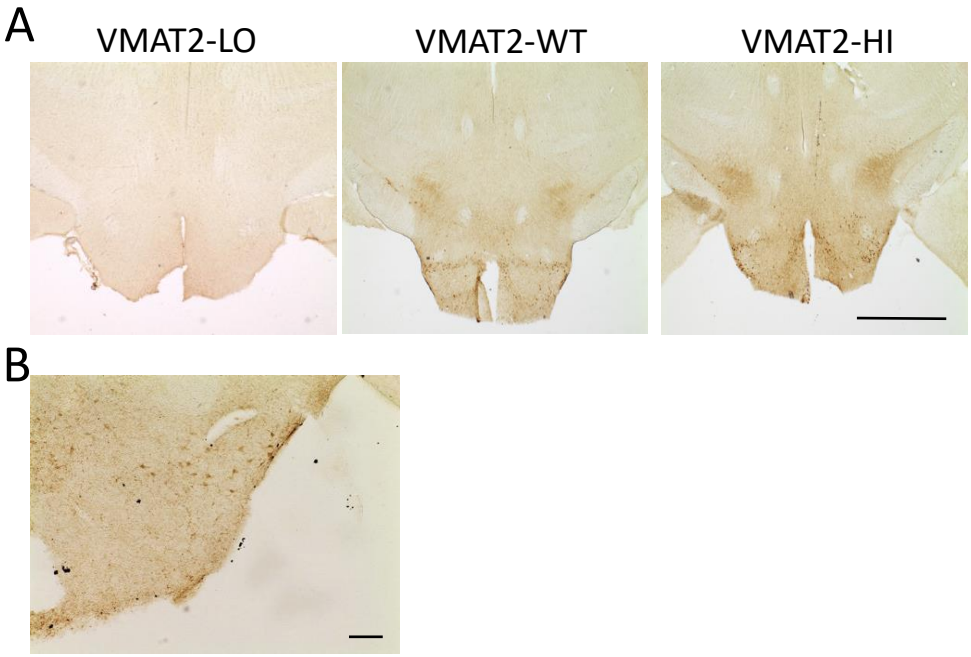

Figure 2-8. VMAT2 immunohistochemistry in a histaminergic nucleus of mouse brain. VMAT2 staining is negligible in a VMAT2-LO tissue. In both VMAT2-WT and -HI tissue, VMAT2 protein is expressed in the histaminergic tuberomammilary nucleus, WT staining shown at higher magnification in B. Polyclonal rabbit anti-VMAT2 was used at 1:50,000 on VMAT2-WT and -HI mice, 1:20,000 for VMAT-2 LO tissue. Scale bar 1 mm in A-C, 100 µm in B.

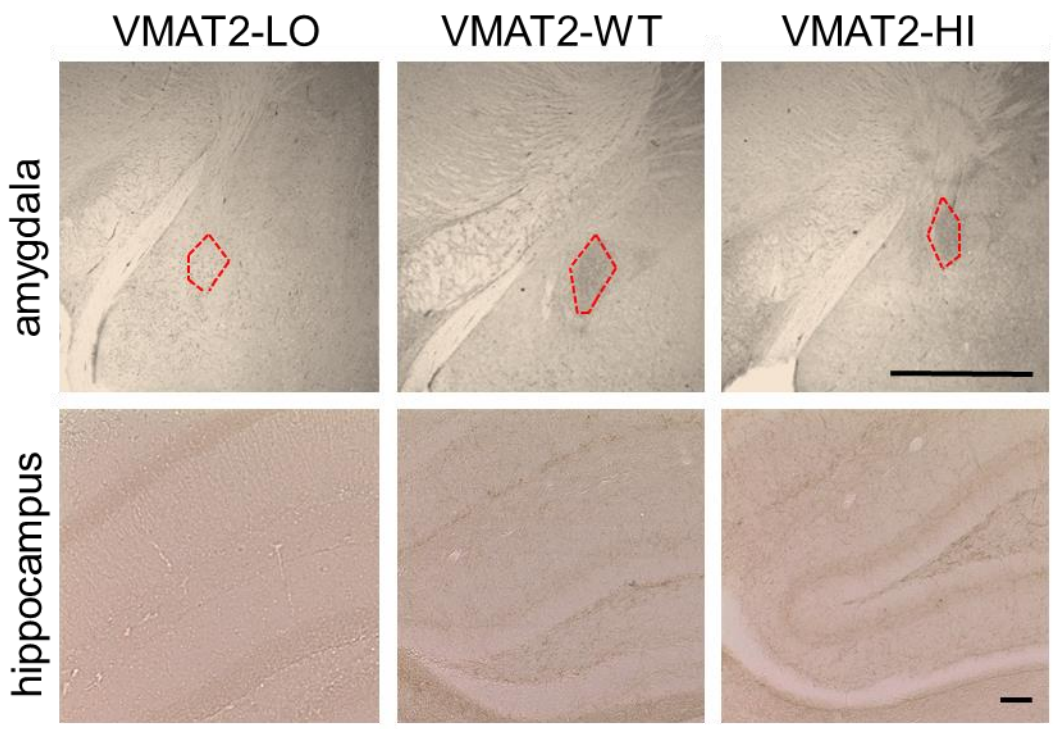

Figure 2-9. VMAT2 immunohistochemistry in mouse amygdala and hippocampus. VMAT2-LO mice show negligible VMAT2 immunohistochemical staining in the amygdala (outlined in red) and hippocampus, while VMAT2-WT and –HI mice show VMAT2 protein expression in these areas. Polyclonal rabbit anti-VMAT2 was used at 1:50,000. Scale bar at 1 mm for amygdala, 100 µm for hippocampus.

III. Chapter 3. VMAT2 transgenic mice represent a continuum of monoaminergic function

A version of this chapter was submitted as part of a manuscript:

Rachel A. Cliburn, James P. Burkett, Jason P. Schroeder, David Weinshenker, Tanja Jovanovic, Gary W. Miller. (2018) Submitted to Neuropsychopharmacology.

ABSTRACT

Vesicular monoamine transporter 2 (VMAT2) is a critical modulator of monoamine neurotransmitters in the central nervous system. Our laboratory has bred transgenic strains of mice that express either 5% of wild type (VMAT2-LO mice) or 200% of wild type levels (VMAT2-HI mice) of VMAT2 protein. We have previously shown that VMAT2-LO and -HI mice express VMAT2 protein in monoaminergic regions of the mouse brain in addition to brain regions critical to the expression of fear and memory. Furthermore, immunohistochemical analysis confirms variation in VMAT2 protein expression in these areas. However, it is yet unknown whether and to what extent variation in VMAT2 protein results in alterations in the function of the monoamine system within the brain. In other words, does the change in the protein amount actually make a difference in the function of monoaminergic neurons? To answer this question, we performed radioactive uptake to measure vesicular storage capacity, high performance liquid chromatography to measure monoamine metabolite content, and fast-scan cyclic voltammetry to measure stimulated dopamine release. We found that VMAT2-LO mice have reduced monoaminergic vesicular storage capacity in both the striatum and frontal cortex, show a pattern of reduced monoamine metabolites, and greatly reduced capacity to release dopamine upon stimulation. VMAT2-HI animals showed improved storage capacity, a pattern of increased monoamine metabolites, and increased capacity to release dopamine upon stimulation. These functional changes in monoaminergic transmission could underlie the behavioral phenotypes observed in VMAT2 transgenic animals.

INTRODUCTION

VMAT2 transports monoamine neurotransmitters (dopamine, serotonin, norepinephrine, epinephrine, and histamine) into presynaptic neuronal vesicles in preparation for release into the synaptic space (Eiden and Weihe, 2011; Peter *et al*, 1995a). We have previously shown that VMAT2 protein is expressed throughout the murine brain. VMAT2 protein expression is observed in monoaminergic cell bodies and terminal regions, including the paraventricular dopaminergic nuclei, the midbrain, the tuberomammilary nucleus, the locus coerleus, and the dorsal and ventral striatum. Furthermore, there is diffuse VMAT2 protein expression in the dentate gyrus of the hippocampus and in the basolateral nucleus of the amygdala. Lastly, based on visual analysis of immunohistochemical staining, VMAT2-LO mice display greatly reduced protein amount in these brain regions, while VMAT2-HI mice seem to show elevated protein content. Reduced VMAT2 protein in VMAT2-LO animals and elevated VMAT2 protein content in VMAT2-HI mice was confirmed via immunoblot analysis from striatal dissections (Chapter 2).

We have yet to establish that this expression and variation in VMAT2 protein results in functional changes to the monoamine system. Though VMAT2 is a critically positioned protein within the synaptic machinery of monoamine release, it is possible that VMAT2-LO mice have compensatory mechanisms of monoamine release despite their reduced VMAT2 protein content. Likewise, it is possible that VMAT2-HI mice do not show functional consequences of increased VMAT2 protein, as there is debate whether a presynaptic vesicle could carry more neurotransmitter even with additional VMAT2

packaging proteins on the plasmalemmenal membrane. Therefore, the purpose of these studies is to test whether changing VMAT2 protein amount changes anything about the normal function of monoaminergic neurons. For these studies, 'normal function' includes storing neurotransmitter into vesicles, producing monoamine metabolites, and releasing neurotransmitters following a stimulation event. Specifically, we hypothesize that VMAT2-LO animals have decreased measures of monoamine function, while VMAT2-HI mice display enhanced measures of monoamine function. To test this, we performed a variety of assays.

First, we perform radioactive vesicular uptake assay in the frontal cortex and striatum. The striatum primarily contains dopamine terminal projections from the midbrain, while noradrenergic and serotonergic neurons, projecting from the locus coerleus and raphe nucleus, respectively, are the primary drivers of vesicular monoamine uptake in the frontal cortex. Testing vesicular monoamine uptake in both the striatum and frontal cortex enables us to characterize how VMAT2 genotype affects the vesicular storage capabilities of various monoamine systems.

Next, we measured total brain metabolite content using high performance liquid chromatography. Since VMAT2 protein is a critical protein to the packaging of monoamines into presynaptic vesicles, but not necessarily critical to the *production* of monoamines, it was an open question whether mice under- or over-expressing VMAT2 would show changes in monoamine metabolite content.

Lastly, we used fast-scan cyclic voltammetry (FSCV) to measure stimulated dopamine release in the dorsal and ventral striatum. At baseline, this comparison elucidates the size of readily releasable pool of dopamine, which corresponds to both the number of

vesicles in the presynaptic terminal and to the amount of dopamine stored within those vesicles. We also use FSCV to measure the biochemical response to cocaine. Cocaine blocks the dopamine transporter (DAT). DAT is a plasmalemmenal protein that transports dopamine molecules from the extracellular space into the presynaptic terminal, so administration of a DAT blocker forces dopamine to stay in the extracellular space for an extended period of time. Interestingly, cocaine also increases the amount of dopamine released from the readily releasable pool. Though this phenomena is not well understood, cocaine likely exerts this effect through some interaction with synapsin-dependent reserve pool (Venton *et al*, 2006). Therefore, adding cocaine to the system of altered presynaptic function can elucidate how altered VMAT2 can contribute to the dopamine-releasing effects of cocaine. As a positive control of the effects of cocaine on dopamine release, we use mice that overexpress DAT (DAT-OE). These mice were developed by the Salahpour laboratory at University of Toronto (Masoud *et al*, 2015). Because of the overexpression of the transporter, dopamine is efficiently packed into the cytosol, but not necessarily quickly sequestered into presynaptic vesicles. Because of this excess in cytosolic dopamine, DAT-OE mice show progressive dopaminergic degeneration as shown by loss of dopamine neurons and signs of oxidative stress. In an effort to truly "max out" the amount of cytosolic dopamine, the Salahpour laboratory crossed DAT-OE mice with VMAT2-LO mice. Theoretically, this would create a system in which dopamine is efficiently transported from the extracellular space into the cytosol, where it languishes unpackaged due to the paucity of VMAT2 protein. In these mice, one would expect a very low level of stimulated dopamine release in the striatum. We performed fast-scan cyclic voltammetry to characterize stimulated dopamine release in the dorsal striatum of DAT

and VMAT2 transgenic mice. We bathed *ex vivo* striatal slices in increasing concentrations of cocaine in order to block DAT. The increase in stimulated dopamine release due to the addition of cocaine gave us a sense of the relative contribution of DAT in that transgenic system.

MATERIALS & METHODS

Mice. Male and female adult VMAT2-LO and -HI animals were used for these assays. VMAT2-LO mice were generated by backcrossing the original mixed-background VMAT2-deficient strain (Caudle *et al*, 2008; Taylor *et al*, 2014) to Charles River C57BL/6 for four generations using a marker-assisted selection (i.e. "speed congenic") approach (Lohr *et al*, 2016). VMAT2-HI mice were generated as previously described (Lohr *et al*, 2014). We used a bacterial artificial chromosome-mediated transgene to insert three additional copies of the murine *SLC18A2* (VMAT2) gene, including its endogenous promotor and regulatory elements. These founders were then backcrossed to a Charles River C57BL/6 background. In these assays, no difference was detected between wild-type littermates from the VMAT2-LO and VMAT2-HI colonies, so these groups were collapsed. We also used DAT-overexpressing mice and DAT-overexpressing/VMAT2-LO mice (DAT-OE or DAT-OE/VMAT2-LO, respectively, both developed in the Salahpour laboratory at University of Toronto (Masoud *et al*, 2015). Each of these genetically altered mice are on a C57BL/6 background. Mice were group housed with *ad libitum* access to food and water in the home cage.

All procedures were conducted in accordance with the National Institutes of Health Guide for Care and Use of Laboratory Animals and were approved by the Institutional Animal Care and Use Committee at Emory University.

Vesicular radioactive monoamine uptake. Striatal and frontal cortical dissections from three to five mice of each genotype were homogenized in homogenization buffer (4 mM HEPES, 0.32 M sucrose, pH 7.4). Homogenates were centrifuged at 1000 x *g* for 10 minutes, and the resulting supernatant was centrifuged at 20,000 x *g* for 20 minutes. The resulting pellet was resuspended in 1.6 mL of 0.32 M sucrose before being transferred to glass/Teflon homogenizer containing 6.4 mL of water and subjected to 10 up-and-down strokes by hand. All contents of the homogenizer were then poured into a tube containing 1 mL each of 250 mM HEPES and 1 M potassium tartrate and inverted to mix. The mixture was then centrifuged at 20,000 x *g* for 20 minutes, and the resulting supernatant was placed in an ultracentrifuge tube and spun at 120,000 x *g* for 2 hours. Vesicles were resuspended in 1.8 mL of buffer (100 mM potassium tartrate, 25 mM HEPES, 0.1 mM EDTA, 0.05 mM EGTA, 1.7 mM ascorbate, pH 7.4). Uptake assays used 300 μL of vesicle solution for each dopamine concentration, with 2% [^{3}H] dopamine as a tracer and 10 μM tetrabenazine (Sigma, St. Louis, MO) to define specific uptake. Samples were incubated for 10 minutes at 30 ^{o}C followed by the addition of [^{3}H] dopamine and further incubation for 5 minutes at 30 ^{o}C. The assay was terminated by addition of 5 mL of ice-cold assay buffer before filtration through 0.5% polyethylenamine-soaked Whatman GF/F filters (Brandel, Gaithersburg, MD). Filters were then placed in scintillation fluid and counted using a Beckman LS6500 (Beckman Instruments, Fullerton, CA). Radioactive activity was

normalized by sample protein amount, which was determined by performing a bicinchoninic acid assay (Thermo Fisher Scientific, Waltham, MA). ANOVA with post-hoc Dunnett's tests were performed to determine differences between genotypes.

High performance liquid chromatography (HPLC). HPLC was performed as described previously (Lohr *et al*, 2014), with a few modifications. Briefly, half brains cut sagittally with the cerebellum removed were sonicated in 10x their weight of 0.1 M perchloric acid and were pelleted at 10,000 x *g* for 10 min. Supernatants were filtered at 0.2 µm. Dopamine (DA), 3,4-dihydroxyphenylacetic acid (DOPAC), norepinephrine (NE), homovanillic acid (HVA), and 5-hydroxyindoleacetic acid (5-HIAA) were detected using an MD-150 x 3.2 mm C18 column (ESA). The mobile phase consisted of a 1.5 mM 1-octanesulfonic acid sodium, 75 mM NaH_2PO_4, 0.025% trimethylamine, and 8% (vol/vol) acetonitrile at pH 2.9. A 20 µL sample was injected. The detected concentrations of three groups of analytes (dopamine group: DA and DOPAC; norepinephrine group: NE; serotonin group: HVA and 5-HIAA) were analyzed using separate two-factor MANOVAs, with genotype (LO, WT, HI) as between-subjects factor and the metabolites as dependent variables. Post-hoc Dunnett's test was performed to determine differences between groups.

Fast scan cyclic voltammetry (FSCV). Slice FSCV was performed in the lateral dorsal striatum of male and female adult VMAT2-LO, -WT, or -HI mice (n = 6 – 10 per genotype). Mice were decapitated and the brain rapidly removed and placed in ice-cold, oxygenated (95% O_2/5% CO_2) sucrose aCSF (193 mM sucrose, 11 mM d-glucose, 1.2 mM dihydrous $CaCl_2$, 4.5 mM KCl, 25 mM $NaHCO_3$, 20.5 mM NaCl, 1.2 mM NaH_2PO_4

monobasic, 2.6 mM $MgCl_2$, adjusted to pH 7.4) then sliced coronally at 300 μM using a vibratome (Leica VT1000 S, Buffalo Grove, IL). Striatal slices were selected and bathed in oxygenated HEPES aCSF (19.7 mM HEPES, 11 mM d-glucose, 2.4 mM dihydrous $CaCl_2$, 25 mM $NaHCO_3$, 126.4 mM NaCl, 2.5 mM KCl, 1.2 mM monobasic NaH_2PO_4, 2.6 mM $MgCl_2$, adjusted to pH 7.4) at 20^oC for 30 mins prior to recording. For recording, a slice was transferred to a slice dish where it was superfused in 30 ^oC HEPES aCSF for the course of the experiment. The recording electrodes, cylindrical carbon-fiber (6 um diameter, Thornel, Greenville, SC) microelectrodes, were fabricated in-house by sealing the carbon fiber in a glass capillary such that the length of the protruding carbon-fiber was approximately 65 μM. A bipolar tungsten stimulating electrode (MicroProbes, Gaithersburg, MD) and a recording electrode were placed on the surface of the slice in the nucleus accumbens core. For each recording, dopamine release was effected via a single computer-generated stimulation (monophasic, 60 Hz, 2.31 V to produce a 700 μA stimulation). Stimulations were separated by five minutes. Application of waveform, stimulus, and current monitoring was controlled by TarHeel CV (University of North Carolina) using a custom potentiostat (UEI, UNC Electronics Shop). The waveform for dopamine detection consisted of a -0.4 holding potential versus an Ag/AgCl (World Precision Instruments, Inc., Sarasota, FL) reference electrode. The applied triangular voltage ramp went from -0.4 V to 1.0 V and back to -0.4 V at a rate of 600 V/s at 60 Hz. The current at the peak oxidation potential for dopamine (0.6 vs Ag/AgCl) was used to evaluate dopamine concentration changes with time. Primary outcome measure was peak dopamine release, which was evaluating by calculating the maximum current and dividing it by the calibration constant for that electrode. Measuring peak dopamine release is a

common practice to determine stimulated neurotransmitter release (Alter *et al*, 2016; Lohr *et al*, 2014; Stout *et al*, 2016) ANOVA with post-hoc Dunnett's tests were performed to determine differences in peak stimulated dopamine release between genotypes.

Application of drugs. Drugs were administered either via intraperitoneal injection (20 mg/kg cocaine, 1 hour before recording) or via bath application to the *ex vivo* slice preparation. For experiments using bath application of cocaine, first, a stable baseline (aCSF) condition was established and cocaine were dissolved at desired concentrations within oxygenated aCSF. Next, I added increasing bath concentrations of cocaine to the aCSF (0, 1, 3, 10 uM). These concentrations were chosen in this order such that each brain slice underwent ascending concentrations of drug sequentially. The slice was incubated in each new cocaine concentration for ten minutes before recording. Relative dopamine release and uptake constants in each drug condition was compared to baseline.

RESULTS

VMAT2 genotype mediates vesicular uptake in multiple brain regions. We first performed radioactive monoamine uptake in isolated vesicles from the striatum and the frontal cortex. Compared to the wild type, vesicles isolated from VMAT2-LO animals transported less radioactive tracer than vesicles isolated from wild-type animals, while VMAT2-HI animals were better able to take up radioactive tracer in both the cortex ($F(2, 33) = 56.09$, $p < 0.05$, Dunnett's test LO<WT $p < 0.0001$ and HI>WT $p < 0.05$) and in the

striatum ($F(2,30) = 115.5$, $p<0.0001$, Dunnett's test LO<WT $p < 0.0001$ and HI>WT $p<0.001$) (Fig 3-1).

VMAT2 genotype mediates total brain metabolite content. We performed HPLC to test whether VMAT2 genotype resulted in changes in monoamine and monoamine metabolite content in the mouse brain. We found that VMAT2 gene dose had an effect on metabolite content in the dopamine group (main effect of genotype, $F(4,28) = 4.712$, $p < 0.01$; LO<WT $p < 0.001$ but WT vs HI was not significant) and norepinephrine group (main effect of genotype, $F(2,14)=4.801$, $p < 0.05$, no significant post-hoc differences) content between VMAT2-LO, -WT, and -HI mice (MANOVA for serotonin group was not significant $F(4,28)=1.3056$, $p=0.29$) (Fig 3-2).

VMAT2 genotype mediates stimulated dopamine release. We performed FSCV to measure stimulated dopamine release in the dorsal striatum. Compared to the wild type, VMAT2-LO tissue exhibited reduced peak stimulated dopamine release while VMAT2-HI exhibited enhanced peak stimulated dopamine release ($F(2,19) = 33.85$, $p < 0.0001$, Dunnett's test LO<WT $p < 0.001$ and HI>WT $p<0.01$) (Fig 3-3).

Pretreatment with cocaine attenuates wild type stimulated dopamine response but enhances VMAT2-HI stimulated dopamine response in the ventral striatum. Wild type and VMAT2-HI mice displayed similar levels of dopamine release in the nucleus accumbens following stimulation. However, in wild-type mice, pretreatment with 20 mg/kg cocaine one hour prior to recording resulted in reduced peak dopamine release (t-test comparing

maximum dopamine release between groups, $p < 0.01$) (Fig 3-4A). Alternately, pretreatment with cocaine resulted in an increased peak dopamine release in VMAT2-HI mice (t-test between maximum dopamine release, $p < 0.05$) (Fig 3-4B).

Overexpression of DAT results in hypersensitivity to the dopamine-releasing effects of cocaine. Wild-type mice release ~7 μM of dopamine in the dorsal striatum upon electrical stimulation, which is rapidly taken back up to the presynaptic terminal. Adding low concentrations of cocaine (1 or 3 μM) both increases peak dopamine release (~12 μM) and increasingly slows rate of reuptake. High bath concentrations of cocaine (10 μM) results in an extremely slow rate of reuptake, but no increase in peak release (Fig 3-5A). VMAT2-LO, DAT-OE, and VMAT2-LO/DAT-OE mice all had reduced stimulated peak release in the baseline condition ($F(3,20) = 9.821$, $p < 0.001$, VMAT2-LO < WT and DAT-OE/VMAT2-LO < WT, $p < 0.001$; DAT-OE < WT, $p < 0.05$; no differences among VMAT2-LO, DAT-OE, DAT-OE/VMAT2-LO) (Fig 3-5B). Furthermore, DAT-OE display an increased responsiveness to cocaine across multiple bath concentrations ($F(3,80) = 12.75$, $p < 0.0001$, DAT-OE > WT at 1 uM, $p < 0.001$, at 3 μM $p < 0.01$, at 10 μM, $p < 0.05$) (Fig 3-5C).

DISCUSSION

VMAT2 acts in all monoaminergic brain regions, and thus variation in its expression has wide-ranging effects on neurochemical transmission in multiple regions (Alter *et al*, 2016; Caudle *et al*, 2007; Lohr *et al*, 2014; Taylor *et al*, 2014). Here, we show

that VMAT2 genotype affects the ability of the vesicle to store monoamine neurotransmitter. The striatum primarily contains dopamine terminal projections from the midbrain, while noradrenergic and serotonergic neurons, projecting from the locus coerleus and raphe nucleus, respectively, are the primary drivers of vesicular monoamine uptake in the frontal cortex. Testing vesicular monoamine uptake in both the striatum and frontal cortex enabled us to characterize how VMAT2 genotype affects the vesicular storage capabilities of various monoamine systems. Our results indicate that VMAT2-LO mice show reduced monoaminergic vesicular storage capacity in vesicles derived from primarily serotonin and norepinephrine nerve terminals in addition to reduced vesicular storage capacity in vesicles derived from primarily dopaminergic nerve terminals.VMAT2-HI animals show increased capacity to store monoamines in these regions. Our laboratory has previously demonstrated that VMAT2-HI animals have increased vesicular storage capacity specifically within the dopaminergic vesicles of the dorsal striatum (Lohr *et al*, 2014) and there are multiple lines of evidence that VMAT2-deficient animals have reduced dopaminergic storage capacity (Caudle *et al*, 2007; Taylor *et al*, 2011). This is the first time showing that this pattern of decreased and increased capacity of VMAT2-LO and -HI mice, respectively, holds true in areas that are not primarily driven by dopamine release.

Furthermore, we show that VMAT2 gene dose results in brain-wide alterations in monoamine metabolite content. One disadvantage of this a whole-brain preparation is that it does not delineate monoamine metabolite difference in specific brain areas. However, we do not believe this to be a major setback: though monoamine metabolite content can vary across brain regions, monoamine content is highly positively correlated between regions (Fitoussi *et al*, 2013).

Lastly, we show that the VMAT2-LO mice have greatly reduced capacity to release dopamine upon stimulation, while VMAT2-HI animals have an increased peak stimulated dopamine response in the dorsal striatum. This complements our finding that vesicles isolated from VMAT2-LO tissue are less able to store neurotransmitter while VMAT2-HI animals are able to store more neurotransmitter. This difference in storage capacity results in altered neurotransmitter release upon forced ejection of the readily releasable pool of dopamine vesicles within the dorsal striatum.

VMAT2-HI animals show an altered dopamine release response to cocaine. Wild-type mice will show a decreased peak dopamine release following an intraperitoneal. injection of cocaine (Keller *et al*, 1992; Singer *et al*, 2017). This is thought to be due to compensatory changes in the release and reuptake machinery that rapidly responds to the increase in extrasynaptic dopamine following initial cocaine exposure. However, VMAT2-HI animals actually show an *increased* peak dopamine release following intraperitoneal injection of cocaine. Interestingly, the VMAT2-HI mice also show a rapid increase in the rate of dopamine re-uptake, which is not observed in wild-type mice that have been exposed to cocaine. One theory that could explain these neurochemical results: cocaine recruits VMAT2-carrying vesicles for rapid release, such that in a mouse model of VMAT2 overexpression, cocaine has an exacerbated effect, which is counterbalanced by an increase in plasmalemmenal DAT that increases the rate of dopamine reuptake in cocaine-exposed VMAT2-HI animals. Indeed, there is evidence that cocaine interacts with presynaptic vesicles to increase release in the striatum, and that DAT can be internalized or membrane-

bound in response to experiences (Brown *et al*, 2001; Heal *et al*, 2014; Maina *et al*, 2012; Maina and Mathews, 2010; Porter-Stransky *et al*, 2011).

Mice with increased DAT and decreased VMAT2 are neurochemically indistinguishable from VMAT2 deficient mice. Dopamine release in the dorsal striatum of these transgenic mice does not clarify the hyperactive behavior observed in the DAT-OE/VMAT2-LO mice. It confirms previous research from our laboratory showing that VMAT2-LO mice have a dramatically reduced stimulated dopamine release response. Indeed, the DAT-OE/VMAT2-LO dopaminergic response to stimulation is indistinguishable from the VMAT2-LO response. This may be because in this particular method, dopamine *release* is the dependent variable, not actual concentration of cytosolic dopamine. In the case of dopamine terminals with reduced VMAT2 protein, the capacity to release dopamine is so stunted that it's difficult to measure any changes all, due to a floor effect. There could be a few methods to circumvent this problem. The first method would be to do microdialysis in the dorsal striatum of these animals. Though that would give a measure of extracelluar (not cytosolic) dopamine, when combined with the fast-scan cyclic voltammetry data, it can give a better picture of what's happening at the dopamine terminal. Another approach would be using a combination of radioactive uptake in synaptosomal versus vesicular fractions of striatal dissections. By subtracting the vesicular uptake from the synaptosomal uptake, it would give a measurement of how much dopamine remained in the cytosol. In any case, it is not entirely unexpected that VMAT2, a packaging protein directly involved in neurotransmitter ejection from the presynaptic terminal, is a better predictor of stimulated dopamine release than a plasmalemmenal transporter protein.

There was a trend towards increased cocaine-induced dopamine release in the VMAT2-LO mice. It is possible that the VMAT2-LO mice show an altered neurochemical response to cocaine, but this study was underpowered to detect such a slight difference, if there is one. It is possible that it appears that VMAT2-LO animals have a trend towards increased cocaine responsiveness simply because the LO animals are already at such a floor of detectible dopamine.

Dopaminergic, serotonerigic, and noradrenergic neurons originate from a relatively few number of cell bodies, but have a highly dense axonal arbor and large terminal fields. These neurons therefore have millions of synaptic or 'en-passant' connections in each cubic millimeter of terminal field. Unlike strictly inhibitory or excitatory neurotransmitters, the monoamines exert their modulatory influence by volume transmission, which overlaps in many brain regions. Thus, changes in the protein machinery of the monoamine system, as we have created via transgenic insertion or removal of VMAT2 in our mouse models, has a dramatic effect on the functioning of these influential neurons.

FIGURES

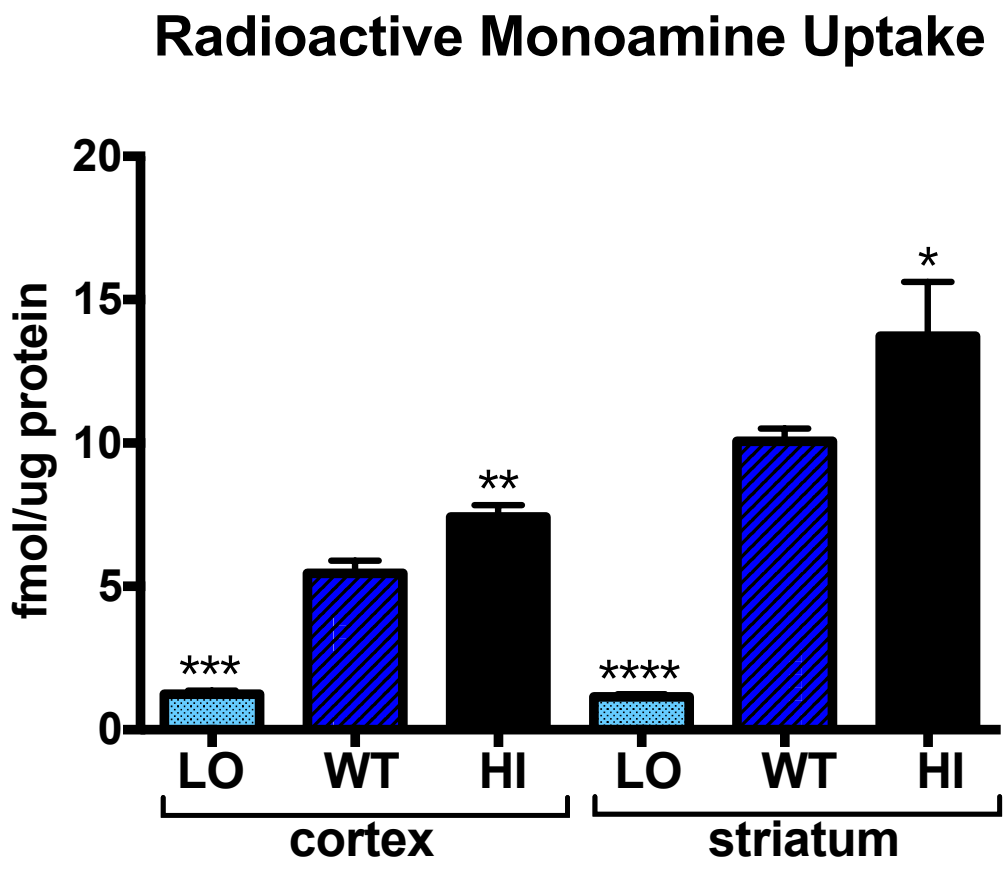

Figure 3-1. VMAT2 genotype mediates monoamine uptake in the cortex and striatum. VMAT2-LO mice show a reduced capacity to take up radioactive monoamine in vesicles isolated from both the frontal cortex and striatum, while VMAT2-HI mice show an increased capacity to take up radioactive monoamine. n = 3-5 for each group * $p < 0.05$; ** $p < 0.01$, *** $p < 0.001$, **** $p < 0.0001$.

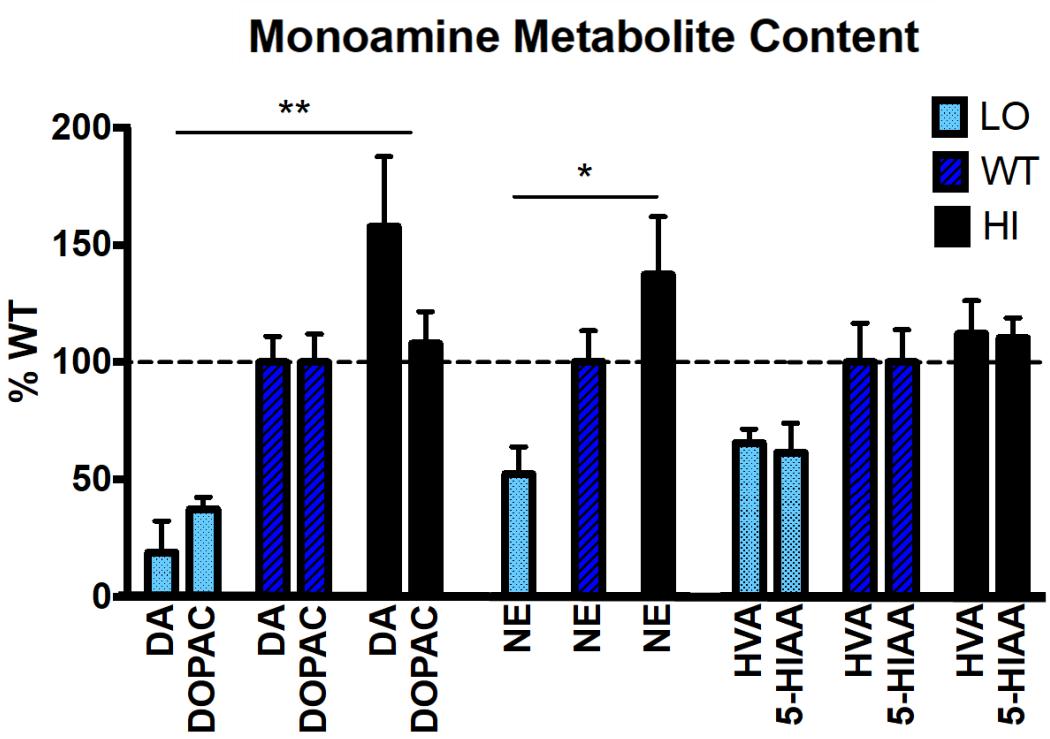

Figure 3-2. VMAT2 genotype mediates monoamine content. Monoamine and monoamine metabolite content varies across VMAT2 genotype. HPLC analysis from half brain homogenate shows a reliable trend towards increased monoamine or monoamine content as gene dose of VMAT2 increases. n = 4 – 8 for each group, * $p < 0.05$; ** $p < 0.01$.

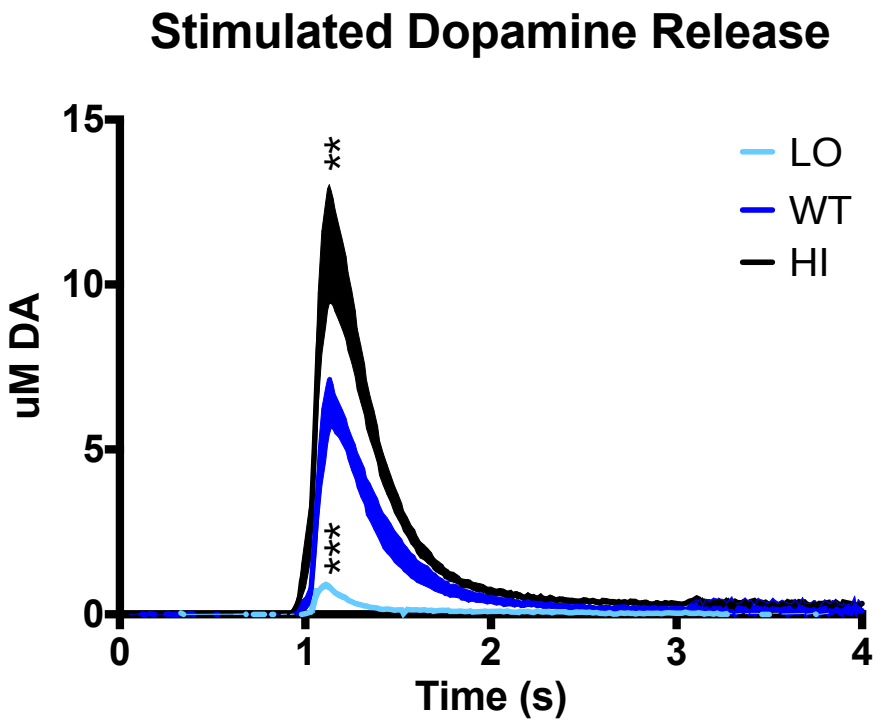

Figure 3-3. VMAT2 genotype mediates stimulated dopamine release in the dorsal striatum. *Ex vivo* slice preparation of VMAT2-HI striata exhibited enhanced stimulated dopamine release while VMAT2-LO striata displayed a reduction in stimulated dopamine release. Trace shows the standard error of the mean of an average dopamine release time course for that genotype. n = 6 – 10. ** $p < 0.01$, *** $p < 0.001$.

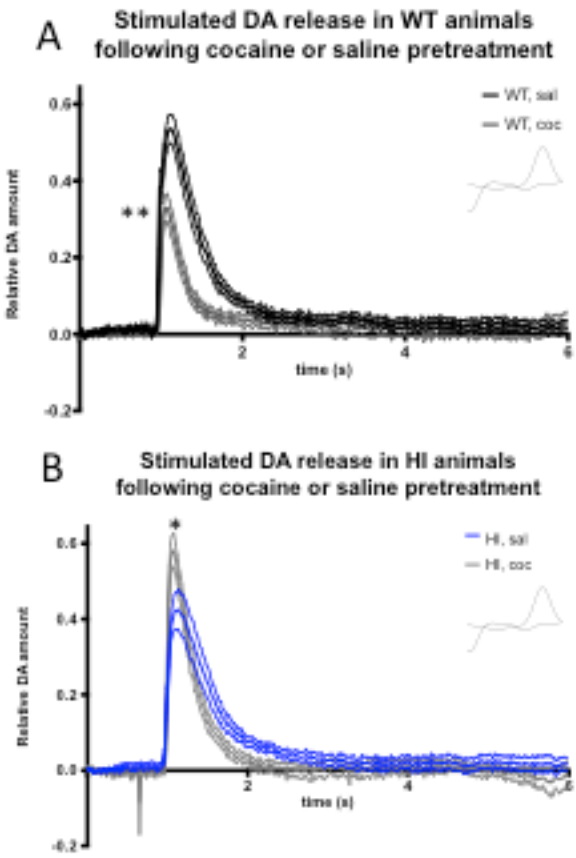

Figure 3-4. Response of stimulated dopamine release after a saline or cocaine pretreatment. A. In WT mice, injecting cocaine (20 mg/kg, I.P) 1 hour before recording resulted in a hypodopaminergic state compared to mice that received a saline pretreatment. B. However, in VMAT2-HI mice, cocaine pretreatment resulted in a heightening of peak DA release and rate of DA uptake. Trace shows the average dopamine release time course for that condition (thick line) and associated standard error of the mean (thin lines). n = 6 – 16 per group * $p < 0.05$, ** $p < 0.01$.

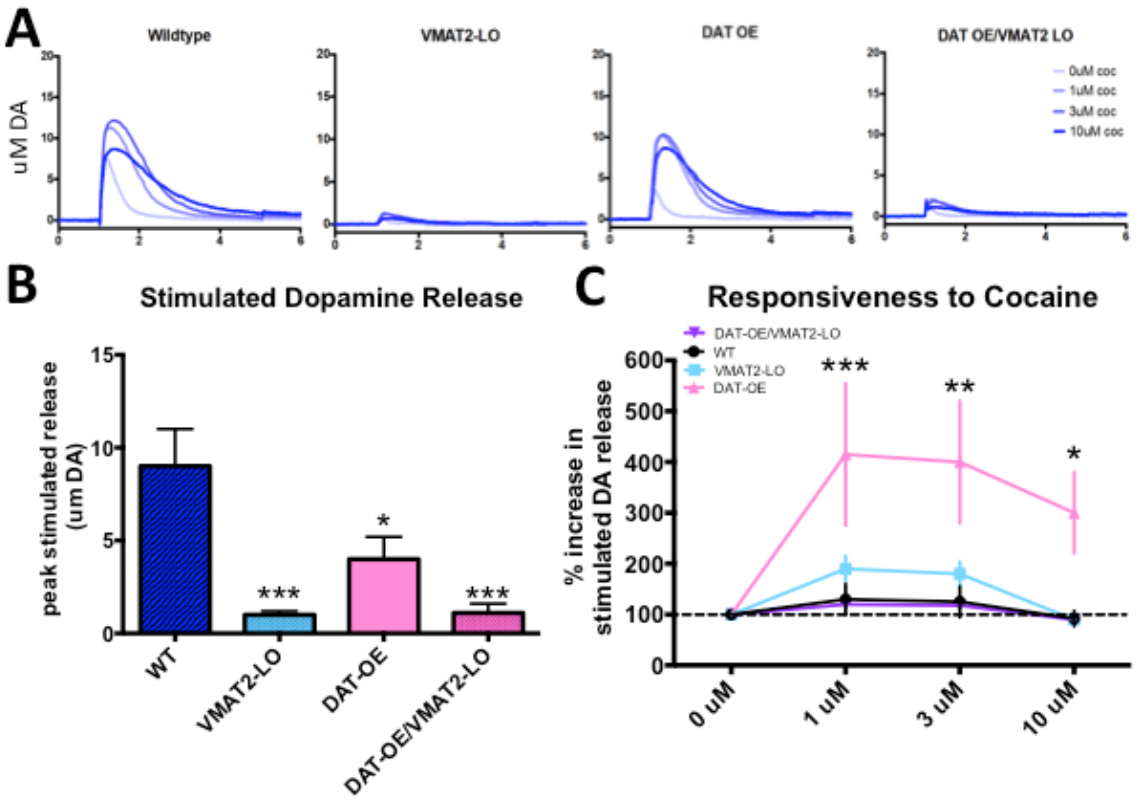

Figure 3-5. The effect of DAT overexpression on stimulated dopamine release and cocaine responsivity. A. Average time course of stimulated dopamine release among wild type, VMAT2-LO, DAT-OE, and DAT-OE/VMAT2-LO transgenic animals under ascending cocaine bath applications. B. In the absence of cocaine, wild-type mice release ~9 uM of dopamine following stimulation in the dorsal striatum. By contrast, VMAT2-LO, DAT-OE, and DAT-OE/VMAT2-LO animals show reduced stimulated dopamine release. C. DAT-OE have increased responsiveness to the dopamine-releasing effects of cocaine. Note that VMAT2-HI animals were not included in this study, and therefore VMAT2 dopamine responses are not depicted in these graphs. * $p < 0.05$, ** $p < 0.01$, *** $p < 0.001$

IV. Chapter 4. VMAT2 gene dose mediates behavioral response to fear

A portion of this chapter was submitted as part of a manuscript:

Rachel A. Cliburn, James P. Burkett, Jason P. Schroeder, David Weinshenker, Tanja Jovanovic, Gary W. Miller. (2018) Submitted to Neuropsychopharmacology.

ABSTRACT

Only a subset of people who are exposed to a traumatic event go on to develop post-traumatic stress disorder (PTSD). Genetic factors mediate part of the risk for developing PTSD following exposure to a traumatic event. Variation in *SLC18A2*, the gene that encodes vesicular monoamine transporter 2 (VMAT2) can confer risk for the development of PTSD in humans. Here, we use transgenic mice that represent a continuum of *Slc18a2* gene-dose to test whether VMAT2 expression level causally alters expression of conditioned fear behavior in mice, a model of dysregulated fear responses that have been observed in PTSD. Mice with dramatically reduced expression of VMAT2 (VMAT2-LO) showed increased cued and contextual fear expression, altered fear extinction, inability to discriminate threat from safety cues, and altered startle response compared to wild-type mice. By contrast, mice overexpressing VMAT2 (VMAT2-HI) were indistinguishable from controls in these assays. Together, these data corroborate and enrich the human genetic data showing that VMAT2 deficiency impacts monoamine function and fear behavior.

INTRODUCTION

Post-traumatic stress disorder (PTSD) is characterized by aberrant fear behaviors including re-experiencing, avoidance, and negative changes in cognitions and mood following a traumatic event (American Psychiatric Association, 2013). Although exposure to severe trauma is relatively common, only a small proportion of those exposed to trauma will go on to develop PTSD (Breslau *et al*, 1999; Keane *et al*, 2009; Kessler *et al*, 1995; Shiromani *et al*, 2009), a risk mediated by genetic and social factors (Binder *et al*, 2008; Charney, 2004; Li *et al*, 2016; Ozer *et al*, 2003). One avenue of research is to examine the genetic differences between trauma-exposed individuals who develop PTSD and those that do not (Norrholm and Ressler, 2009). As is common in complex behavioral disorders, no single gene directly causes all diagnoses. In a recent candidate gene analysis of more than 3,000 single nucleotide polymorphisms across more than 300 genes, the *SLC18A2* locus, which encodes the vesicular monoamine transporter 2 (VMAT2), was identified as a risk haplotype for PTSD diagnosis in a cohort of 2,538 European women and replicated in an independent cohort of 748 male and female African Americans (Solovieff *et al*, 2014).

VMAT2 transports monoamine neurotransmitters (dopamine, serotonin, norepinephrine, epinephrine, and histamine) into presynaptic neuronal vesicles in preparation for release into the synaptic space (Eiden and Weihe, 2011; Peter *et al*, 1995a). Animal studies show that innervations from multiple monoaminergic systems converge on the amygdala (Goldstein *et al*, 1996), a key structure for the expression of fear and anxiety responses in both rodents and humans (Davis, 1992; Phelps *et al*, 2001). Much research has focused on the role of specific monoamines within fear expression circuits (Bauer,

2015; Bocchio *et al*, 2016). However, neurotransmitter-specific manipulations do not represent the state of globally altered monoaminergic transmission suggested by the human genetic literature.

This large human genetic study points to VMAT2 as a mechanism in the etiology or expression of PTSD risk (Solovieff *et al*, 2014), but experimental data is needed to establish directionality and causality in the relationship between VMAT2 and PTSD. For these reasons, the causal link between VMAT2 expression and PTSD phenotype merits further analysis. Behavioral studies in VMAT2 knock-out mice are impossible, as completely eliminating VMAT2 is neonatal lethal (Wang *et al*, 1997). To circumvent this issue, our laboratory has developed and characterized strains of transgenic mice that provide a continuum of VMAT2 gene dose (Chapter 2; Cliburn *et al*, 2016). Specifically, these mice express differing amounts of VMAT2: 95% reduced (VMAT2-LO) (Caudle *et al*, 2007; Taylor *et al*, 2009), normal (VMAT2-WT), or 200% elevated levels (VMAT2-HI) (Lohr *et al*, 2014, 2016). Our laboratory and others have previously demonstrated that VMAT2-LO mice show progressive degeneration of the midbrain nuclei and locus coerelus, resulting in decreased extracellular dopamine and norepinephrine concentration compared to wild type mice (Taylor *et al*, 2009, 2011; Wang *et al*, 1997). VMAT2-LO mice also display decreased serotonergic signaling (Alter *et al*, 2016). Alternately, VMAT2-HI mice show an increased capacity to store and release monoamines (Chapter 3; Branco *et al*, submitted; Lohr *et al*, 2015). Thus, VMAT2 is a critical modulator of monoaminergic neurotransmission throughout the brain, and our continuum of VMAT2 transgenic mice reflect reduced or increased capacity to transmit monoamines.

We have bred VMAT2-HI and -LO lines to be on identical genetic backgrounds (C57BL/6J). In our studies of these mice, the wild-type littermates of VMAT2-LO mice and the wild-type littermates of VMAT2-HI mice show no difference in neurochemical or behavioral outcomes. This indicates that VMAT2 gene dose is driving the observed differences in behavior among VMAT2-LO, -WT, and -HI mice. VMAT2-LO mice show sleep disturbances (Taylor *et al*, 2009) and depressive- and anxiety-like phenotypes whereas VMAT2-HI mice show improved outcomes in these assays (Lohr *et al*, 2015; Taylor *et al*, 2009). This continuum of VMAT2 expression is an ideal tool for testing whether the functional dysregulation of VMAT2 is a causal factor in producing an aberrant fear response.

We tested how VMAT2 gene dose affects PTSD-like fear phenotypes, which relies on a number of behavioral assays that measure different aspects of the human condition. Because the architecture of fear biology is highly conserved in mammals, mice serve as a useful tool for studying fear behavior in humans (Flandreau and Toth, 2017). Fear conditioning paradigms capitalize on this shared circuitry and can be used in rodents and humans to model fear-related phenotypes (Jovanovic *et al*, 2005; Jovanovic and Ressler, 2010), including fear acquisition (Norrholm *et al*, 2015a; Orr *et al*, 2000), extinction (Guthrie and Bryant, 2006), startle responses (Grillon *et al*, 1996; Pole, 2007), and fear generalization (Kaczkurkin *et al*, 2017; Levy-Gigi *et al*, 2015; Morey *et al*, 2015a; Wicking *et al*, 2016). We also performed a test to measure the behavioral response to stress by administering exogenous murine stress hormone corticosterone at a level that mimics that of chronic behavioral stress (Gourley *et al*, 2008), then testing for freezing behavior following fear conditioning. We hypothesized that decreased presynaptic monoaminergic

function leads to increased PTSD-like outcomes, while increased presynaptic monoaminergic function results in decreased trauma resilience.

Materials & Methods

Mice. VMAT2-LO mice were generated by backcrossing the original mixed-background VMAT2-deficient strain (Caudle *et al*, 2008; Taylor *et al*, 2014) to Charles River C57BL/6 for four generations using a marker-assisted selection (i.e. "speed congenic") approach (Lohr *et al*, 2016). VMAT2-HI mice were generated using a bacterial artificial chromosome-mediated transgene to insert three additional copies of the murine *Slc18a2* (VMAT2) gene, including its endogenous promotor and regulatory elements (Lohr *et al*, 2014). These founders were then backcrossed to a Charles River C57BL/6 background. 6-11 month old male and female mice were used for all experiments. Mice were singly-housed and received food and water *ad libitum* on a 12:12 light cycle. There were no significant differences between wild-type mice from the VMAT2-HI and VMAT2-LO colony, so all graphs show collapsed data from VMAT2-HI and -LO wild-type littermate controls.

All procedures were conducted in accordance with the National Institutes of Health Guide for Care and Use of Laboratory Animals and were approved by the Institutional Animal Care and Use Committee at Emory University.

Fear acquisition, contextual fear, cued fear, and fear extinction. On day 1, mice were placed in the fear conditioning apparatus (7" W, 7" D, 12" H, Coulbourn Instruments,

Whitehall, PA) composed of plexiglass with a metal shock grid floor and were allowed to explore the enclosure for 3 min. Following this habituation period, 3 presentations of a conditioned stimulus (CS) (tone, 20 s, 10 kHz, 85 dB, 1 min inter-trial interval) co-terminated with 3 presentations of an unconditioned stimulus (US) (foot shock, 2 s, 0.5 mA). Shock was delivered via a Precision Animal Shocker (Coulbourn Instruments) connected to each fear-conditioning chamber. One min following the last CS-US presentation, animals were returned to their home cage. On day 2 mice were presented with a context test, during which they were placed in the same conditioning chamber used on day 1 for 7 min and the amount of freezing was recorded via FreezeFrame 3 (Coulbourn Instruments, Holliston, MA). No shocks were administered during the context test. On day 3, a tone test was presented, during which mice were placed in a novel compartment with a texturally distinct metal floor. Initially, animals were allowed to explore the novel context for 2 min. Following this habituation period, the CS was presented for 6 continuous min without shocks, and the amount of freezing behavior was recorded. On day 4 the tone test was repeated, and freezing during the continuous tone over time was taken as a measure of extinction. Freezing threshold was determined individually for each mouse using FreezeFrame 3 (Coulbourn Instruments, Holliston, MA). For each assay, we performed a two-way ANOVA with genotype (LO, WT, HI) as a between-subjects factor and time as a repeated measure. Time was binned different for each test, as each test at different protocols. For the fear acquisition test, time was binned into seven groups: seconds 0-180, 180-200, 200-260, 260-280, 280-340, 340-360, 360-420. For the contextual and cued fear test, time was binned into 8 groups: seconds 0-60, 60-120, 120-180, 180-240, 240-300, 300-360, 360-420, and 420-460. For the habituation test, time was binned into each minute

of continuous tone exposure (six minutes total). Post-hoc Dunnett's tests were used to analyze differences between genotype (GraphPad Prism, San Diego, CA).

Acoustic startle and prepulse inhibition. Startle assays were performed as described in Flandreau et al. (2015). Mice underwent multiple sessions in order to assess startle magnitude and prepulse inhibition. In one block of testing, there were five presentations each of 80, 90, 100, 110, and 120 dB pulses, presented in randomized order. In a separate block of testing for prepulse effects, there were five each of 67, 70, 74, or 80 dB prepulses to a 120 dB tone after a 100 ms lag. Because mice that are physically heavier produce a more robust startle response and VMAT2-LO mice tend to be physically smaller than VMAT2-WT and -HI mice, each startle response was normalized to that mouse's average startle response to a very loud tone (120 dB). For each assay, a separate two-way ANOVA with genotype (LO, WT, HI) as between-subjects factor and tone intensity (80, 90, 100, 110 dB for startle test, 67, 70, 74, 80 dB for prepulse test) as a repeated measure was performed. Post-hoc Dunnett's tests were used to analyze differences between genotypes (GraphPad Prism, San Diego, CA).

Fear discrimination. VMAT2-LO and -WT mice were trained using the protocol described in McHugh et al. (2015). VMAT2-LO and -WT were selected for this study based on the previous fear and startle data that shows that VMAT2-LO mice exhibit altered behavior compared to wild-type mice, but VMAT2-HI mice are behaviorally indistinguishable from wild-type mice in these assays. Briefly, on the first day, the mice habituated to the fear chambers and were exposed to the auditory tones. For days 2-4, mice

were trained to associate one tone (CS+) with a foot shock while another tone (CS-) was never associated with a foot shock. Each auditory tone (one of three tones: tone 1, 10 kHz, 85 dB, 30 s; tone 2, 7 kHz, 85 dB, 30 s; tone 3, 2.9 kHz, 85 dB, 30 s) was randomly assigned to be CS+ or CS- for each mouse. On the fifth and final day of this protocol, mice were moved to a new fear testing apparatus in order to reduce contextual fear, and were exposed to multiple presentations of the auditory cues. Each mouse's freezing behavior was recorded during habituation, training days, and the final testing day.. Freezing threshold was determined individually for each mouse using FreezeFrame 3 (Coulbourn Instruments, Holliston, MA). Learning in response to each tone was calculated by subtracting percentage of time spent freezing to that tone during the pre-test from percentage of time spent freezing to that tone following training. Each genotype was evaluated for whether there was a difference in freezing response between the CS- and CS+ using paired t-tests. Freezing response to all tone types was compared between genotypes via student's t test. Bonferonni correction was used to account for multiple comparisons. Similarly, response to tones *before* they were associated with any fear or safety signal was measured. The WT and LO response to the 'to-be CS+ or CS-' tones were compared via student's t-test.

Response to corticosterone administration. This protocol was taken from Gourley *et al*, 2013. Corticosterone (CORT, 4-pregnen-11β-21-DIOL-3-20-DIONE-21-hemisuccinate; Steraloids, Newport, RI) was dissolved in water and administered for 20 days (25 μg/ml free-base, translating to ~4.97 mg/kg/day). Control animals received regular drinking water during this time. Following the 20 day CORT exposure, mice underwent a ten day washout period in which they received regular drinking water. At this

time, mice underwent the fear acquisition, contextual fear, cued fear, and fear extinction protocol as described above. A two-way ANOVA with genotype (LO, WT, HI) and CORT treatment status (CORT or H2O) as factors. Post-hoc Dunnett's tests were used to analyze differences between genotypes (GraphPad Prism, San Diego, CA). It should be noted that the there were fewer mice in both the LO-CORT and the LO-H2O group (n's of 2-3) compared to all other groups (n's of 5-8). In order to test whether this is a sufficiently powered experiment, we performed a post hoc power analysis using G*Power software (Dusseldorf, Germany). We found that this experiment was severely underpowered (power = 0.22).

RESULTS

VMAT2-LO mice display increased fear acquisition, increased cued and contextual fear responses, and altered extinction. VMAT2-LO exhibit increased freezing in a variety of contexts. When mice are first put into the fear-conditioning chamber, before a tone is played, VMAT2-LO mice display a small but significant elevated freezing rate ($F(2,78) = 3.528$, $p < 0.05$; Dunnett's test LO>WT, $p<0.01$). VMAT2-LO mice displayed increased fear acquisition compared to wild-type controls, as shown by increased freezing during CS-US pairings on the training day (main effect of genotype $F(2,107)=16.16$, $p < 0.0001$; Dunnett's test LO<WT, $p < 0.0001$) (Fig 4-1A). Furthermore, compared to wild-type controls, VMAT2-LO froze more in response to a context previously paired with foot shocks (Fig 4-1B, main effect of genotype $F(2, 632) = 17.87$, $p < 0.0001$; Dunnett's test LO<WT, $p < 0.0001$) as well as to the auditory tone previously associated with a fearful

stimulus (Fig 4-1C, main effect of genotype $F(2,576) = 19.62$, $p < 0.0001$; Dunnett's test LO<WT, $p < 0.0001$). Lastly, VMAT2-LO mice showed a slowed rate of fear habituation (genotype x time interaction effect, $F(10,35) = 1.997$, $p < 0.05$; Dunnett's test LO<WT at minute 2, $p < 0.01$) (Fig 4-1D). By contrast, performance of VMAT2-HI mice was indistinguishable from wild type in all assays

VMAT2-LO mice displayed altered startle reactivity. We tested two different aspects of startle reactivity. The first test measured the mouse startle response to tones of varying loudness. VMAT2-LO mice startled more in response to these auditory tones overall (main effect of genotype $F(2, 252) = 5.888$, $p < 0.01$) (Fig 4-2A). In a separate assay, we tested for the ability of an auditory tone (called a 'prepulse') to inhibit a startle response to a very loud tone (120 dB) that immediately follows the prepulse. Typically, the louder the prepulse tone, the greater the inhibition to the following 120 dB tone that immediately follows the prepulse. While the 70 dB prepulse had no effect on startle in wild-type and VMAT2-HI mice, it potentiated startle in VMAT2-LO mice. Prepulse inhibition at the higher decibels prepulses were equivalent in the three genotypes (genotype x intensity interaction $F(6,756) = 2.173$, $p < 0.05$; Dunnett's test LO<WT at 70 dB, $p < 0.001$) (Fig 4-2B).

VMAT2-LO showed inability to discriminate threat and safety cues. As expected, VMAT2-WT mice responded with higher freezing to a danger cue and lower freezing to a safety cue, indicating that they can distinguish between a danger signal and a safety signal (WT CS+ ≠ WT CS-, $t(22) = 3.989$, $p < 0.01$).By contrast, VMAT2-LO did not show a

difference in freezing response to a fear and safety cue (for LO CS+ compared to LO CS-, $t(21)=1.797$, $p = 0.2601$). Furthermore, following CS-US training, VMAT2-LO mice froze more in response to both cues overall ($t(88) = 3.840$, $p < 0.001$) (Fig 4-3A). This VMAT2 generalization effect was not due to an increased tendency to freeze to all stimuli, as VMAT2-LO mice showed less freezing to novel tone presentations ($t(90) = 3.208$, $p < 0.01$) (Fig 4-3B).

Corticosterone administration increased freezing response following fear training. Consistent with data from Fig 4-1, VMAT2 genotype mediated freezing response (main effect of genotype, $F(2,29) = 3.582$, $p < 0.05$). Furthermore, the group of mice that received corticosterone froze more than the mice that received drinking water (main effect of treatment, $F(1,29) = 5.179$, $p < 0.05$). However, there was no interaction between genotype and corticosterone treatment ($F(2,29) = 0.1971$, $p = 0.8222$) (Fig 4-4). However, it must be taken into account that post hoc power analysis determined that we were underpowered to determine whether corticosterone has a differential effect on LO, WT, and HI mouse freezing behavior.

DISCUSSION

Here we show that reduced expression of VMAT2 produces an altered fear phenotype in mice. In combination with human genetic data, our work implicates VMAT2 as a potential target for the future treatment or prevention of fear disorders in vulnerable populations.

VMAT2 acts in all monoaminergic brain regions, and thus variation in its expression has wide-ranging effects on neurochemical transmission in multiple regions (Alter *et al*, 2016; Caudle *et al*, 2007; Lohr *et al*, 2014; Taylor *et al*, 2014). It is difficult to attribute any one of the behavioral phenotypes described in this paper to a particular neurotransmitter system or brain region. Indeed, genetic variation in multiple monoaminergic systems has been implicated in risk for PTSD (Naß and Efferth, 2017). All three major central monoamine systems—dopamine, norepinephrine, and serotonin—interact with each other, and individually to contribute to PTSD outcomes. The relationship between these neurotransmitters and the expression and maintenance of fear symptomology is complex. Though norepinephrine is crucial to the expression of startle and other panic-related behaviors (Kao *et al*, 2015; O'Donnell *et al*, 2004), increasing extracellular norepinephrine actually has an anxiolytic effect (Estrada *et al*, 2016; Montoya *et al*, 2016) and, along with dopamine, plays a role in the synaptic plasticity necessary for memory reconsolidation following trauma (Fitzgerald *et al*, 2015; Lee *et al*, 2017; Lee and Kim, 2016; Otis *et al*, 2015). Serotoninergic transmission in the amygdala facilitates the expression of fear (Johnson *et al*, 2015), yet inhibiting the reuptake of serotonin is a mainstay of pharmacological treatment for PTSD (Kelmendi *et al*, 2016) and this synaptic serotonin is necessary for pharmacologically-mediated acceleration of fear extinction learning (Young *et al*, 2017). VMAT2 itself can be responsive to stimuli, as a single prolonged stress in a rodent model can reduce VMAT2 protein level in amygdala and hippocampus (Lin *et al*, 2016).

The relative contributions of each monoamine neurotransmitter systems could be teased out using optogenetics or through the use of cre/lox mice to selectively inhibit or

express VMAT2. While we think that there is value in the use of genetic knockdown and genetic overexpression to investigate the causal relationship of VMAT2 protein amount and fear expression, further investigation of specific circuits via optogenetics could provide more specific treatments or better tease out the role of specific circuits in these behaviors. The Giros lab has bred VMAT2(lox/lox) mice with DBHcre, SERTcre, and DATcre mice to create conditional VMAT2 knockout in norepinephrine, serotonin, or dopamine circuits, respectively. In studying the heterozygotes of these knockout lines, the Giros lab reports no difference in assays of motor or affective assays (Isingrini *et al*, 2016). These conditional knock-out mice would be ideal tools for initial testing which neurotransmitter system is critical for the VMAT2-depletion effects on fear behavior.

The VMAT2-LO mice show a variety of fear-related phenotypes, including increased fear acquisition, increased contextual fear, increased cued fear, altered rate of fear extinction, altered startle reactivity, and inability to discriminate between threat and safety cues. Dysregulated fear responses have been observed in patients with PTSD, including poor discrimination between threat and safety cues, impaired inhibition of fear to safety signals, deficits in fear extinction, and heightened fear expression during extinction (Careaga *et al*, 2016; Jovanovic *et al*, 2010, 2012; Milad *et al*, 2009; Morey *et al*, 2015b; Norrholm *et al*, 2011, 2015b). These fear phenotypes are likely behavioral indices of amygdala hyperactivity, which has been frequently reported in PTSD neuroimaging studies (Rauch *et al*, 2000; Shin *et al*, 2006; Stevens *et al*, 2013, 2017) Though VMAT2-LO show a non-significant trend towards decreased movement throughout these tests, the results of the assay do not change after correcting for overall movement. Though VMAT2-LO mice show a slight elevation of baseline levels of

freezing, this observation does not account for the increase in freezing observed during fear-cued assays. These behavioral fear phenotypes, in conjunction with our previously published literature showing that VMAT2-LO mice show altered sleep patterns, and anxiety- and depressive-like phenotypes (Taylor *et al*, 2011), indicate that the VMAT2-LO mice model a variety of human PTSD symptomology.

In a post-mortem analysis of human brains, VMAT2 protein abundance was reduced in PTSD patients relative to controls (Bharadwaj *et al,* 2016). The results of this study build off this human literature that suggests that VMAT2 plays a role in PTSD risk. We show that reduction of VMAT2 leads to aberrant fear phenotypes. We also show that overexpression of VMAT2, though it results in biological changes in monoamine metabolite levels, does not alter fear behavior as measured in these assays. Indeed, in our laboratory, we have yet to observe any deleterious effects of increasing VMAT2 function (Lohr *et al,* 2014). We have demonstrated that VMAT2-HI animals do indeed show functional differences in ability to transport and release monoamine neurotransmitters (Chapter 3). It is possible that we have reached a 'ceiling' effect using these assay, such that we do not observe differences between wild-type and VMAT2-HI animals. It is possible that increasing the intensity of the unconditioned stimulus or exposing the mice to early life stress would result in some difference among wild-type and VMAT2-HI mice. Certainly, we are interested in the VMAT2-HI mice as a genetic model of 'resilience,' and further experimentation is needed to test whether increasing VMAT2 is a promising avenue of behavioral resilience.

We anticipate that the results described here may guide future research in a number of ways. First: individuals with constitutively lower VMAT2 function may be candidates

for prevention strategies or special monitoring if they will be exposed to a potentially traumatic environment (i.e. active duty service members deploying to a war zone). Second: PTSD is a heterogeneous disorder with multiple subtypes (Norrholm and Jovanovic, 2010). It is possible that one or more of these PTSD subtypes corresponds to 'VMAT2-LO' genetic risk. This is a testable hypothesis, given that VMAT2 function is readily assessed in humans using PET ligands (Okamura *et al*, 2010). Lastly, these results point to VMAT2 as a potential therapeutic target for the treatment of fear disorders. The canonical pharmacological tools for PSTD and other fear disorders are selective serotonin reuptake inhibitors, which are not universally effective (Kelmendi *et al*, 2016). Augmenting vesicular function would lead to an action potential dependent increase in synaptic transmission, an approach that could reduce unwanted side effects common in drugs that affect synaptic machinery or increase extracellular monoamine levels in an unregulated way. Future drug discovery and development aimed at agonists or positive allosteric modulators of VMAT2 may produce candidate pharmacological therapeutics for the treatment of PTSD.

FIGURES

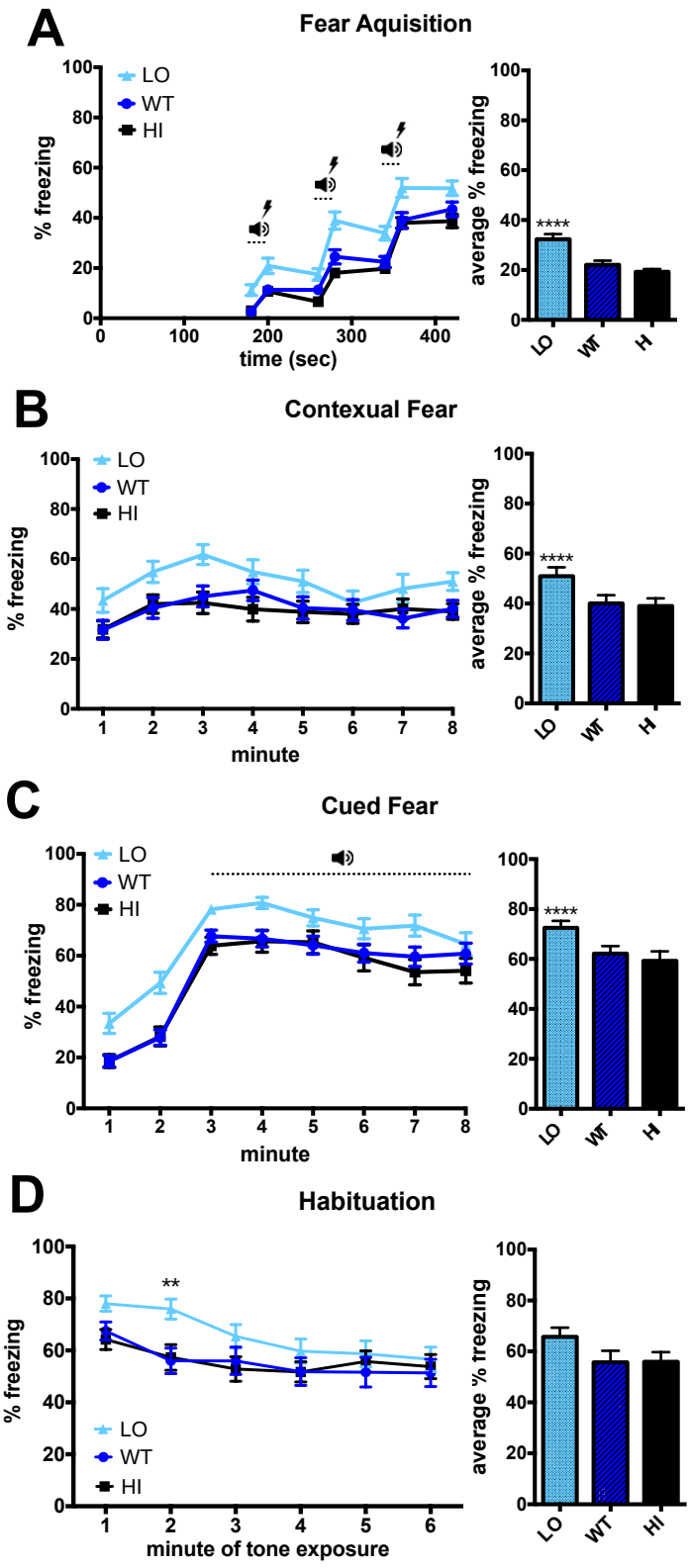
A
Fear Aquisition
LO
WT
HI
% freezing
time (sec)
average % freezing
****
B
Contexual Fear
minute
C
Cued Fear
D
Habituation
**
minute of tone exposure

Figure 4-1. VMAT2-LO mice display increased fear behavior. A. VMAT2-LO mice show increased fear learning during CS-US pairings. B. VMAT2-LO mice show increased freezing in response to context previously associated with foot shocks C. VMAT2-LO mice show increased freezing response to an auditory tone previously associated with a foot shock D. VMAT2-LO mice show an altered rate of fear habituation. n = 22 – 40 animals per group, ** $p < 0.01$, **** $p < 0.0001$.

A

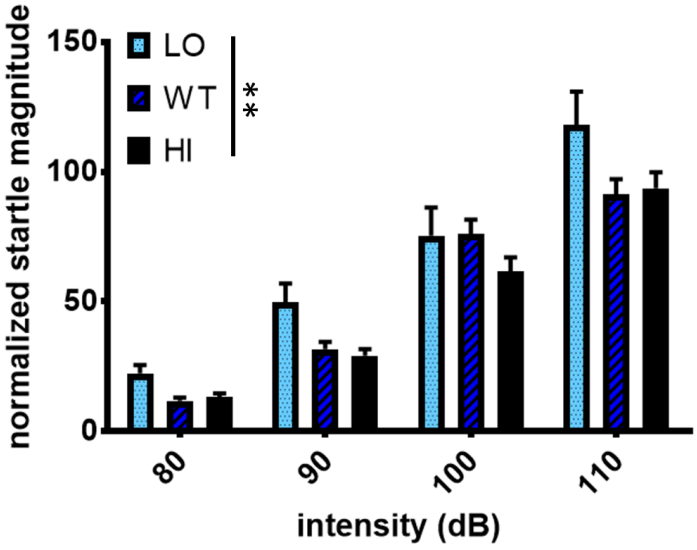
normalized startle magnitude
150
100
50
0
LO
WT
HI
**
80
90
100
110
intensity (dB)

B

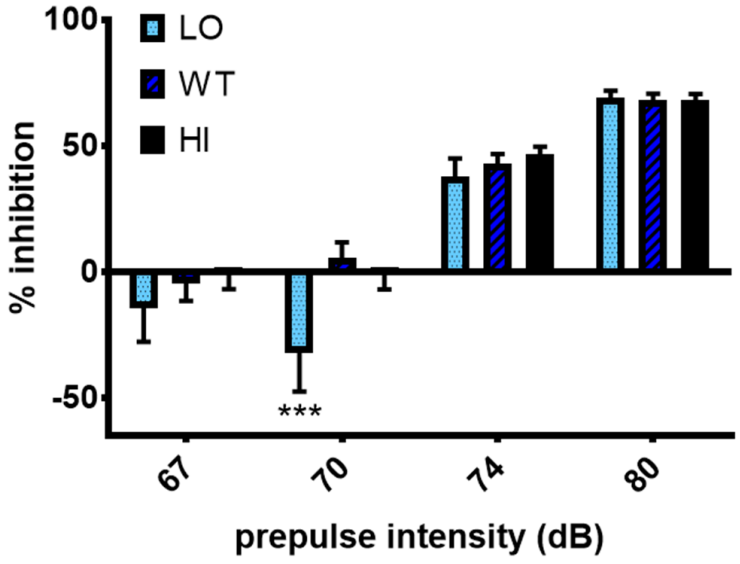
% inhibition
100
50
0
-50
LO
WT
HI
***
67
70
74
80
prepulse intensity (dB)

Figure 4-2. VMAT2-LO mice show altered startle responses. We tested VMAT2 transgenic animals for magnitude of startle in response to a number of acoustic cues. A. VMAT2-LO mice displayed increased corrected acoustic startle magnitude in response to a range of acoustic stimulus intensities. B. VMAT2-LO mice were less able to inhibit a startle response with lower-intensity prepulse tones. n = 11 - 20 animals per group, ** $p < 0.01$; *** $p < 0.001$.

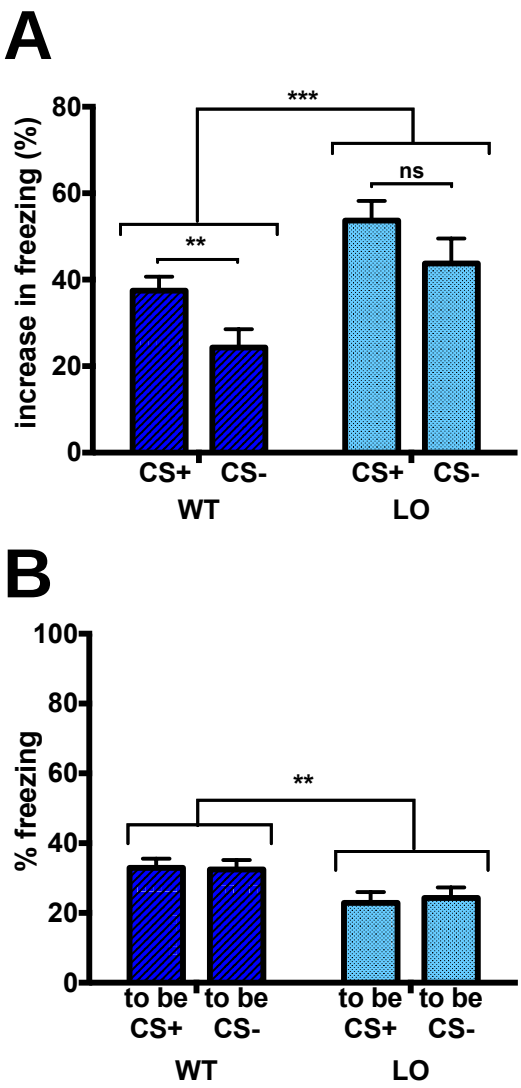

Figure 4-3. A. VMAT2-LO mice show increased fear generalization and increased fear response to multiple cues. A. Following training to associate one auditory cue with a foot shock (CS+) and another auditory cue with safety (CS-), VMAT2-LO mice have an increased freezing response across both tone types and fail to discriminate between a tone that reliably predicts a foot shock (CS+) compared to a tone that does not predict foot shock (CS-). B. This increase in freezing is not due to an increased tendency for VMAT2-LO to freeze to novel tones. VMAT2-LO mice freeze less in response to novel tones compared to VMAT2-WT. n = 22 – 25 mice per group, * $p<0.05$, ** $p<0.01$, ns = not significant.

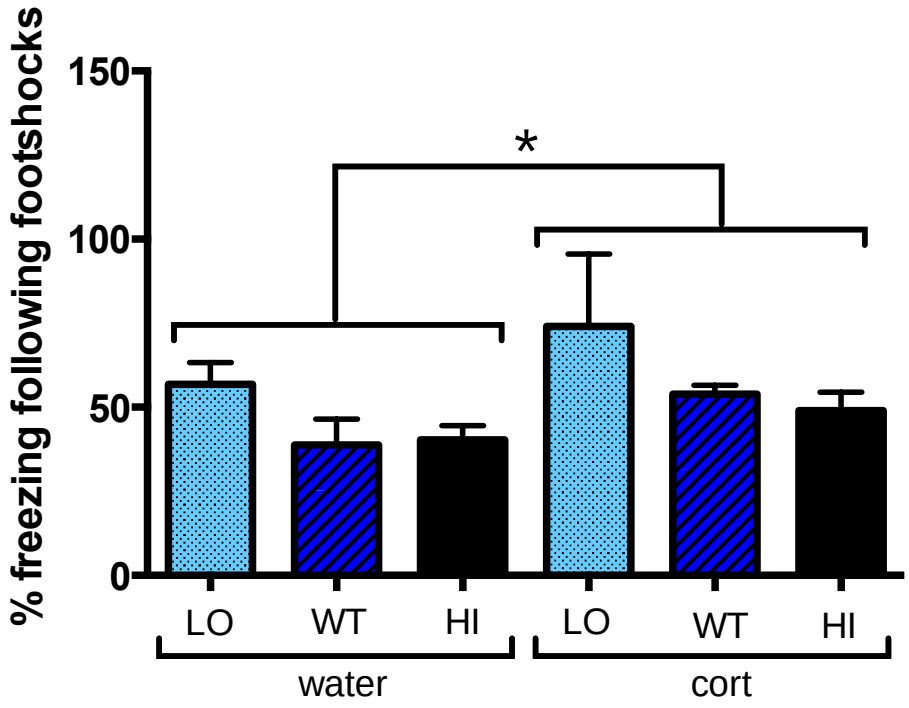

Figure 4-4. A. Pretreatment with corticosterone in mouse drinking water increases freezing response following fear training. VMAT2-LO, -WT, and -HI animals were individually housed and given either regular drinking water or water with the murine stress hormone corticosterone ("cort") dissolved in it for 20 days. Following a washout period, these mice underwent training to associate an auditory stimulus to a foot shock. VMAT2-LO mice showed increased freezing compared to WT mice, and administration of corticosterone increased freezing response, but there was no significant interaction. n = 2 – 8 per group, * $p<0.05$.

V. Chapter 5. The effect of VMAT2 gene dose on sensory, affective, social and appetitive assays.

ABSTRACT

Vesicular monoamine transporter 2 (VMAT2) is a critical modulator of dopamine, serotonin, and norepinephrine in the brain. Variation in VMAT2 has been associated with a variety of psychiatric disorders, including posttraumatic stress disorder, autism, bipolar disorder, and substance use disorder. To test whether VMAT2 protein amount plays a causal role in deleterious phenotypes associated with these disorders, we tested transgenic mice that represent a continuum of VMAT2 gene dose in a variety of sensory, affective, social, and appetitive assays. We found that mice with dramatically reduced VMAT2 protein amount tend to show a high-anxiety phenotype, but no deficits in sensory or social function. By contrast, mice that overexpress VMAT2 protein responded similarly to wild-type mice in most assays, with some evidence of a reduced anxiety phenotype. These behavioral characterizations of VMAT2 transgenic mice may help characterize subsets of highly heterogeneous psychiatric disorders in humans.

INTRODUCTION

Normal monoaminergic neurotransmission is critically dependent on VMAT2 for vesicular uptake of monoamine molecules. Faulty monoaminergic neurotransmission has been implicated in a variety of disorders including schizophrenia, attention deficit hyperactivity disorder, dystonia, Huntington's disease, addiction, depression, post-traumatic stress disorder (PTSD), and Parkinson's Disease (PD) (Caudle *et al*, 2007; Coppen, 1967; Eisenberg *et al*, 1988; Hornykiewicz, 1998; Klawans *et al*, 1972; Pifl *et al*, 2014; Rilstone *et al*, 2013; Ritz *et al*, 1988; Song *et al*, 2012). Specifically, aberrations in VMAT2 functioning have been associated with a variety of diseases and disorders. Previous research indicates reduced vesicular uptake in patients with PD, changes to VMAT2 binding patterns in patients with schizophrenia and bipolar disorder type I, and decreased VMAT2 expression in the ventral tegmental area (VTA) and nucleus accumbens (NAC) in a rat model of depression (Pifl *et al*, 2014; Schwartz *et al*, 2003; Zubieta *et al*, 2001). Additionally, in a study with trauma-exposed European-American women of 3742 single nucleotide polymorphisms (SNPs) in more than 300 genes, a significant association was found between the haplotype for the gene that encodes VMAT2, and PTSD (Solovieff *et al*, 2014). Moreover, in a post-mortem analysis of PTSD-affected brains and control brains, the brains of patients diagnosed with PTSD had significantly reduced mRNA for the VMAT2 protein in multiple brain areas (Bharadwaj *et al*, 2016). Furthermore, a mouse model of reduced VMAT2 function recapitulates a hyperarousal fear phenotype (Chapter 4).

The implication that VMAT2 has a role in PTSD indicates that VMAT2 could have an effect on various complex behaviors. Previous research indicates that animal models with reduced VMAT2 function show anxiety-like behavior (Taylor *et al*, 2009; Wang *et al*, 2016) and depressive-like behavior (Fukui *et al*, 2007). To build on this initial data, we tested for additional phenotypic evidence of risk or resilience to ancillary aspects of PTSD in our VMAT2 transgenic mice, including anhedonia (Hopper *et al*, 2008; Spitzer *et al*, 2018; Vujanovic *et al*, 2017), anxiety (Modlin, 1967), depressive symptoms (Anderson *et al*, 2018; Bajor *et al*, 2013; Lai *et al*, 2015), and altered response to drugs of abuse (Kulka *et al*, 1988).

Furthermore, the implication of VMAT2 in other disorders such as bipolar disorder and schizophrenia that often contain an aspect of social anxiety and/or dysfunction indicates that VMAT2 gene dose could mediate social behavior in mice (American Psychiatric Association, 2013; Schwartz *et al*, 2003; Zubieta *et al*, 2001). The neural circuitry underlying social behavior is another indicator that VMAT2 could have an effect on social behavior in mice. In the mesolimbic dopamine system, dopamine cells originating in the ventral tegmental area (VTA) project to the nucleus accumbens (NAc), medial prefrontal cortex (mPFC), and amygdala (Swanson, 1982). The mesolimbic dopamine system is critical for social behavior, maternal behavior, and appetitive drugs of abuse (O'Connell and Hofmann, 2011; Young *et al*, 2011). The dopaminergic projections from VTA, a neural region known to express VMAT2, to various neural regions implicated in appetitive behaviors, pleasure, and social behavior further indicates that changes in VMAT2 expression could be associated with changes in social behavior (Cliburn *et al*, 2016; O'Connell and Hofmann, 2011; Swanson, 1982). Furthermore, serotonin, another

monoamine packaged by VMAT2, has been implicated in social deficits and repetitive behaviors (Kane *et al*, 2012). Mice lacking serotonin display social deficits, communication deficits, and an increased incidence of repetitive behaviors, thus recapitulating many behaviors observed in autism spectrum disorder (ASD) (Veenstra-VanderWeele *et al*, 2012). Given the changes in social and repetitive behavior seen in patients with ASD, it is likely that VMAT2 gene dose also has an effect on repetitive behaviors. Additionally, patients with schizophrenia, another disorder associated with aberrant VMAT2 function often also exhibit repetitive behaviors, thus supporting the idea that VMAT2-transgenic mice likely have alterations in repetitive behaviors (Luchins *et al*, 1992). As VMAT2 can affect neurotransmission in the mesolimbic dopamine system as well as serotonergic neurotransmission, more research is needed to understand how varying levels of VMAT2 expression specifically affect social and repetitive behaviors.

Cocaine abuse has persisted as a major public health concern in the United States, yet currently no FDA-approved pharmacotherapies are available for its treatment. Cocaine's abuse-related effects are predominantly attributed to increases in dopamine levels, particularly within mesocorticolimbic brain pathways. However, most nonselective antagonists have proven unsuccessful in clinical trials of substance abuse treatment, in part because they exhibit an undesirable profile of side effects that limits compliance and retention. The behavioral response to drugs of abuse is driven by biochemical events. Dopamine release within the nucleus accumbens is critical to expression and maintenance of a motivated response to a drug or other appetitive cue. We have demonstrated that VMAT2-transgenic mice display an altered dopamine release response in the presence of cocaine (Chapter 3). To study the whether this altered biochemical response affects the

behavioral response to cocaine, we test VMAT2-transgenic animals for appetitive and locomotor responses to cocaine. Because VMAT2 has also been implicated in alcohol use disorder and because alcohol is also reliant on the mesolimbic dopamine pathway, we also test VMAT2 transgenic animals for the behavioral response to ethanol.

Collectively, these studies show that VMAT2 could be a promising pharmacological target for a variety of diseases; thus, more research is needed to understand the contribution of VMAT2 to complex behaviors, specifically, affective, social, and appetitive behaviors. Despite converging lines of evidence indicating that VMAT2 gene dose could mediate social and motivated behavior, little research has explored the effect of over- and under-expression of VMAT2 on affective, social or appetitive behavior in mice. To that end, we performed a variety of assays to test the contribution of VMAT2 gene dose to complex behavior in mice. We hypothesize that VMAT2-LO mice will display deleterious outcomes in these assays, while VMAT2-HI mice will have improved outcomes. Overall, these studies will provide a basis for understanding the contribution of VMAT2 to the changes in affective, social, and appetitive behaviors seen in a variety monoamine-related disorders.

MATERIALS & METHODS

Mice. VMAT2-LO mice were generated by backcrossing the original mixed-background VMAT2-deficient strain (Caudle *et al*, 2008; Taylor *et al*, 2014) to Charles River C57BL/6 for four generations using a marker-assisted selection (i.e. "speed congenic") approach (Lohr *et al*, 2016). VMAT2-HI mice were generated as previously

described (Lohr *et al*, 2014). Briefly, we used a bacterial artificial chromosome-mediated transgene to insert three additional copies of the murine *SLC18A2* (VMAT2) gene, including its endogenous promotor and regulatory elements. These founders were then backcrossed to a Charles River C57BL/6 background. Thus, VMAT2-LO, -WT, and -HI mice share an identical genetic background. Mice received food and water *ad libitum* on a 12:12 light cycle. All mice were 6-11 months at time of testing, which is before any evidence of neurodegeneration even in the VMAT2-LO mice (Caudle *et al*, 2007). All procedures were conducted in accordance with the National Institutes of Health Guide for Care and Use of Laboratory Animals and were approved by the Institutional Animal Care and Use Committee at Emory University.

Buried food test. The protocol was adapted from Yang et al. (2009) to assess mouse olfactory sensation. All food was removed from each mouse cage sixteen hours prior to testing. Precautions were taken to ensure that no pellets were in the bedding. To ensure that the food was palatable, each mouse was given one Fruit Loop. In all cages, the Fruit Loop was consumed during the overnight period prior to formal testing. Each mouse was placed in a clean cage and allowed 5 minutes of habituation. The mouse was placed back in original cage while the experimenter buried one Fruit Loop in the bottom right corner of the cage approximately 1 cm below the surface of the bedding. The mouse was placed in the top left of the cage and total time to uncover the cereal was recorded by a live experimenter blind to the experimental groups. ANOVA with post-hoc Dunnett's test was performed to determine differences between groups. There were n = 5 LO animals, n = 7 WT animals, and n = 4 HI animals in this assay.

Hot plate assay. A hot plate assay was used to test the mouse's pain sensitivity. The mouse was placed on a hot plate set at 52-53 °C and enclosed within a cylinder such that the mouse could not escape. The amount of time before the animal reacted with either paw licking, jumping, or making noise, was recorded. To prevent lasting tissue damage, the mouse was immediately removed upon showing any indication of pain, and the mouse was removed after 30 seconds even in the absence of a response. Decreased pain sensitivity was indicated by a longer amount of time before any reaction. ANOVA with post-hoc Dunnett's test was performed to determine differences between groups. There were n = 5 LO animals, n = 7 WT animals, and n = 5 HI animals in this assay.

Open field test. Mice were individually placed in a large circular chamber and allowed ten minutes to freely explore. Time spent in the center of the apparatus, time spent in the side of the apparatus, and total movement was recorded by TopScan 2.0. CleverSysm Inc (Reston, VA). ANOVA with post-hoc Dunnett's test was performed to determine differences between groups. There were n = 9 animals per group in this assay.

Sucrose preference. For a period of five days, a bottle of 2% sucrose and a bottle of plain water was placed in the hoppers of individually housed mice. Each day, the bottles were weighed to determine the amount of liquid consumed. The relative positions of the bottles were switched each day to eliminate side preferences. Percent sucrose preference was determined by dividing the amount of sucrose water consumed divided by the total amount of liquid consumed. Difference among genotype was determined using ANOVA

with post-hoc Dunnett's tests (Graphpad Software, La Jolla, CA). There were n = 11 LO animals, n = 9 WT animals, and n = 9 HI animals in this assay.

Forced swim test. Forced swim test assays were administered as previously described (Lohr et al. 2014). Briefly, mice were placed in glass cylinders (24 x 16 cm) with 15 cm of water maintained at 25ºC and were video recorded for 6 minutes. After the first 2 min, videos were scored in 5 second bins and the primary behavior (either immobile, passive swimming, or active struggle) was scored for each bin. Behavior as measured by a rater blind to the experimental groups had over 95% concordance between independent scoring sessions. Differences among genotypes was determined using ANOVA with post-hoc Dunnett's test. Experimental observers noticed different patterns of behavior during the forced swim test that were not captured simply by measuring immobility time, so videos were re-analyzed and proportion of time spent immobile, passively swimming, and actively struggling were compared between VMAT2-LO and VMAT2-WT mice using a chi-square test (Graphpad Software, La Jolla, CA). There were n = 9 LO animals, n = 8 WT animals, and n = 5 HI animals in this assay.

Marble burying. Mice were placed in their home cages with the nestlet, food, and water removed from the cage for the duration of the test. Extra bedding was added to each cage such that there was about 6 inches depth of bedding throughout the cage. In each cage, twenty marbles were arranged evenly in 5 rows of 4 marbles. The mouse was placed in the cage for 30 minutes and the number of marbles at least 2/3 covered was recorded. ANOVA

with post-hoc Dunnett's test was performed to determine differences between groups. There were n = 5 LO animals, n = 6 WT animals, and n = 5 HI animals in this assay.

Repetitive behaviors. Mice were individually placed in a clean, new cage and allowed to habituate for 20 minutes. After habituation, mice were recorded for ten minutes using a GoPro Hero 5 Session. Videos were played via QuickTime movie player and duration of repetitive behaviors was timed via hand-held stopwatch. Amount of time spent self-grooming was recorded. ANOVA with post-hoc Dunnett's test was performed to determine differences between groups. There were n = 19 LO animals, n = 24 WT animals, and n = 16 HI animals in this assay.

Social Approach. A social approach assay was used to quantify social approach behavior and social memory in mice (Yang et al., 2011). Mice were individually placed in the center chamber of a 3-chambered apparatus and allowed 10 minutes to habituate. The sides were then opened and the mouse was allowed 10 minutes to habituate to the whole apparatus. Time spent in each chamber was later analyzed through video recordings. A stimulus mouse was then placed under a mesh wire cup (3.8-cm bottom diameter, rust-proof/rust-resistant, noncorrosive, steel wire with space between bars to allow for interaction) on one side of the chamber, and an identical empty upside-down cup was placed on the opposite side. To prevent the subject mouse from climbing on top of the cup, a right-side up Solo cup was placed on top of the inverted cup and a weight was placed in the Solo cup. The subject mouse was given 10 minutes to freely explore the apparatus. Time spent near the stimulus mouse under the cup (novel mouse) and time spent near the

inverted cup without the mouse (novel object) was later analyzed through video recordings. The relative placement of the novel mouse was counterbalanced across all subjects. In the final stage, the original stimulus mouse was moved to the opposite side of the chamber, and a new subject mouse was placed under a cup on the original side. The subject mouse was given 10 minutes to explore the apparatus, and time near the novel and familiar stimulus mouse was observed through video recordings. The apparatus was cleaned between subjects. All videos were scored by an experimenter blind to the experimental groups. ANOVA with post-hoc Dunnett's test was performed to determine differences between groups. There were n = 11 LO animals, n = 18 WT animals, and n = 10 HI animals in this assay.

Cocaine conditioned place preference (CPP) and cocaine-induced locomotion. During cocaine CPP, each mouse was placed in a cage that has two distinct contexts, separated by a neutral center area. The two contexts could be discriminated using visual cues (stripes vs. solid) and tactile cues (rough vs. smooth floor). During a 20 minute pre-conditioning test, each mouse could freely explore both environments. During three days of conditioning, a saline solution was administered (i.p.) in the morning and each mouse placed in one of the two distinct contexts for 30 minutes. Then in the afternoon, a cocaine solution was administered (5, 10, or 20 mg/kg, i.p.) and each animal placed in the other context for 30 minutes. Assignment of compartments to either saline or cocaine was done in a counterbalanced manner. On the fifth and final day, mice could once again freely explore both environments, and the difference in the amount of time the mouse spent in the cocaine-paired versus the saline-paired context was taken as a measure of cocaine

conditioned place preference. Exclusion criteria were greater than 67% of total pretest time in the center or more than 70% of non-center pretest time in one context. Number of beam breaks within the enclosed space was used to measure mouse movement after saline injections and after cocaine injections, and the increase in number of beam breaks following cocaine injection was taken as a measure of cocaine-induced locomotion. Two-way ANOVA with genotype (LO, WT, HI) and cocaine concentration (5 mg/kg, 10 mg/kg, 15 mg/kg) as factors with post-hoc Dunnett's test to determine differences between groups. N's for each group were as follows:

[Cocaine]	LO	WT	HI
5 mg/kg	-	8	15
10 mg/kg	9	21	18
20 mg/kg	-	4	4

Two bottle ethanol choice. We used a modified version of the two bottle choice protocol previously described by our laboratory (Reveron *et al*, 2002; Savelieva *et al*, 2006). Immediately following fear assays mice remained individually housed and given continuous access to two 50 ml bottles. One bottle contained water and other bottle contained an escalating concentration of ethanol (0%, 3%, 6%, 10%, 15%; 6 – 8 days per concentration). The relative positions of the bottles were changed every day to control for side preferences. Bottles were weighed daily to determine the amount of liquid consumed. Food was available ad libitum and the mice were weighed every four days. Leakage was measured individually for each bottle by placing a full bottle in an empty cage for two days and measuring the change in the volume of liquid. Consumption (g/kg) was calculated for each mouse by dividing the amount of ethanol solution consumed by the total amount of liquid consumed, after correcting for leak. Two-way ANOVA with genotype (LO, WT,

HI) and ethanol concentration (0%, 3%, 6%, 10%, 15%) as factors with post-hoc Dunnett's test was used to determine differences between groups. There were n = 11 LO animals, n = 9 WT animals, and n = 9 HI animals in this assay.

Drinking-in-the-dark (DID) assay. To complement our studies using two-bottle choice, we used the binge-like model of drinking-in-the-dark (DID) (Harris *et al*, 2017; Rhodes *et al*, 2005, 2007; Thiele *et al*, 2014). DID takes advantage of the circadian rhythm-based fluctuations in ethanol consumption. This maximizes the consumption allowing a more binge-like pattern. Ethanol is made available for only a few hours each day and water is not offered during that time. The drinking-in–the-dark paradigm is thought to represent a better model of binge drinking, which is relevant to the AUD behaviors observed in those with PTSD (Harris *et al*, 2017; Rhodes *et al*, 2005, 2007; Thiele *et al*, 2014). We are fortunate that our mice have been generated on a C57BL/6J strain; the same strain used to establish the DID paradigm. A recent paper explored the transcriptome in animals selectively bred for high drinking in the dark. There was a clear enrichment in several gene pathways associated with synaptic vesicle function (Hitzemann *et al*, 2017). Moreover, in the network analysis illustrated in the paper all of the affected gene sets converge on the synaptic vesicle. This suggests that our mice, which have altered filling and release of monoamines, are likely to have a differential response in the DID paradigm. DID has been optimized for use in C57BL/6J mice, which tend to consume higher level of ethanol than other strains. Mice were individually housed for one week before testing. The mice were on a reverse light cycle (7:00 am off, 7:00 pm on). Three hours after lights off water bottles were replaced with bottles containing 20% ethanol in tap water. Mice had access to the

ethanol for two hours. On day four, ethanol was available for four hours (with content measured at 2 and 4 hours). The amount of ethanol consumed during the final two hours of the assay was taken as a measure of binge-like ethanol consumption. ANOVA with post-hoc Dunnett's test was used to determine differences between genotypes. There were n = 11 LO animals, n = 9 WT animals, and n = 9 HI animals in this assay.

Core body temperature. A small probe (Physiotemp, Clifton, NJ) was lubricated with petroleum jelly and inserted into the anal cavity of restrained mice. ANOVA with post-hoc Dunnett's test was used to determine differences between genotypes. There were n = 3 LO animals, n = 11 WT animals, and n = 11 HI animals in this assay.

Power analysis. Because the sample sizes vary in these assays, we performed a power analysis to determine how many animals would be appropriate to determine if differences exist between three groups using an ANOVA. For a moderate effect size (f = 0.7), a sample of at least 8 mice per group is needed to for $\alpha = 0.05$ and $1 - \beta = 0.8$. This effect size after reviewing past effect sizes observed in behavioral tests of VMAT2-deficient animals (Baumann *et al*, 2016; Taylor *et al*, 2011; Wang *et al*, 2016). More mice would be needed to gain power to detect smaller effect sizes. Assays that are underpowered for an effect size of f=0.7 are the buried food assay, the hot plate assay, the forced swim test, marble burying, cocaine conditioned place preference test (particularly at 20 mg/kg and comparing the LO animals), and a test of core body temperature.

RESULTS

VMAT2 transgenic mice show no differences in olfaction or nociception. In a test of olfactory capability, there was no effect of VMAT2 genotype on amount of time to find a hidden piece of food ($F(2,13) = 2.19$, $p = 0.1515$) (Fig 5-1A). Similarly, there was a trend for an effect of VMAT2 genotype on amount of time to retract a paw from a heated plate ($F(2,14) = 3.44$, $p = 0.0611$) (Fig 5-1B). However, the trend was actually for VMAT2-LO to display *increased* tolerance to pain, as evidenced by a longer time spent until paw retraction. However, it should be noted that a post hoc power analysis using the observed effect size of these of these experiments determined that I was underpowered to detect differences among groups for both the buried food test (power = 0.48) and the hot plate assay (power = 0.55) at the observed effect sizes.

VMAT2 genotype mediates some affective behaviors in mice. In a series of assays meant to measure the effect of VMAT2 gene dose on anxiety- and depressive- like behavior, there was variation due to genotype in some measures but not in others. There was no difference due to genotype in the amount of time spent close to the edges of an enclosure compared to time spent in the middle of an enclosure ($F(2,24) = 0.0689$, $p = 0.9336$) (Fig 5-2A). VMAT2-HI mice buried fewer marbles in a marble burying assay, but there was no difference between VMAT2-LO and wild-type mice ($F(2,13) = 53.18$, $p < 0.0001$, HI>WT $p < 0.0001$) (Fig 5-2B). VMAT2-LO mice exhibited a decreased preference for a 2% sucrose solution ($F(2,26) = 8.372$, $p < 0.01$, LO<WT, $p<0.001$) (Fig 5-2C). There was a nonsignificant trend towards increased self-grooming in the VMAT2-LO mice ($F(2,55) = 3.134$, $p = 0.0514$) (Fig 5-2D). VMAT2-LO mice spent less time

immobile during a forced swim test ($F(2,15) = 4.983$, $p < 0.05$, LO<WT, $p < 0.05$) (Fig 5-2D). However, during observation of the forced swim test assay, we noticed that the VMAT2-LO mice seemed to be actively attempting to climb the container walls more than wild-type mice, who would paddle, but not climb. In a post hoc test, we show that VMAT2-LO mice show different swimming behaviors due to an increase in active climbing ($\chi^2(1) = 79.5$, $p < 0.0001$) (Fig 5-2E). We also performed power analysis for each of these assays, since the number of mice used for each group varied among each test.

Core body temperature. VMAT2-LO mice show an elevated core body temperature relative to wild-type mice ($F(2,22) = 4.820$, $p < 0.05$, LO<WT, $p < 0.05$) (Fig 5-3).

VMAT2 transgenic animals show similar patterns of social memory. There were no differences among VMAT2-LO, -WT, and –HI mice in regards to amount of time spent exploring a novel mouse versus a novel object ($F(2,36) = 1.518$, $p = 0.2328$) (Fig 5-4A) or in the amount of time spent exploring a novel mouse versus a familiar mouse ($F(2,36) = 0.2158$, $p = 0.8069$) (Fig 5-4B).

VMAT2-HI mice show a trend towards decreased cocaine conditioned place preference, but no difference in cocaine induced locomotor activity. There was a trend towards decreased preference for a context associated with cocaine in VMAT2-HI mice compared to wild-type mice ($F(1,62) = 3.007$, $p = 0.0879$) (Fig 5-5A). However, VMAT2-HI and wild-type mice showed no differences in locomotor response to cocaine ($F(1,22) = 0.0308$, $p = 0.8620$) (Fig 5-5B). VMAT2-LO mice were only tested at 10 mg/kg, and were

not different than WT in regard to cocaine conditioned place preference ($F(2,45) = 0.9905$, $p = 0.37$) (data not shown). Notably, this test is underpowered to detect differences among groups and any interaction effects. Therefore, these results are considered as a preliminary trend, but not definitive.

VMAT2 genotype does not mediate behavior response in a test of ethanol preference or ethanol binge-drinking paradigm. VMAT2 genotype did not mediate amount of 20% ethanol consumed during the last two hours of a binge-drinking paradigm ($F(2,26) = 0.0137$, $p = 0.9864$) (Fig 5-6A). In a test of two bottle choice with an ascending ethanol concentration, there was a main effect of ethanol concentration ($F(4,96) = 7.897$, $p < 0.0001$) but no effect of VMAT2 genotype ($F(2,24) = 2.521$, $p = 0.1014$) (Fig 5-6B).

Half of the assays that were underpowered did not risk reporting a false negative. Because of the power analysis that determined an n of 8 was necessary for an effect size of $f=0.7$ at $\alpha = 0.05$ and $1- \beta = 0.8$, we knew that several assays were at risk of reporting false negatives due to underpowered sample sizes. Assays that are underpowered for an effect size of $f=0.7$ are the buried food assay, the hot plate assay, the forced swim test, marble burying, cocaine conditioned place preference test (particularly at 5 mg/kg and comparing the LO animals), and a test of core body temperature. However, the forced swim test, marble burying test, and test of core body temperature definitively did not show false negatives, as they actually showed a difference among groups despite the small sample sizes. We performed post-hoc power analysis on these three assays to determine what power was achieved even with the small sample sizes, which is summarized below:

Test	Observed effect size	Total n	Power achieved
Forced swim	0.76	17	0.71
Marble burying	4.72	16	~1
Core body temp	0.85	25	0.95

DISCUSSION

Here, we show that VMAT2 transgenic animals display differences in some but not all assays of complex behavior, primarily as it relates to affective measures.

First, we show that there is no measurable difference in mouse olfaction or nociception, which can influence other behavioral assays. VMAT2-immunoreactivity has been observed in cells that project from the subventricular zone to the olfactory bulb, and VMAT2 is expressed in the monoaminergic olfactory tubercle (Xu, 1996; Cliburn et al., 2016). The olfactory tubercle is implicated in the reward system and sensory integration (Ikemoto, 2007; Wesson and Wilson, 2011). In rodents, odors are used for communication and to convey information about sex, species, social dominance, health status, and reproductive status (Arakawa et al., 2008; Harvey et al., 1989; Lin et al., 2005). Therefore, any deficit in olfaction could influence the interpretation of social tests. Previous research has shown a progressive decline in olfactory acuity for the VMAT2-LO mice (Caudle et al., 2007; Taylor et al., 2009; Braak et al., 2003; Langston, 2006), but we did not observe this deficit in the mice that we tested that were relatively younger mice and of a different background than those used to test progressive loss of olfactory function. The finding that,

at least as measured via hot plate assay, VMAT2-LO mice do not show a hypersensitivity to unpleasant stimuli is informative for the interpretation of foot-shock paradigms. Though these tests were underpowered, these results are consistent with past data that demonstrates that reduced VMAT2 does not affect sensory abilities at this age (Taylor *et al*, 2007).

Next, we show that VMAT2-LO mice show an anhedonic-like phenotype, as measured by decreased preference for a sucrose solution. The increased escape-like behavior observed in our VMAT2-LO mice in the forced swim test is consistent with the increase in escape behavior observed in mice with 95% depletion of VMAT2 in SERT-expressing neurons (Narboux-Nême *et al*, 2011). This increase in active struggling occurs despite the severe age-dependent motor deficits seen in VMAT2-LO mice (Caudle et al. 2007; Taylor et al. 2011). Previous researchers have suggested that this pattern of behavior is indicative of a high-anxiety panic-like phenotype. Furthermore, the implication of the serotonergic system in autism spectrum disorder that is associated with changes in both social and repetitive behaviors as well as the presence of repetitive behaviors in other disorders associated with VMAT2 collectively indicates that VMAT2 gene dose could also affect repetitive behaviors (Silverman et al., 2012; Veenstra-Vanderweele et al., 2012; Luchins et al., 1992). We observed a trend towards increased repetitive self-grooming in the VMAT2-LO mice. Altered self-grooming behavior can be symptomatic of a state of disorder (Kalueff et al., 2015). Multiple studies indicate that self-grooming behavior is altered by acute stress, and it can also be a sign of both discomfort and comfort in the environment (Denmark et al., 2010; Kalueff and Murphy, 2007; Minuer et al., 2003; Kalueff, 2004).

Rodents prefer to be in the presence of a social odor than no odor indicating that social odors could be inherently rewarding (Nelson and Panksepp, 1996; Trezza et al., 2011). The aforementioned VMAT2 distribution indicates that VMAT2-overexpression could alter sensory integration of rewarding stimuli. A three-chambered apparatus was used to test both social exploration and social memory in VMAT2-transgenic mice. When the mice were given a choice between a novel mouse and a novel object, all genotypes spent significantly more time exploring the mouse than the object. These results indicate that overall, VMAT2-transgenic mice exhibit sociability, defined as significantly more time spent exploring the mouse than the object (Yang et al., 2011). During the final phase, the subject mouse could investigate either a novel mouse on one side of the apparatus or a familiar mouse on the other side of the apparatus. Previous research indicates that wild-type C57BL/6J mice show a significant preference for the novel mouse (Nadler et al., 2004). However, in this study, none of the genotypes had a significant preference for the novel mouse. Genotype had no effect on the extent of preference for the mouse compared to a novel object or on the preference for a novel compared to familiar mouse. These data do not support the initial hypothesis that the VMAT2-LO mice would display reduced social behavior. The VMAT2-LO mice exhibited no difference in sociability from the VMAT2-WT or VMAT2-HI mice. Similarly, VMAT2-HI mice did not show any difference in sociability from the VMAT2-WT mice. These social tests involved interactions with a novel mouse, however, interactions with a novel mouse do not encapsulate the range of social deficits or social anxiety phenotypes exhibited in other disorders (PTSD, bipolar disorder, schizophrenia, depression) in which VMAT2 is implicated (Zubieta et al., 2001; Schwartz et al., 2003; DSMV, 2013). These disorders

often include aspects of social anxiety, social withdrawal, social dysfunction, and altered empathic responses (Zubieta et al., 2001; Schwartz et al., 2003; DSMV, 2013). In humans, the social issues associated with these disorders are not limited to interactions with novel individuals. In order to better address the role of VMAT2 in the social components of these disorders, mice should be tested in assays that involve their behavior towards familiar conspecifics, thus more closely mirroring the social phenotype seen in humans. This could include studies evaluating the subject's response to the distress of a familiar cage- or littermate compared to the distress of a novel mouse, studies of prosocial behavior, studies of social recognition, and studies examining ultrasonic vocalizations (Langford et al., 2006). Differences in these assays could be indicative of a social deficit analogous to aberrant social behavior in humans.

Furthermore, VMAT2-LO exhibit an elevated core body temperature. This could be a result of altered peripheral serotonergic innervation, which can regulate body temperature (Ishiwata *et al*, 2017). In fact, the observed characteristic phenotype of the VMAT2-LO mice is consistent with the symptoms of serotonin syndrome. The symptoms of mild serotonin syndrome include high body temperature, hyper-arousal, and increased rate of gastric emptying – all symptoms that are observed in VMAT2-LO mice. In humans, serotonin syndrome occurs when extracellular levels of serotonin rise, often due to unintended combinatorial effects of drugs (Cheshire, 2016). Certainly, the VMAT2-LO mice do not suffer from an abundance of synaptically available serotonin. However, some research has indicated that the symptoms are due to increased sensitivity in 5-HT_{1A} and 5-HT_{2A} receptors (Isbister *et al*, 2004), which could be the case in VMAT2-LO mice. Changes in core body temperature has long been associated with psychiatric disorders,

though most research indicates that a lower core body temperature is most associated with disorders like depression in humans. However, it is possible that the behavioral hyperarousal we observe in the VMAT2-LO mice in fear and affective assays are exacerbated by peripheral discomfort or dysregulation of body temperature.

Lastly, we tested how VMAT2 gene dose affects appetitive response to reinforcing drugs. Originally, we hypothesized that the VMAT2-HI mice would show *increased* preference for psychostimulants, since VMAT2-HI mice have increased capacity to release dopamine into the extracellular space. We did not observe an increased preference for cocaine in VMAT2-HI mice: if anything, VMAT2-HI mice show a trend towards *decreased* cocaine preference overall, driven by decreased preference at 20 mg/kg cocaine. This trend needs to be replicated and reproduced in other types of appetitive assays, including self-administration. Interestingly, VMAT2-HI mice had an identical locomotor response to cocaine compared to wild-type mice. There may be a few reasons why changes in the VMAT2 system may change appetitive but not motor responses to psychostimulants. First: the dopamine neurons that project from the ventral tegmental area to the ventral striatum along the mesolimbic dopamine pathway, which underlies the rewarding response to drugs of abuse, co-release glutamate and dopamine. Dopamine neurons that project from the substantia nigra to the dorsal striatum, which underlie motor behavior, release only dopamine. Therefore, application of a DAT-blocker such as cocaine may have a different response on one system versus the other. Secondly, VMAT2-HI mice may have compensatory mechanisms for rapid clearance of extracellular dopamine since they constitutively tend to release more dopamine from nerve terminals compared to wild-type animals. These compensatory clearance mechanisms may be independent of DAT, such as

increased degradation via catechol-o-methyltransferase and monoamine oxidase, or alternative reuptake via the organic cation transporter-3.

To further explore how VMAT2 gene dose affects appetitive behavior, we tested VMAT2 transgenic mice for their behavioral response to ethanol. We observed no differences in either ethanol preference or binge-drinking behavior. However, even after correction for bottle leak, the VMAT2-WT mice displayed a preference for the water bottle compared to the to-be ethanol bottle when it contained 0% ethanol, which indicates that this experiment may not contain appropriate controls.

The present study provides a foundation for future research to further examine the effect of VMAT2 on aspects of social behavior and repetitive behaviors. Because VMAT2 is a potential pharmacological target for a variety of disorders, understanding how VMAT2 mediates social behavior across a range of studies could aid the development of pharmacological interventions as well as mouse models to study other diseases and disorders.

FIGURES

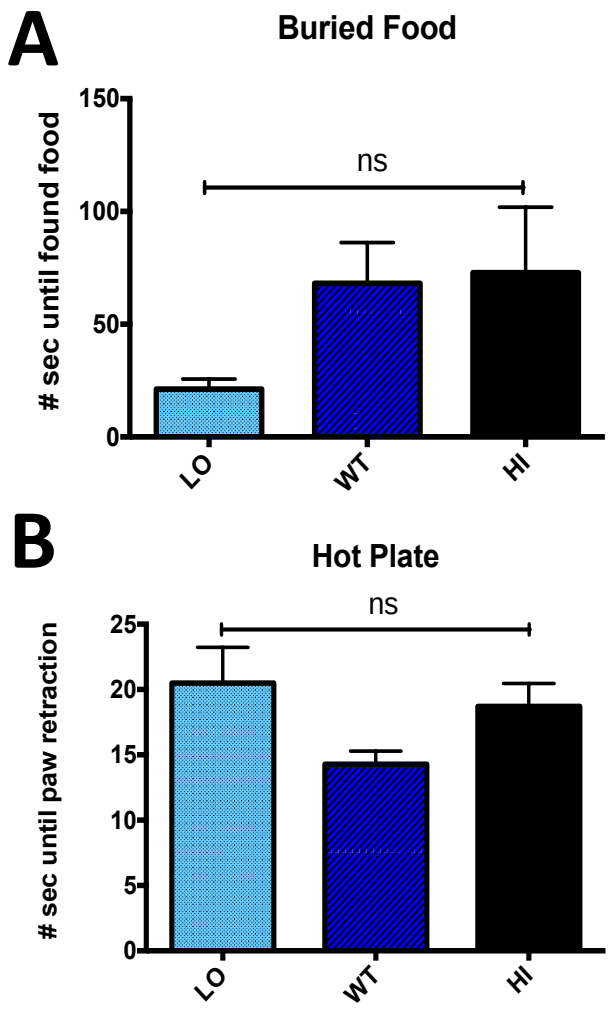

Figure 5-1. There were no differences in observed olfactory or nociceptive sensation in VMAT2 transgenic mice. A. In a test of olfactory function, mice were timed for how long until they approached a hidden piece of food. There was no difference in time to approach hidden food due to VMAT2 genotype. B. In a test of nociception, mice were placed on a hot plate and measured for the amount of time until they retracted a paw. There was no difference in time to paw retraction due to VMAT2 genotype. n = 4 -7 animals per group. ns = not significant.

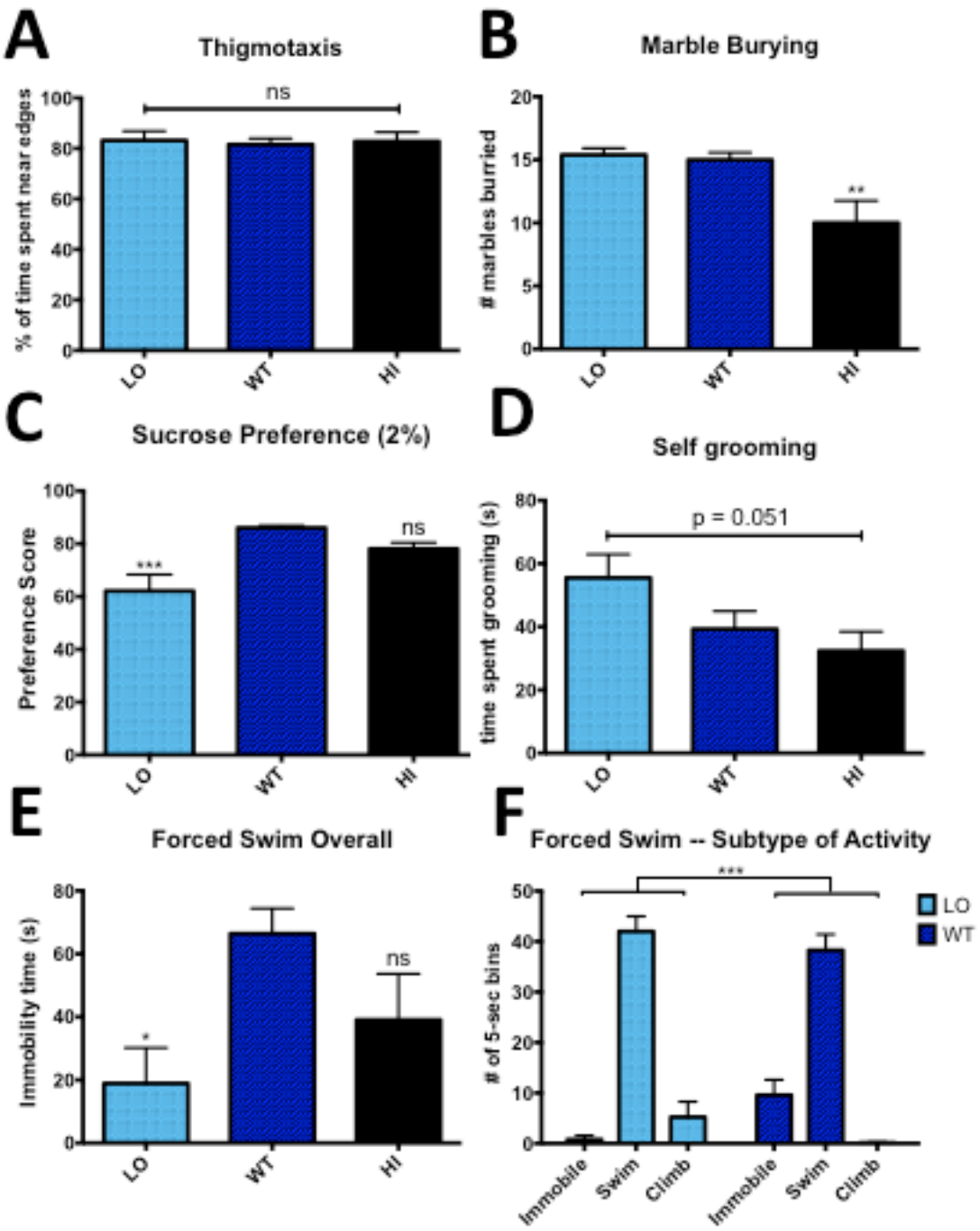
A
Thigmotaxis
% of time spent near edges
ns
LO
WT
HI
B
Marble Burying
marbles burried
**
C
Sucrose Preference (2%)
Preference Score
***
ns
D
Self grooming
time spent grooming (s)
p = 0.051
E
Forced Swim Overall
Immobility time (s)
*
F
Forced Swim -- Subtype of Activity
# of 5-sec bins
Immobile
Swim
Climb

Figure 5-2. VMAT2-LO animals show alterations in some tests of depressive- and anxiety- like behavior. VMAT2 transgenic animals underwent a number of assays to determine affective behavioral phenotypes. A. VMAT2 transgenic animals did not vary in the amount of time spent near the edges of an open enclosure. B. VMAT2-HI mice bury fewer marbles in a test a marble-burying assay. C. VMAT2-LO mice have a reduced preference for sucrose-sweetened drinking water. D. VMAT2 may mediate time spent self-grooming, as variation in this behavior due to VMAT2 genotype was on the cusp of significance. E. VMAT2-LO spend less time immobile in a forced swim test. F. The reduction in VMAT2-LO immobility time is due to an increase in climbing (i.e. actively struggling to climb up the walls of the forced swim apparatus), not due to an increase in amount of time treading water. n = 5 – 24 animals per group * $p < 0.05$, ** $p < 0.01$, *** $p < 0.001$, ns = not significant.

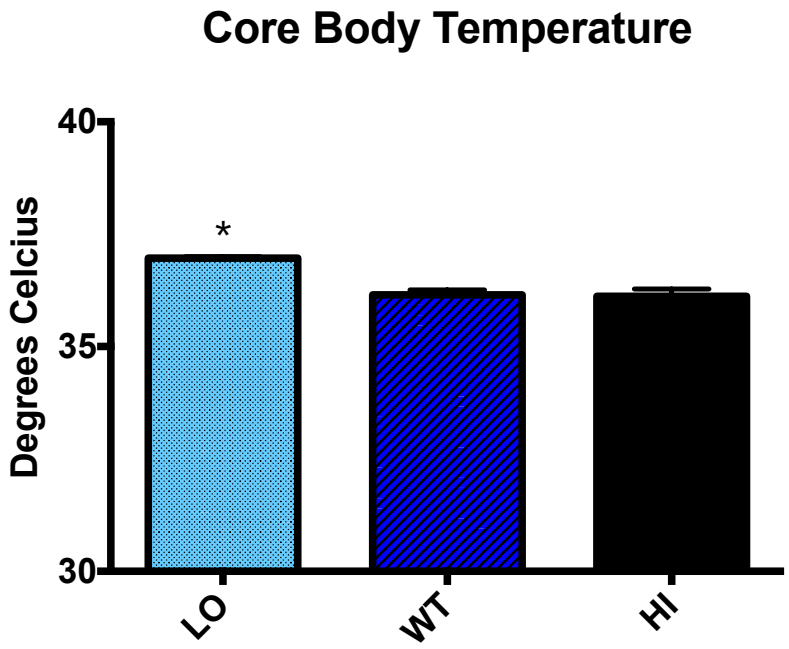

Figure 5-3. VMAT2-LO mice have elevated core body temperature. VMAT2-LO animals show a slight but significant increase in core body temperature as measured via thermometer insertion into the anal cavity. n = 3 – 11 animals per group * $p < 0.05$

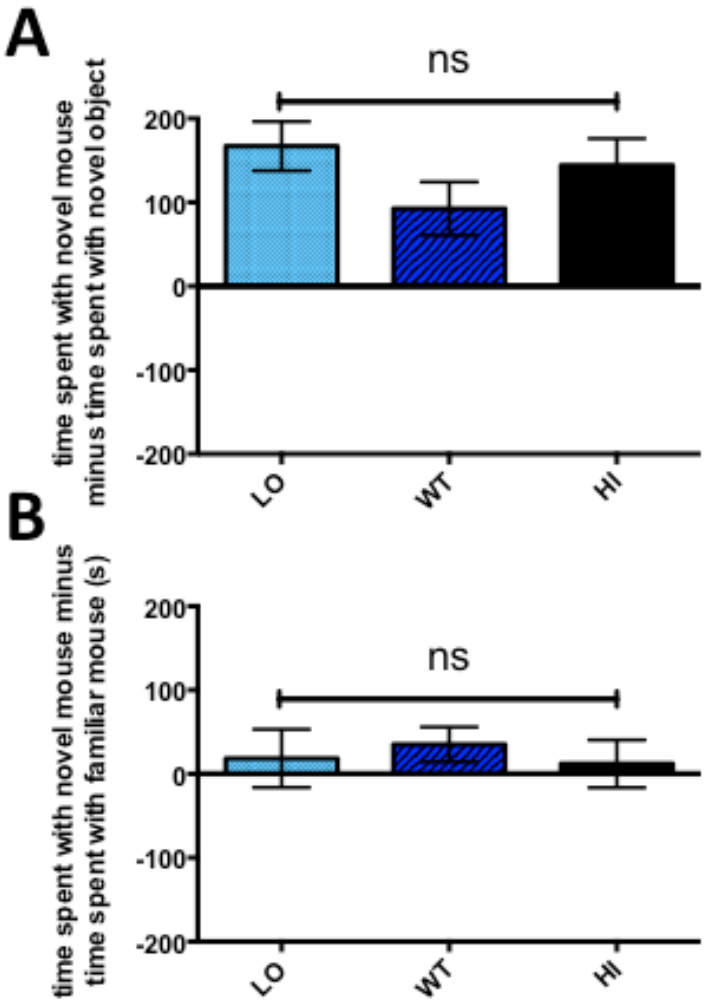

Figure 5-4. VMAT2 transgenic animals show no difference in social memory. We performed two tests to assess social behavior in VMAT2 transgenic animals. A. In a test comparing time spent near a novel conspecific and a novel inanimate object, all mice showed a preference for spending time near the novel mouse. There was no difference in preference due to VMAT2 genotype. B. In a test comparing time spent near a novel mouse versus time spent near a familiar mouse, there was a trend towards increased preference for the novel mouse, but no differences in preference due to genotype. n = 10 – 18 per group. ns = not significant.

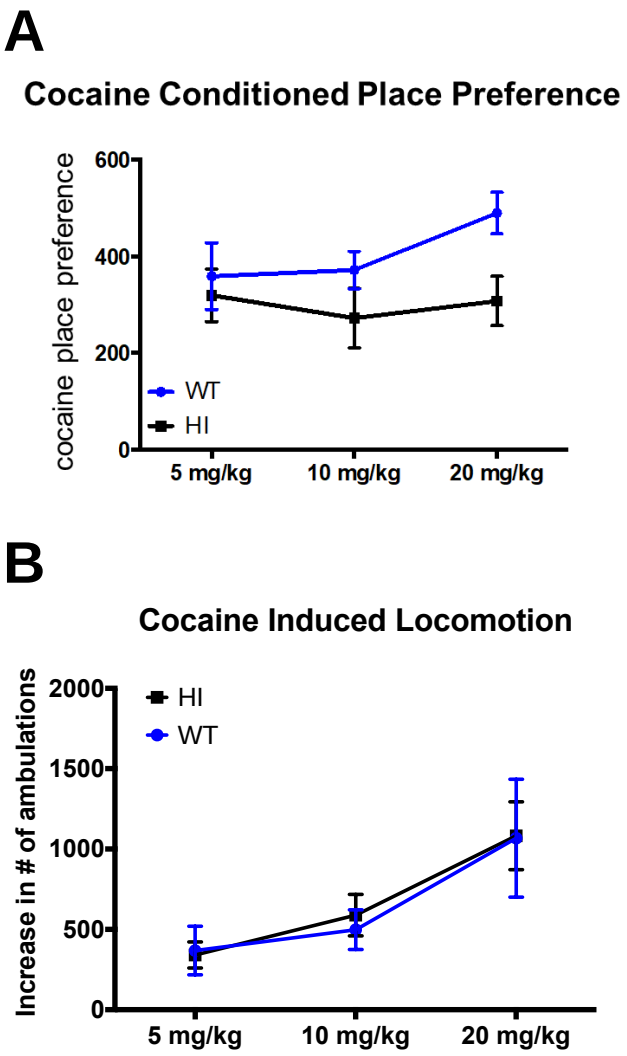

Figure 5-5. VMAT2-HI animals show a trend towards decreased cocaine preference. A. VMAT2-HI mice were compared with wild-type mice in their cocaine place preference. All animals exhibited a preference for the cocaine-paired side, but there was a trend towards reduced cocaine place preference in VMAT2-HI animals. B. As cocaine dose increased, mouse locomotion increased. There was no difference in cocaine-induced locomotion due to VMAT2 genotype. n = 4 – 21 animals per group.

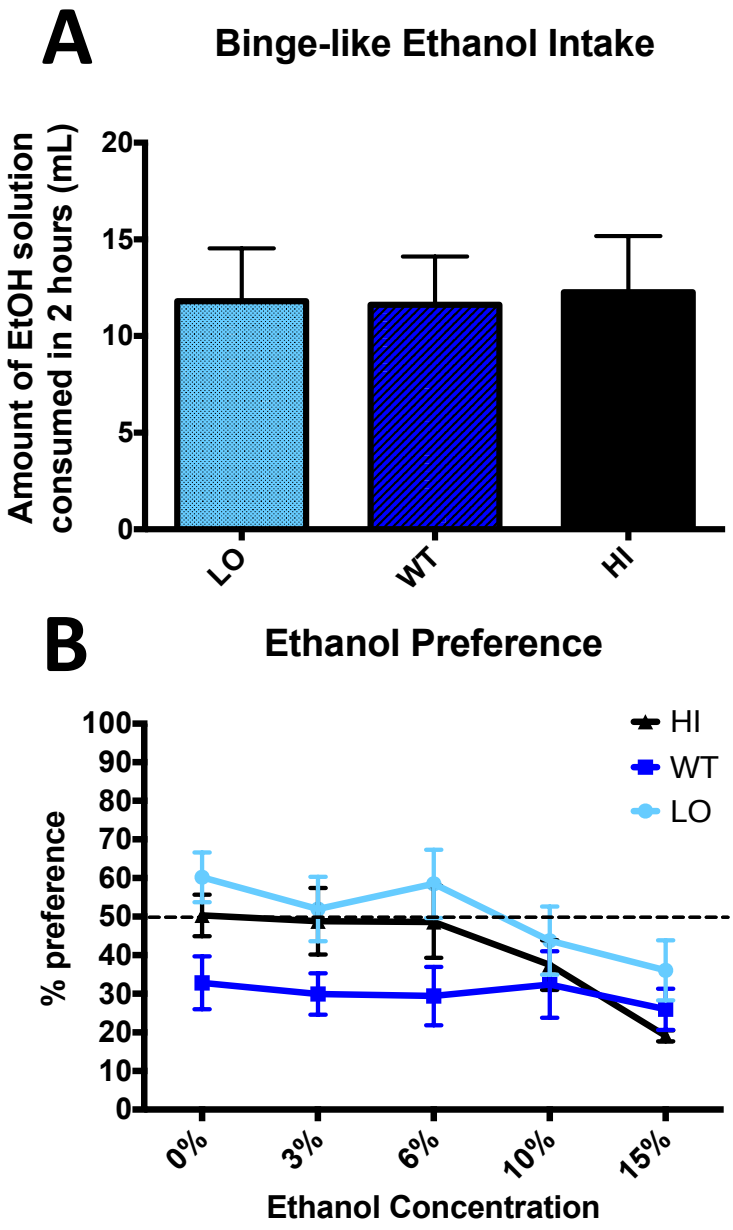
A
Binge-like Ethanol Intake
Amount of EtOH solution consumed in 2 hours (mL)
20
15
10
5
0
LO
WT
HI
B
Ethanol Preference
% preference
100
90
80
70
60
50
40
30
20
10
0
HI
WT
LO
0%
3%
6%
10%
15%
Ethanol Concentration

Figure 5-6. There is no difference in ethanol consumption behavior among VMAT2 transgenic mice. A. Mice were given restricted access to a high concentration of ethanol (20%) for 2-4 hours of their active cycle for four consecutive days. Ethanol consumption during the last two hours of this test was taken as a measure of binge-like drinking behavior. There was no difference in binge-like drinking behavior due to VMAT2 genotype. B. Mice were given continuous access to either a bottle full of regular drinking water or a bottle filled with ethanol solution (ascending in order from 0%, 3%, 6%, 10%, and 15%, 6-8 days per concentration). VMAT2 genotype did not determine ethanol preference, though there was a slight trend towards increased ethanol preference in the VMAT2-LO mice. n = 9 – 11 animals per group.

VI. Chapter 6. Discussion, future directions, and concluding remarks.

Summary of findings. The overarching hypothesis of this dissertation was that **VMAT2 protein expression in the brain is inversely correlated to PTSD-associated outcomes** such that animals with reduced VMAT2 will show more reduced monoaminergic function and a PTSD-like behavioral phenotype whereas animals with increased VMAT2 expression will show enhanced monoaminergic function and improved outcomes on tests of PTSD-like behavior**.** I explored this hypothesis in four chapters, each chapter addressing progressive questions relating to VMAT2 and PTSD-associated outcomes:

Chapter 2: Where is VMAT2? In this chapter, I demonstrated that VMAT2 protein is expressed in areas pertinent to fear or non-fear symptomology of PTSD, and that VMAT2 protein amount varies by VMAT2 genotype. Specifically, VMAT2 protein is seen in the cell body and terminal regions of serotoninergic, noradrenergic, dopaminergic, and histaminergic regions of the brain. Notably, VMAT2 is diffusely expressed in the amygdala and hippocampus, regions that are critical for the expression and maintenance of fear. Furthermore, VMAT2 protein amount varies in accordance with VMAT2 gene-dose, as demonstrated by our VMAT2-transgenic mice, the VMAT2-LO and VMAT2-HI mice. These results were made possible via use of a novel VMAT2 antibody that we created in-house.

Chapter 3: Does change in VMAT2 protein result in functional changes in the monoamine system? In this chapter, I demonstrated that the changes in VMAT2 protein amount resulted in functional consequences to monoamine storage,

content, and signaling. As predicted, VMAT2-LO mice demonstrated reduced monoamine content, reduced ability to store monoamine within presynaptic vesicles, and reduced stimulated neurotransmitter release. VMAT2-HI mice show enhanced results in each of these measures.

Chapter 4: Does VMAT2 mediate the fear-related symptomology of PTSD? In this chapter, I show that VMAT2 gene dose causally influences behavioral response to aversive stimuli. Specifically, mice with deficient VMAT2 show enhanced freezing responses to fear-paired stimuli, exaggerated startle responses, and inability to discriminate between a fear and safety cue. Alternately, mice overexpressing VMAT2 showed no differences compared to wild-type mice in these assays. These results are the first demonstration of PTSD-relevant fear phenotypes in VMAT2-deficient mice.

Chapter 5: Does VMAT2 mediate non-fear related symptomology of PTSD? In this chapter, I used VMAT2 transgenic mice to test whether changes in VMAT2 amount causally produces aberrant sensory, affective, social, or appetitive behaviors. We found that mice with dramatically reduced VMAT2 protein amount tend to show a high-anxiety phenotype, but no deficits in sensory function, social function, or response to ethanol or cocaine. Conversely, mice that overexpress VMAT2 protein responded similarly to wild-type mice in most assays, with some evidence of a reduced anxiety phenotype and reduced preference for cocaine.

In summary, in this dissertation I show that altering VMAT2 protein amount (Chapter 2) results in biochemical functional changes (Chapter 3) and that VMAT2 deficiency leads to altered fear (Chapter 4) and non-fear (Chapter 5) behavior related to PTSD. As expected, decreasing or increasing VMAT2 protein amount via transgenic models results in decreased or increased monoamine function across multiple neurotransmitter systems. This change in monoaminergic function results in behavioral changes in the VMAT2-LO mice: VMAT2-LO mice showed increased cued and contextual fear expression, altered fear extinction, inability to discriminate threat from safety cues, altered startle response compared to wild-type mice, and show a high-anxiety phenotype, but no deficits in sensory or social function. By contrast, VMAT2-HI mice are similar to wild-type mice in most behavioral assays, with some evidence of a reduced anxiety phenotype. Together, these data corroborate and enrich the human genetic data showing that reduced VMAT2 expression impacts monoamine function and fear behavior, and may be an exciting target for future pharmacotherapies for disorders like PTSD.

The potential role of VMAT1 and peripheral epinephrine. Another consideration of reduced VMAT2 function that was not explored in this body of work is the idea that monoaminergic tone can significantly alter basic growth and health of the body. As alluded to in the above studies, VMAT2-LO mice show an increased baseline core body temperature and show a consistently smaller and lighter body size. Often, the temptation is to talk about VMAT2 as an *exclusively* central nervous system protein. While it's true that VMAT2 primarily exerts its effects in the central nervous system, specifically, the brain, there are other cell types that normally express VMAT2. VMAT2 resides on the membrane

of secretory vesicles in the gastrointestinal, endocrine, hematopoietic, and immune systems, and is often co-expressed in the periphery with its non-neuronal isoform, VMAT1 (Anlauf et al., 2006, 2004, 2003; Erickson et al., 1992; Erickson et al., 1996; Henry et al., 1994; Peter et al., 1995a; Schuldiner et al., 1995; Tillinger et al., 2010; Weihe et al., 1994). So, in our VMAT2 transgenic mice, we assume that VMAT1 is 'picking up the slack' in the absence of a robust VMAT2 expression in these non-neuronal cells. However, we have not verified that this is the case, and the paucity of VMAT2 in these peripheral cell types may be influencing the health and growth of our VMAT2-LO line of transgenic mice.

Furthermore, even if VMAT1 is totally accounting for the missing VMAT2 in these animals, the central nervous system does indeed have influence on peripheral function. We do not ever directly measure this. There is some unpublished evidence of altered epinephrine content in VMAT2-LO mice (personal communication with Shawn Alter). Epinephrine (alias: adrenaline) is a both a catecholamine neurotransmitter and a circulating hormone. It is produced by adding a methyl group to the amine group of the norepinephrine molecule via the enzyme phenylethanolamine *n*-methyltransferase. As a member of the monoamine family of neurotransmitters, it is stored into presynaptic vesicles in the central nervous system by VMAT2. The overwhelming majority of epinephrine in the brain is produced by the adrenal gland, and acts as a circulating hormone that is particularly important in the physiological response to stress. However, ~10% of total epinephrine is produced in the reticular formation and the aqueductal grey of the brain stem (Mefford *et al*, 1977). It is possible that in our VMAT2-LO mouse model, VMAT1-mediated peripheral expression of epinephrine is 'ramped up' in response to a lack of centrally-produced epinephrine. This would account for the increase in core body temperature, increased rate

of gastrointestinal clearance, and potentially the lower body weight due to a constitutively higher metabolism. This is an interesting possibility and merits further investigation, as peripherally increased epinephrine could account for the behavioral anxiety-like and hyper-arousal symptoms observed in our VMAT2-LO mice.

Interestingly, the peripheral compensation for reduced VMAT2 function may operate differently in humans. In rodents, VMAT1 is expressed in peripheral cell types, and transiently in the central nervous system during development—there is no evidence of central VMAT1 in adulthood (Erickson *et al*, 1996b; Weihe *et al*, 1994). However, in humans, there is some evidence that VMAT1 is co-expressed with VMAT2 in adults, and that variation in the gene encoding VMAT1 is also associated with anxiety, affective, and appetitive disorders (Lohoff, 2010; Lohoff *et al*, 2006; Vaht *et al*, 2016). The relationship between expression of VMAT1 and VMAT2 in human central nervous system certainly merits further analysis. Initial impression of existing evidence seem to indicate that VMAT1 and VMAT2 do *not* compensate for deficiencies in the others' function, as many groups have reported specific single nucleotide variants in VMAT1 or VMAT2 that are associated with behavioral changes (Schwartz *et al*, 2003; Zubieta *et al*, 2001; Zucker *et al*, 2002).

Elucidating the contribution of specific neurotransmitters. The relative contributions of each monoamine neurotransmitter systems could be teased out using optogenetics or through the use of cre/lox mice to selectively inhibit or express VMAT2. While we think that there is value in the use of genetic knockdown and genetic overexpression to investigate the causal relationship of VMAT2 protein amount and fear

expression, further investigation of specific circuits via optogenetics could provide more specific therapeutic treatments or better tease out the role of specific circuits in these behaviors. The Giros laboratory at McGill University has bred VMAT2(lox/lox) mice with DBHcre, SERTcre, and DATcre mice to create conditional VMAT2 knockout in norepinephrine, serotonin, or dopamine circuits, respectively. In studying the heterozygotes of these knockout lines, the Giros lab reports no difference in assays of motor or affective assays (Isingrini *et al*, 2016). These conditional knock-out mice would be ideal tools for initial testing of which neurotransmitter system is critical for the VMAT2-depletion effects on fear behavior.

VMAT2 deficiency as a predictor of psychiatric risk. We demonstrate that deficiency in VMAT2 is a causal factor for symptoms of anxiety, hyper-arousal, and increased fear responsiveness in mice. This adds to a body of evidence from human genetic studies showing that genetic variation in VMAT2 is associated with PTSD and the disorders that are most commonly comorbid with PTSD (Araújo *et al*, 2014; Bajor *et al*, 2013; Kessler *et al*, 1995; Schwartz *et al*, 2003; Zubieta *et al*, 2001; Zucker *et al*, 2002). Genetic variation in VMAT2 expression that leads to decreased VMAT2 function may account for the common comorbid disease phenotype often observed in humans. Since the mechanisms underlying the etiology of these diseases are functionally diverse, understanding that a subset of patients' disease may derive from a common presynaptic dysregulation mechanism may lead to precision medicine treatments in these individuals.

Previous work shows that PTSD symptoms tend to cluster into three classes: re-experiencing, numbing, and hyperarousal—accurate identification of the patient's

particular symptom cluster is paramount to effective treatment (Norrholm and Jovanovic, 2010). The fear phenotype observed in VMAT2-LO mice is most consistent with the "numbing" and "hyperarousal" symptom clusters, as shown by the anhedonic sucrose response, increase in contextual fear response, blunted fear response to an ambiguous fear cue, and increase in escape behavior. It's possible that humans with PTSD with reduced VMAT2 expression may also tend to disproportionately experience these symptom clusters. This is a testable hypothesis, given that VMAT2 function is readily assessed in humans using PET ligands (Okamura *et al*, 2010).

Ideas for future VMAT2-mediated treatment. The results of these studies add enthusiasm to the search for a positive allosteric modulator of VMAT2. We have observed biochemical changes (i.e. increased dopamine release capacity, increased neurotransmitter vesicular storage capacity) due to increased VMAT2 protein, but the behavioral phenotypes of increasing VMAT2 function are quite subtle and – as far as we have measured – not deleterious. If anything, increased VMAT2 protein results in a subtle anti-anxiety phenotype and a potential decreased preference for psychostimulants with no concurrent decrease in preference for natural rewards (i.e. sucrose, social interaction). Furthermore, increasing VMAT2 function could have other potentially useful pharmacological benefits in the treatment of the neurodegenerative disorder Parkinson's disease (Lohr and Miller, 2014).

VMAT2 protein expression is known to be modifiable, since at least two compounds—the pituitary adenylate cyclase-activating polypeptide (PACAP) and oxytocin—can produce long-term upregulation of VMAT2 expression in rodent models

(Guillot *et al*, 2008a; Jovanovic *et al*, 2014). However, these compounds either do not cross the blood-brain barrier or exhibit low bioavailability via rapid blood clearance. PACAP is an interesting therapeutic target, as genetic abnormalities in the PACAP receptor have been associated with PTSD symptoms (Ressler *et al*, 2011) There are ongoing efforts to make PACAP into a more stable formulation (Bourgault *et al*, 2011) as well as to make clinically useful oxytocin agonists (Lacivita *et al*, 2017; Manning *et al*, 2012). Past treatments for both PTSD and AUD target specific neurotransmitter systems. Notably, each of these pharmacological strategies includes unwanted side effects, which often contribute to the patient ceasing treatment. Increasing VMAT2 functionality would be a much more subtle, activity dependent pharmacotherapy that could potentially avoid the side-effect profile pitfalls of other monoaminergic drugs. Our lab, in partnership with medicinal chemists at Emory, has already set up an assay that can be used to perform a high-throughput screen of VMAT2-binding compounds using stably-transfected VMAT2+ human embryonic kidney cells in order to identify positive allosteric modulators of VMAT2. If successful, a positive allosteric modulator of VMAT2 may be an exciting potential therapeutic agent for PTSD in humans.

VII. Appendix 1: The effect of D_2 and D_3 receptor blockade on cocaine-induced increase in dopamine release

This chapter includes work that is part of an in-preparation manuscript:

D.F. Manvich*, **R.C. Branco***, A.K. Petko*, K.A. Stout, A.H. Newman, G.W. Miller, D. Weinshenker, C.A. Paladini. 2018. Dual presynaptic and postsynaptic mechanisms in the nucleus accumbens core contribute to the differential modulation of the effects of cocaine in mice following selective antagonism of dopamine D2 vs D3 receptors. *Neuropsychopharmacology*. [in preparation]

*denotes authors contributed equally to this publication. Dr. Manvich performed all behavioral experiments, while Ms. Branco performed neurochemical experiments.

ABSTRACT

Dopamine D_3 receptors are upregulated upon exposure to drugs of abuse and are expressed in brain regions implicated in drug seeking and relapse behaviors. D_3 receptors may therefore be a potential therapeutic target for drug addiction. However, high sequence homology between D_2 and D_3 has long complicated the search for D_3-selective ligands. Recent advancements in receptor-specific pharmacological tools have allowed behavioral and neurochemical studies of the specific effects of D_2 and D_3 receptor antagonism. D_3 and D_2 antagonism exerts opposing behavioral effects: a D_3-selective ligand, PG01037 (PG) enhances cocaine-induced locomotor sensitization while a D_2-selective ligand, L741626 (L7) attenuates cocaine-induced locomotor sensitization. In this study, we tested the presynaptic neurochemical effects of the PG and L7 in an attempt to explain these divergent behavioral effects of dopamine receptor antagonism in male and female C57/BL6 mice. We found that the two drugs exert similar effects on the presynaptic dopamine terminal as measured by fast-scan cyclic voltammetry.

INTRODUCTION

Cocaine abuse has persisted as a major public health concern in the United States, yet currently no FDA-approved pharmacotherapies are available for its treatment. Cocaine's abuse-related effects are predominantly attributed to increases in dopamine levels, particularly within mesocorticolimbic brain pathways. However, most nonselective antagonists have proven unsuccessful in clinical trials of substance abuse treatment, in part because of deleterious side effects.

Dopamine receptors can be classified into two families: the D1-like family (D_1R and D_5R subtypes) and the D2-like family (D_2R, D_3R, and D_4R subtypes). Compounds exhibiting selectively for one of these subtypes may reduce the incidence of side effects while still exerting sought-after effects on cocaine-seeking behavior. The D_3R in particular has emerged as a promising target because it is highly and selectively expressed within target regions of dopaminergic mesolimbic projections known to be involved in the abuse-related effects of cocaine and related psychostimulants (Levant, 1998). Preliminary studies have indicated that pretreatment with both partial agonists or antagonist of the D_3R attenuates several behavioral effects of cocaine in experimental animals (Newman *et al*, 2005, 2012), but the specific neuropharmacological mechanisms underlying these results remain unknown.

Work by Dr. Dan Manvich determined whether selective D_3R antagonism (using PG01037, "PG") alters the behavioral-stimulant effects of acute cocaine in mice. For comparison, the effects of selective D_2R antagonist (L741,626, "L7") were also assessed. D_3R blockade enhances but D_2R blockade attenuates cocaine-induced locomotor

sensitization. PG treatment significantly enhanced cocaine-induced locomotion compared to vehicle-treated mice. Contrastingly, L7 attenuated cocaine-induced locomotion compared to vehicle treated mice.

The goal of this study was to determine the potential presynaptic mechanisms by which D_3R and D_2R antagonism modulates cocaine effects. Since D_2R and D_3R can be both pre- and post-synaptic, and have specific regions of expression in the brain, the known effects of D_2R and D_3R-acting drugs on dopamine release is summarized below:

Effects on DA release	D2	D3	both
Agonist	-D2 agonists inhibited DA release in both dorsal and ventral striatum (Maina and Mathews, 2010) -D2 agonist inhibits dopamine cell firing in VTA, SNpc, and caudate putamen (Bowery *et al*, 1996) -D2 agonist –mediated reduction in striatal DA release can last several hours (Abraini *et al*, 1994) -D2 agonist decreased cocaine potency (McGinnis *et al*, 2016) -CB1 receptor agonist attenuates the inhibitory effects of D2 agonists on dopamine release (O'Neill *et al*, 2009)	-D3 agonist inhibited DA release, much more so in the ventral striatum than in the dorsal striatum (Maina and Mathews, 2010) -D3-preferring agonist increases rate of uptake (Zapata and Shippenberg, 2002) -IP administration of a D3 agonist reduced volume of DA release in the NAc (Gilbert *et al*, 1995) -D3 agonist had no effect on cocaine potency (McGinnis *et al*, 2016)	-D2/D3 agonist inhibits DA release in the NAc (Roberts *et al*, 2006)

Antagonist	-D2 antogonist increases stimulated dopamine release in dorsal and ventral striatum (Stamford *et al*, 1988) -D2 antagonist (haloperidol) primarily exerts its DA enhancing effects by reducing uptake. D2 antagonist modestly increased DA release only at low frequencies (Wu *et al*, 2002) -D2 antagonist partially prevents the amphetamine-induced decrease stimulated DA release (Schmitz *et al*, 2001)	-D3 antagonism alone has little effect on dopamine release in NAc (Roberts *et al*, 2006) -Though it can increase extracellular DA concentrations by blocking uptake (Zapata and Shippenberg, 2002) -D3 antagonist pretreatment potentiates cocaine-induced increase in extracellular DA in NAc in anesthesized rats (Congestri *et al*, 2008) -Cocaine blockade of DAT enhanced by D3 antagonism, but not by D2 antagonism, suggestive of a D3/DAT interaction (McGinnis *et al*, 2016)	-D2/D3 antagonist raclopride increases firing rate and extracellular concentration of DA in DA neurons in the VTA and SNpc (Andersson *et al*, 1994) -In combination with low-dose of psychostimulant modafinal, D2/D3 antagonist raclopride elicits DA transients in dor and ventral striatum. Modafinil alone increases stimulated DA release. (anesthetized rats) (Bobak *et al*, 2016) -animals who were chronically exposed to METH had a smaller increase in dopamine release in response to D2/D3 antagonism and DAT blockade (Robinson *et al*, 2014)

MATERIALS & METHODS

Mice. Adult male and female C57BL/6 mice were used for each assay. Eight animals were used per group. Mice were group housed with *ad libitum* access to food and water in the home cage.

Fast scan cyclic voltammetry (FSCV). FSCV was performed as described in Chapter 3, with the some modifications. FSCV was performed in the nucleus accumbens core of only males between the age of four to seven months. After establishing a stable baseline (aCSF) condition, drug was dissolved at desired concentrations within oxygenated aCSF. Drug conditions for each slice were either: aCSF → 1 uM cocaine → 1 uM cocaine + 1 pM PG01037 → 1 uM cocaine + 100 pM PG01037 → 1 uM cocaine + 1 nM PG01037; aCSF → 1 pM PG01037 → 100 pM PG01037 → 1 nM PG01037; aCSF → 1 uM cocaine → 1 uM cocaine + 1 pM L-741,626 → 1 uM cocaine + 100 pM L-741,626 → 1 uM cocaine + 1 nM L-741,626; aCSF → 1 pM L-741,626 → 100 pM L-741,626 → 1 nM L-741,626. These concentrations were chosen in this order such that each brain slice underwent ascending concentrations of drug sequentially. The slice was incubated in each new drug condition for ten minutes before recording. Relative dopamine release and uptake constants in each drug condition was compared to baseline.

RESULTS

Selective blockade of D_2R or D_3R produces similar effects on cocaine-mediated increases in presynaptic dopamine release. We first quantified stimulated presynaptic dopamine release in the presence of D_2R or D_3R antagonism alone or in the presence of cocaine using *ex vivo* fast scan cyclic voltammetry (FSCV) in the NAc of mouse brain slices. Although the application of L-741,626 modestly trended towards increased dopamine release, one-way repeated measures ANOVA failed to detect a significant main effect of L-741,626 concentration ($F(3,9) = 2.23$, $p = 0.229$) (Fig A1-1A-C). In a test of

dual cocaine and L-741,626 application, there was a significant main effect of treatment condition ($F(4,16) = 18.32$, $p < 0.01$) (Fig A1-1D-F). Post hoc Dunnett's tests were used to compare the application of cocaine alone to all other conditions, which revealed two important findings. First, cocaine enhanced stimulated dopamine release compared to baseline as has been reported previously. Second, while L-741,626 did not significantly affect stimulated dopamine release alone, application of 100 pM potentiated the cocaine-induced increase in dopamine release. The highest concentration of L-741,626 (1 nM) trended towards this same effect but narrowly missed statistical significance.

We next asked whether PG01037 would exhibit similar effects on basal and cocaine-enhanced stimulated dopamine release. We repeated the FSCV experiments described above but substituted L-741,626 with the D_3R antagonist PG01037 in all conditions. Similar to L-741,626, application of PG01037 alone did not significantly alter stimulated dopamine release ($F(3,6) = 0.18$, $p = 0.837$) (Fig A1-2A-C). Application of cocaine again produced the expected potentiation of stimulated dopamine release, and this effect was further enhanced following application of 100 pM and 1 nM concentrations of PG01037 ($F(4,24) = 13.61$, $p < 0.01$, post-hoc Dunnett's test compared to cocaine alone, $p < 0.05$) (Fig A1-2D-F).

DISCUSSION

Previous work has shown that selective antagonism of D_2R via L7 functionally antagonizes the locomotor-stimulant effects of cocaine. By contrast, selective antagonism of D_3R functionally enhances the locomotor-stimulant effects of cocaine. To help

understand the mechanism of these opposing behavioral results, we performed FSCV. Taken together, the FSCV studies indicate that both selective D_2R or D_3R antagonism produced a facilitation of cocaine-induced increases in peak presynaptic DA release within the NAc.

It is noteworthy that these effects were observed at concentrations of each drug that failed to alter basal dopamine release. The finding that both D_2R and D_3R antagonism similarly potentiated cocaine-induced dopamine release indicates that this is likely not the mechanism by which they imparted opposing influences on cocaine's locomotor stimulant effects. Addition of L7 to a cocaine bath solution slightly increases cocaine-induced stimulated dopamine release while addition of PG to a cocaine bath solution dramatically increases cocaine-induced stimulated dopamine release.

Since L7 and PG act similarly on dopamine release both alone and in their interaction with cocaine effects, it would be helpful to perform electrophysiology on post-synaptic neurons to record differential responses to these drugs. Likely, the antagonists are acting on presynaptic dopamine receptors to increase dopamine release in a way that interacts with presence of cocaine. These results point to D_2R selective blockade as an interesting therapeutic strategy for the treatment of cocaine dependence.

FIGURES

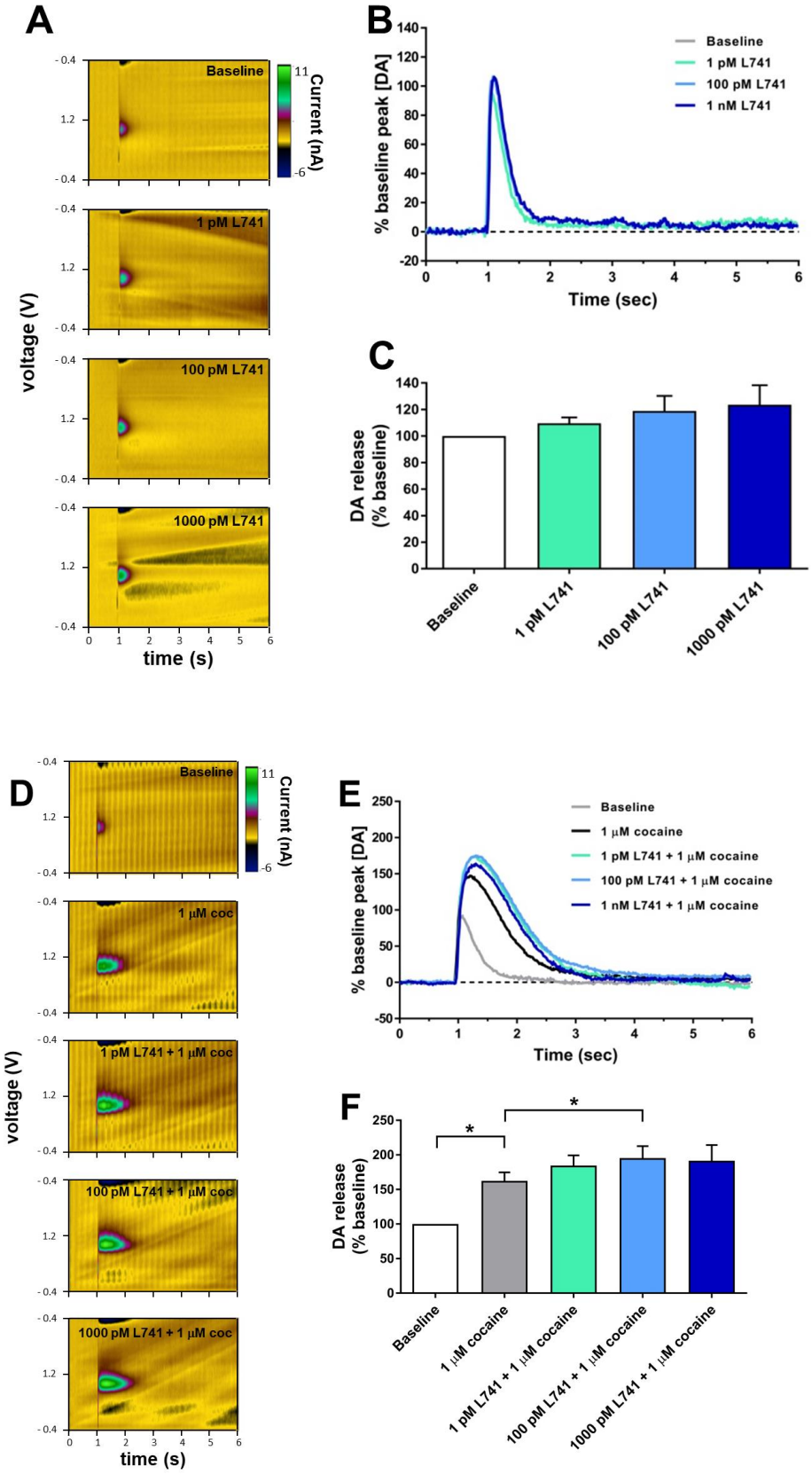
A
Baseline
1 pM L741
100 pM L741
1000 pM L741
Current (nA)
11
-6
voltage (V)
time (s)
B
Baseline
1 pM L741
100 pM L741
1 nM L741
% baseline peak [DA]
Time (sec)
C
DA release (% baseline)
Baseline
1 pM L741
100 pM L741
1000 pM L741
D
Baseline
1 μM coc
1 pM L741 + 1 μM coc
100 pM L741 + 1 μM coc
1000 pM L741 + 1 μM coc
Current (nA)
voltage (V)
time (s)
E
Baseline
1 μM cocaine
1 pM L741 + 1 μM cocaine
100 pM L741 + 1 μM cocaine
1 nM L741 + 1 μM cocaine
% baseline peak [DA]
Time (sec)
F
DA release (% baseline)
*
*
Baseline
1 μM cocaine
1 pM L741 + 1 μM cocaine
100 pM L741 + 1 μM cocaine
1000 pM L741 + 1 μM cocaine

Figure A1-1. Bath administration of L7 and cocaine results in increased stimulated presynaptic dopamine release. A. Representative colorplots of dopamine release under ascending bath concentrations of L7. B. Voltammogram of dopamine release under ascending bath concentrations of L7. C. As L7 bath concentration increases, there is a non-significant trend towards modestly increased stimulated dopamine release. D. Representative colorplots of dopamine release under ascending bath concentrations of L7 in the presence of 1 uM cocaine. E. Voltammogram of stimulated dopamine release under ascending bath concentrations of L7 in the presence of 1 uM cocaine. E. 1 uM cocaine increases stimulated dopamine release compared to baseline condition, and application of 100 pM L7 further potentiates the dopamine-releasing effects of cocaine. * $p < 0.05$

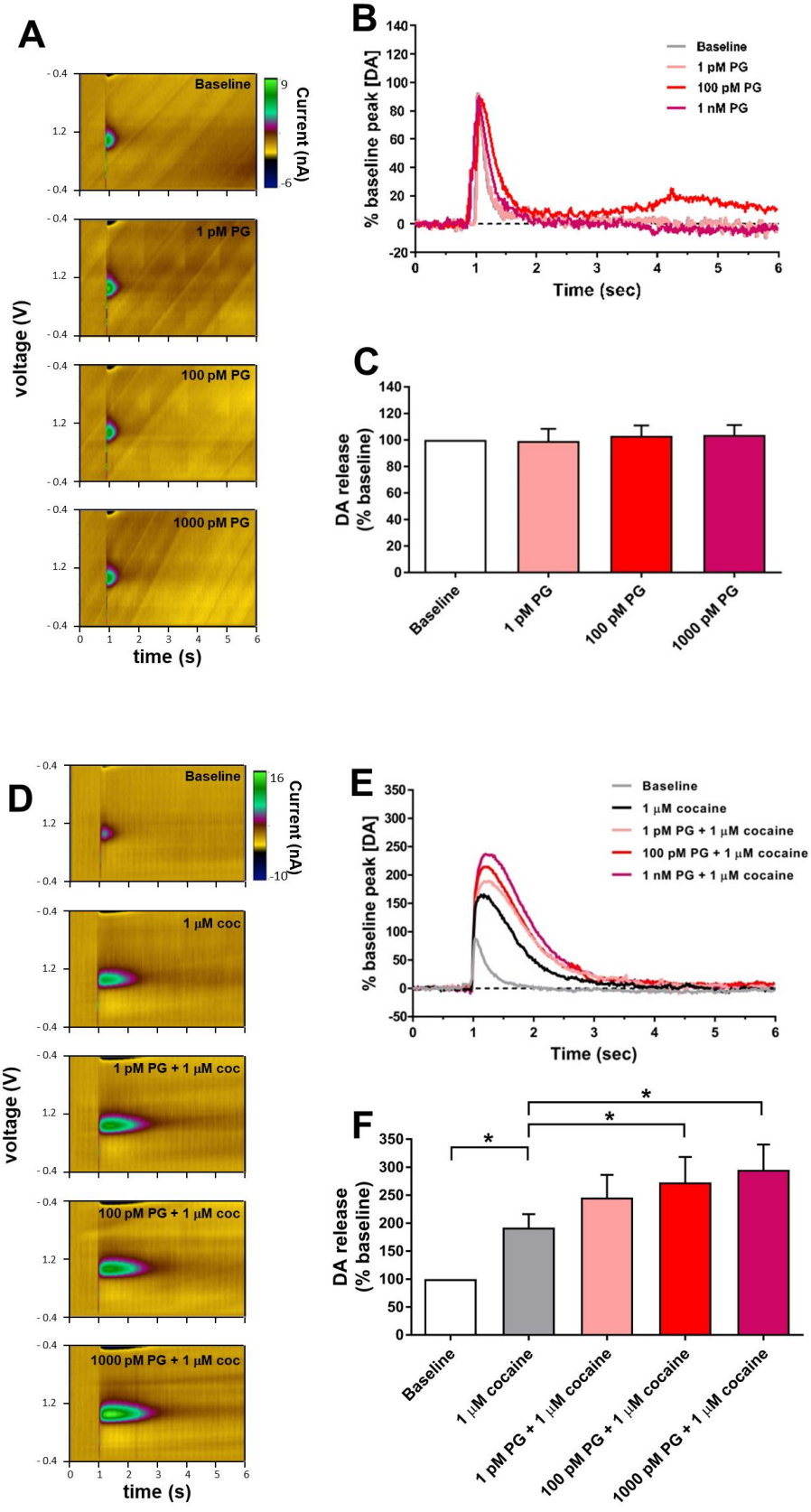
A
Baseline
1 pM PG
100 pM PG
1000 pM PG
Current (nA)
9
-6
voltage (V)
time (s)
B
Baseline
1 pM PG
100 pM PG
1 nM PG
% baseline peak [DA]
Time (sec)
C
DA release (% baseline)
Baseline
1 pM PG
100 pM PG
1000 pM PG
D
Baseline
1 µM coc
1 pM PG + 1 µM coc
100 pM PG + 1 µM coc
1000 pM PG + 1 µM coc
Current (nA)
16
-10
voltage (V)
time (s)
E
Baseline
1 µM cocaine
1 pM PG + 1 µM cocaine
100 pM PG + 1 µM cocaine
1 nM PG + 1 µM cocaine
% baseline peak [DA]
Time (sec)
F
DA release (% baseline)
Baseline
1 µM cocaine
1 pM PG + 1 µM cocaine
100 pM PG + 1 µM cocaine
1000 pM PG + 1 µM cocaine

Figure A1-2. Bath administration of PG and cocaine results in increased stimulated presynaptic dopamine release. A. Representative colorplots of dopamine release under ascending bath concentrations of PG. B. Voltammogram of dopamine release under ascending bath concentrations of PG. C. As PG bath concentration increases, there is a non-significant trend towards modestly increased stimulated dopamine release. D. Representative colorplots of dopamine release under ascending bath concentrations of PG in the presence of 1 uM cocaine. E. Voltammogram of stimulated dopamine release under ascending bath concentrations of PG in the presence of 1 uM cocaine. E. 1 uM cocaine increases stimulated dopamine release compared to baseline condition, and application of 100 pM or 1000 PG further potentiates the dopamine-releasing effects of cocaine. * $p < 0.05$

Chapter VIII. Appendix 2. Levodopa and dopamine dynamics in Parkinson's disease metabolomics

This chapter is adapted from a preprint manuscript:

Rachel C Branco, William Ellsworth, Megan M Niedzwiecki, Laura M Butkovich, Doug I Walker, Daniel E Huddleston[4], Dean P Jones, Gary W Miller. (2018). BioRxiv. https://doi.org/10.1101/306266

ABSTRACT

Parkinson's disease (PD) is a progressive neurological disorder caused by a combination of genetic and environmental factors. Metabolomics is a powerful tool that can be used to screen for potential biomarkers, exogenous toxicants, and metabolic network changes associated with disease states. Here, we used high-resolution metabolomics to compare over 10,000 plasma metabolic features from older adults with and without PD in an untargeted approach. We performed a network analysis that demonstrates that the presence of the PD drug levodopa influences variation observed between PD and control patients. Metabolome wide association studies and discrimination analysis identified significant differentiation in the metabolomics profile of older adults with and without PD. Notably, 15 metabolic features (ten of which we putatively identified) differed between PD and control adults with $p < 0.05$ and a corrected false discovery rate less than 20%. Furthermore, 13 metabolic networks were identified to be functionally different between PD and non-PD patients. Lastly, the dopaminergic toxic intermediate DOPAL differed between PD and non-PD populations, which supports the dopaminergic sequestration model of PD. These individual metabolites and metabolic networks have been implicated in past PD pathogenesis models, including the beta-carboline harmalol and the glycosphingolipid metabolism pathway including the ganglioside GM2. We recommend that future studies take into account the confounding effects of levodopa in metabolomic analyses of disease versus control patients, and encourage validation of several promising metabolic markers of PD.

Statement of impact. Prognostic diagnosis of disease is key for identifying treatment options that slow disease progression and improve patient quality of life. This is particularly important in Parkinson's disease, where patients could greatly benefit from treatment before their latent sickness becomes problematic. Past studies have compared the blood of Parkinson's patients with the blood of healthy adults in an effort to find a biomarker for Parkinson's disease—however, in most of these past studies, the patients with Parkinson's disease were taking the Parkinson's medication levodopa. In our study, we analyzed the plasma metabolomics profiles of people with and without Parkinson's disease. We found that the presence or absence of levodopa was the main difference between the blood of people with and without Parkinson's disease. Furthermore, levodopa was associated with alterations in other metabolic pathways in a way that makes it hard to determine which differences are due to the disease and which are drug-related. Despite this complicating factor, we identified compounds and pathways that differ between Parkinson's and control patients, including harmalol and the glycosphingolipid pathway. With further testing, these markers may help doctors identify Parkinson's risk earlier in life.

INTRODUCTION

Parkinson's disease (PD) is a common progressive neurodegenerative disorder. Though PD pathology affects multiple systems, the most distinctive symptom of PD is motor dysfunction, including bradykinesia, rigidity, and postural instability (Beitz, 2014). PD is caused by the loss of nigrostriatal dopamine neurons (Hornykiewicz, 1970), though

other brain regions are affected in PD pathology (Braak and Braak, 1991; Hornykiewicz, 1998). At the time of PD diagnosis, approximately 60% of nigrostriatal dopamine neurons are already lost (Dauer and Przedborski, 2003). To counteract the loss of dopamine neurotransmission after dopamine cell loss, patients take an oral medication containing levodopa (L-dopa), a dopamine precursor that can cross the blood-brain barrier and helps overcome the paucity of endogenous dopamine in the brain (Birkmayer and Hornykiewicz, 1962). In this way, L-dopa acts to slow the progression of motor symptoms (Hornykiewicz, 2017). However, there are no treatments to either halt or reverse PD progression. Despite the cluster of unwanted complications associated with treatment, L-dopa remains the mainstay pharmacotherapy for PD.

Because earlier identification of PD is critical to effective treatments, research has focused on the identification of biomarkers, protective factors, and/or relevant pathways that characterize PD risk and pathology. High-resolution metabolomics methods provides a powerful tool to characterize the molecular profile present in biological samples. Untargeted metabolomics can simultaneously characterize thousands of endogenous and exogenous compounds within a biological sample – collectively called the *metabolome* (Alonso *et al*, 2015; Gowda *et al*, 2008; Uppal *et al*, 2016; Yu *et al*, 2013).

Due to the treatment considerations of sampling human patients, most metabolomics studies of human PD have sampled from PD patients that are actively taking L-dopa or that are L-dopa deprived for a only short period of time prior to sample collection (Chang *et al*, 2018; Luan *et al*, 2015b; Roede *et al*, 2013). The first aim of this study was to test how much L-dopa accounts for the metabolic differences between PD patients and controls. We found that the majority of metabolic profile differences between Parkinson's

and control patients can be explained by the presence of L-dopa, even in metabolic networks theoretically independent from dopamine metabolism. In this way, this paper acts as a warning to future biomarker and metabolomics researchers to account for the effects of treatment when evaluating effects of pathology.

The second aim of this study was to evaluate biomarker metabolites or pathways that differ between PD and control patients. Despite the complicating effects of L-dopa, we identified metabolic differences that are likely due to PD pathology rather than the L-dopa treatment. Our findings are consistent with past experimental literature suggesting that the antioxidant beta-carboline harmalol and the glycosphingolipid pathway are altered in PD and provides the first demonstration showing these metabolic variations are detectable in peripheral blood. Furthermore, this metabolic analysis underscores the altered dopamine dynamics present in PD patients.

MATERIALS & METHODS

This study was approved by the human subject committee of Emory University. Subjects participated after written informed consent was obtained in accordance with the Declaration of Helsinki.

Study Population Characteristics. The plasma samples analyzed were collected from patients recruited through the Emory Movement Disorders Clinic and controls recruited in the Atlanta area from 2012-2013. The final study population contained 21 PD

patients and 13 control patients. Demographic information was collected from all participants and is summarized in Table 1.

Clinical Data Collection. Clinical data was collected from all PD patients, including disease duration and daily L-dopa equivalent dosage of antiparkinsonian medications. All participants had UPDRS-III motor assessments by a fellowship-trained movement disorders neurologist (Goetz *et al*, 2007). All participants had cognitive assessments with the Montreal Cognitive Assessment (MOCA), and all participants completed the Non-Motor Symptoms Questionnaire (NMSQ) (Chaudhuri *et al*, 2006; Nasreddine *et al*, 2005). Prior to plasma collection, patients were not required to fast nor to stop their PD medications. Exams and sample collections were typically conducted between 9 am and 11 am. Blood samples were collected in EDTA tubes, and immediately placed on ice. They were then transferred on ice an centrifuged at 2200 RPM for 15 min. The plasma was transferred to a transport vial and frozen at -80 °C until mass spectrometry analysis. The time from sample collection to storage in the -80 °C freezer was less than 2 hours.

Mass spectrometry. Samples were prepared as previously described (Roede *et al*, 2013). Briefly, 65 μL of plasma was treated with 130 μL of acetronitrile containing a mixture of 14 stable isotope standards. After mixing and incubation at 4 °C for 30 min, precipitated proteins were pelleted via centrifugation for 10 min at 16,100 x *g* at 4°C. Supernatants were transferred to autosampler vials and stored at 4°C until analysis. Sample extracts were analyzed in triplicate by liquid chromatography-Fourier transform mass

spectrometry (Dione Ultimate 3000;Thermo Scientific Q-Exactive HF High-Resolution Mass Spectrometer) with 10 uL injection volume and a formic acid/acetonitrile gradient as described previously (Walker *et al*, 2016). Electrospray ionization was used in the positive ion mode. Mass spectral data were collected at a resolution of 70,000 and scan range 85 to 1250 *m/z* (Uppal *et al*, 2013; Yu *et al*, 2013). Raw data files were extracted and aligned using apl CMS with modifications by xMSanalyzer with each feature uniquely defined by *m/z* (mass-to-charge ratio), retention time, and sample ion intensity (integrated ion intensity for the peak*).*

Metabolomics data analysis. R was used to analyze the metabolomics data. We first eliminated features that had greater than 35% variability within technical replicates. This reduced the data set from a total of 10,471 m/z values to 9,071 m/z values. Features detected only in PD cases were not removed from the dataset, as the potential measurement of exogenous compounds was one of the major aims of this study. Since a detection value of zero did not imply the absence of the feature, but rather that the amount of feature present was below the threshold of detection, we imputed half of the minimum detected value to all zero values. We then applied a generalized log transformation as described in MetaboAnalyst (Xia *et al*, 2016), which resulted in an approximately normal distribution.

To determine which features differed between PD versus control plasma, two-sample t-tests were conducted for each feature. P-values were adjusted using the FDR correction; features were sorted using the adjusted p-values. This analysis was performed using MetaboAnalyst software (Xia *et al*, 2016) and original R code to verify results. To determine which metabolic pathways were most affected by PD drug treatments, we also

performed a metabolome-wide association study restricted to PD patients wherein we calculated the correlations of the abundance of primary PD drug metabolite (*m/z* = 212.092, retention time = 71) with every other metabolite feature, then created a network of metabolites that most significantly correlated with PD.

The degree of association between two variables was analyzed via linear correlation analysis and reporting the r squared value and direction of association where appropriate.

Pathway analyses were performed in Mummichog (Li *et al*, 2013). The "force primary ion" option was chosen, ensuring that any predicted metabolites were present in at least their primary adduct ($M+H^+$). A *p* threshold of 0.05 was selected. Pathways identified in Mummichog were visualized in Cytoscape (Shannon *et al*, 2003). Identity of networks was visualized using Tableau (Seattle, Washington).

For orthogonal partial least squares-discriminant analysis (OPLS-DA), the data was mean-centered prior to analysis (van den Berg *et al*, 2006; Vinaixa *et al*, 2012). OPLS-DA was performed and visualized both using R and MetaboAnalyst tools.

Putative identities of metabolite features was determined via multiple parallel methods: a custom deconvolution and identification algorithm (Emory University, Atlanta, Georgia), xMSanalyzer (Uppal *et al*, 2013), and manual lookup in various online metabolite databases (Human Metabolome Database, Kyoto Encyclopedia of Genes and Genome) (Tanabe and Kanehisa, 2012; Wishart *et al*, 2012).

RESULTS

There were no differences in the proportions of men and women between the PD and control group, but differences were found in age, race, and educational level, with the PD group more likely to be Caucasian, younger, and less educated. As expected, PD and control groups also differed in motor and non-motor symptoms of PD (Table A2-1).

We performed t-tests to identify *m/z* features differentially expressed in patients with PD based upon a false discovery rate (FDR) correction threshold of 20%. Fifteen *m/z* features were different between the two groups (Figure A2-1, Table A2-2). Predictably, the five top annotated compounds were either PD drugs or their metabolites, all of which were elevated in PD patients (Figure A2-2A). These PD drug metabolites met at least 2 criteria for identity, i.e., accurate mass match to predicted adduct (Level 5 identity (Schymanski *et al*, n.d.)), co-elution with authentic standard, ion dissociation spectrum matching that of known compound, or association with known pathway or metabolic network (Table A2-3), are indicated by metabolite name. Other features are denoted by associated accurate mass match to known metabolite (Level 5 identity) along with *m/z* and retention time, as indicated. Additionally, the toxic dopamine metabolite 3,4-dihydroxyphenylacetaldehyde (DOPAL) was elevated in PD patients (Figure A2-2B). Several compounds, including harmalol, were elevated in control patients relative to PD patients (Figure A2-2C). Five of the fifteen metabolic features provided no matches in chemical databases.

Each patient's L-dopa equivalent dose was highly correlated with the primary L-dopa metabolite (*m/z* 212.092, $r^2 = 0.6559$). Furthermore, L-dopa metabolite abundance and Unified Parkinson's Disease Rating Scale Part III (UPDRS) scores were highly correlated ($r^2 = 0.4562$), indicating that, as expected, patients with more severe PD symptoms tended to have more L-dopa in their blood.

We performed orthogonal partial least squares-discriminate analysis (OPLS-DA), which uses supervised learning to determine the principal components that most differentiate populations across multiple dimensions (Wiklund *et al*, 2008). Using OPLS-DA, the metabolic profile of PD and control patients differentiated into two distinct groups (Figure A2-3). Within the OPLS-DA analysis, we identified features that most contributed to the model using the covariance and correlation between the features and the class designation. As expected, the features that were most influential in driving the OPLS-DA model corresponded to the features identified as most significantly different between PD and controls in the t-test analysis. To evaluate if OPLS-DA merely stratified patients according to presence of L-dopa, we completed a second OPLS-DA after manually eliminating signals corresponding to L-dopa or direct L-dopa metabolites. Even with these PD drug features removed, the two populations differentiated into two distinct groups (Figure A2-5).

However, the removal of L-dopa and its direct metabolites from the OPLS-DA analysis does not guarantee that the downstream effects of L-dopa are eliminated. In order to test the correlation between L-dopa and other metabolites, we performed a separate analysis to predict which metabolites correlated with L-dopa (Figure A2-6). We then performed pathway analysis to elucidate the metabolic pathways that were altered between PD and control patients (Fig A2-7). By comparing the results of these metabolic pathway analyses, we identified several major metabolic pathways altered in PD patients and correlated with plasma L-dopa (Figure A2-4, Table A2-4). Notably, every metabolic network that was different between PD and control plasma metabolites was also affected by the presence of L-dopa.

DISCUSSION

L-dopa confounds PD versus control comparisons. The top five differential features measured in PD and control patients' plasma were a PD drug and its metabolites. The elevated levels of these L-dopa metabolites in PD patient plasma acted as a de facto positive control. The known oral dose of L-dopa strongly correlated with *m/z* 212.092, which was identified as 3-methyltyrosine. Therefore, we deemed the *m/z* 212.092 feature as an acceptable proxy for L-dopa concentration in patient plasma samples:

Feature reduction analysis using OPLS-DA showed that the metabolic profiles of PD versus control patients were distinctly different across two principal components. We also performed OPLS-DA on PD versus control patient plasma metabolites after manually removing the metabolic features corresponding to L-dopa or direct L-dopa metabolites. This approach also resulted in distinct clustering of PD and control populations across two principal components. However, this result does not prove that PD drugs did not drive the separation of the two groups, as the biological response to L-dopa could have driven the separation between PD and control groups despite the omission of L-dopa itself. Indeed, L-dopa is correlated with many metabolic networks, so it is likely that downstream effects of L-dopa alter critical metabolite features that define each metabolic profile and underlie the OPLS-DA identified differences between PD and control patients.

The comparison of metabolic pathways between PD and control patients revealed a number of biological pathways that were different in PD. However, in this analysis, it was impossible to tell whether metabolic pathways are altered due to PD pathology or by

PD treatment. To this end, we performed a separate pathway analysis restricted to PD patients to identify which biological pathways were most strongly associated with L-dopa. All pathways that were identified using metabolites that were different between PD and control patients were also correlated with the presence of L-dopa. This includes networks that we would expect to be perturbed by L-dopa administration, such as tyrosine and biopterin metabolism. However, many of these pathways were correlated with L-dopa despite the lack of any *a priori* suspicion of biological interaction. In previous studies, these pathways were assumed to be altered in PD patients due to PD pathology, but the analysis shows that L-dopa is a confounding factor to that interpretation.

These results provide a warning to future metabolomics studies using prevalent disease cases the extent to which treatment of the disease confounds identification of underlying pathology. Since L-DOPA levels correlate well with many non-dopamine metabolic pathways, simply removing L-DOPA from the dataset after the data collection is likely not sufficient to reduce confounding effects of the drug.

It is not surprising that the treatment of the condition (in this case, L-dopa for PD) has a close relationship with pathways that are pathological in the disease state (i.e. dopamine metabolism). Dopamine dynamics are undoubtedly altered in PD patients (Hornykiewicz, 1970, 1998; Pifl *et al*, 2014) — it is impossible to tease apart the contribution of the treatment and of the disease in this paradigm. A small number of studies have looked at metabolomics of peripheral fluids in PD (Chang *et al*, 2018; Luan *et al*, 2015b; Roede *et al*, 2013), few of which include PD patients without L-dopa (Ahmed *et al*, 2009; Bogdanov *et al*, 2008; Trupp *et al*, 2014). Several studies have looked at plasma or urine metabolites in PD versus controls, and found similar results to those described here

(Bogdanov *et al*, 2008; Hatano *et al*, 2016; Johansen *et al*, 2009; Luan *et al*, 2015a, 2015b; Roede *et al*, 2013; Trupp *et al*, 2014). However, since these patients did not abstain from PD medication, these results are likely driven by PD treatment rather than PD pathology. This highlights a challenge facing these type of biomarker studies and underscores the need for longitudinal studies and creative ways to correct for treatment effects.

Peripheral markers of dopamine dynamics. Our analysis identified elevated levels of DOPAL in the plasma of PD patients compared to controls. DOPAL is a cytosolic product of dopamine that is metabolized by monoamine oxidase-A in the outer mitochondrial membrane (Eisenhofer *et al*, 2004). DOPAL is a neurotoxin that selectively kills dopamine neurons (Burke *et al*, 2003; Mattammal *et al*, 1995; Panneton *et al*, 2010). Toxic DOPAL buildup due to insufficient sequestration by vesicular proteins has been hypothesized to be the precursor to dopamine cell death in PD pathogenesis (Goldstein *et al*, 2013, 2015). It is possible that L-dopa treatment in our PD patient population mediated the elevated DOPAL content. However, while in the total patient population L-dopa dosage and DOPAL plasma concentration were associated ($r^2 = 0.365$), this correlation was absent when we restricted analysis to PD patients only. We were surprised to observe that DOPAL content differed between PD and control patients in the peripheral blood. The detection of DOPAL in plasma suggests that a test could be devised to measure the DOPAL:DA ratio as an indicator of vesicular dopamine function.

Differences between PD and control plasma. Despite the confounding effect of L-dopa in this analysis, variations in harmalol and ganglioside GM2 (a metabolite of the

glycosphingolipid pathway) associated with PD suggests additional biological changes were detected. Both were identified as elevated in control patient plasma compared to PD patients. To our knowledge, there is not a readily apparent biological mechanism through which PD medication might lower endogenous levels of either harmalol or ganglioside GM2. Therefore, these differences may be due to pathological or physiological differences between patients with and without PD diagnosis, rather than due to an effect of taking PD medication.

Harmalol is an indole beta-carboline alkaloid found in a variety of tissues, including brain, and in a variety of consumable plants, most notably in the leaves of tobacco plants (Airaksinen and Kari, 1981; Holmstedt and Lindgren, 1967; Moloudizargari *et al*, 2013). Despite early therapeutic promise (Cooper and Gunn, 1931), studies demonstrating neurotoxic effects of beta-carbolines dampened clinical enthusiasm (Cobuzzi *et al*, 1994; O'Hearn and Molliver, 1993; Storch *et al*, 2004). Later studies found that at low doses, beta-carbolines can be neuroprotective, as demonstrated in PC12 cells (Han *et al*, 2005; Kim *et al*, 2001; Park *et al*, 2003), primary cell culture (Polanski *et al*, 2010), and in a rat model of PD (Wernicke *et al*, n.d.). Beta-carbolines, particularly harmalol and harmine, exert this effect at the surface of the mitochondrial membrane of dopaminergic cells, preventing oxidative damage from free-radicals (Pari *et al*, 2000).

Certainly, our findings that harmalol is elevated in plasma from control patients is exciting given the therapeutic potential of the alkaloid. It is unclear whether control patients display elevated concentrations of harmalol due to an elevated endogenous production of the chemical, or if their elevated harmalol levels are due to a history of consuming of harmalol-containing products. This difference could point to whether individuals who do

not develop PD have an antioxidant-mediated protection factor, or whether they engage in habits that lower the risk of PD development. As beta-carboline alkaloids are found in tobacco plants and nicotine is known to independently reduce risk of developing PD (Dunn *et al*, 2017), the elevated harmalol in control patients may be an artifact of the protective effect of smoking (Soto-Otero *et al*, 1998). Although we cannot rule out the possibility, we do not believe it is likely that smoking drove the difference in harmalol in these patients. Concentration of plasma harmalol was not associated with plasma cotinine, a marker for smoking activity ($r^2 = 0.073$). Nonetheless, this does not rule out confounding entirely. For instance, participants in the study did not fast prior to serum collection, so it is plausible that dietary differences between cases and controls could account for some of the metabolic variability. Furthermore, while we have no knowledge of link between administration of L-dopa and changes in beta-carboline metabolism, this experiment cannot rule out the effect of PD drugs. In our sample of PD patients, L-dopa plasma concentration did weakly correlate with harmalol concentration ($r^2 = 0.1901$), while other studies have shown no correlation (Kuhn *et al*, 1996). In addition, patients may or may not have been on some other medication that could have confounded the observed metabolic differences. Lastly, it is unknown whether blood plasma harmalol concentration correlates with harmalol levels in the brain. Elevated plasma levels of a compound do not always correspond with elevated levels in the brain (Grimmer *et al*, 2009), and there is evidence that PD patients actually show elevated beta-carboline levels in cerebrospinal fluid (Kuhn *et al*, 1996; Matsubara *et al*, 1995).

Gangliosides are a group of glycosphingolipid compounds that are especially common in the brain but are also found in blood. Gangliosides have been implicated in a

variety of neurodegenerative diseases (Kolter, 2012). We identified the ganglioside GM2 and the glycosphingolipid biosynthesis metabolic pathway in our pathway analysis. GM2 levels were lower in PD patients and correlated negatively with motor function as measured by UPDRS-III ($r = -0.492$). Our work implies that reduced peripheral GM2 could indicate central nervous system dysfunction. GM1 ganglioside is a potential therapeutic target for PD, and a recent study has further suggested GM1's disease-modifying effect on PD (Bisel *et al*, 2014; Schneider *et al*, 2015). While GM1 has been extensively implicated in human PD, the role of GM2 remains unclear. Other researchers have found that deletion of GM2/GD2 synthase—the enzyme that produces GM2 and GD2 gangliosides—causes a Parkinsonian phenotype, likely due to downstream effects on GM1 (Wu *et al*, 2011). Furthermore, the pathological fibrillation of α-synuclein, which is characteristic of PD, can be inhibited by GM2 (and even more so by GM1) (Martinez *et al*, 2007). As with harmalol, confounding—whether due to diet, L-DOPA administration, or some other factor—cannot be ruled out entirely. However, considered together, this analysis points towards ganglioside metabolism and GM2 in particular as potential biomarkers or therapeutic targets for future research. Our analysis identified elevated levels of DOPAL in the plasma of PD patients compared to controls. DOPAL is a cytosolic product of dopamine that is metabolized by monoamine oxidase-A in the outer mitochondrial membrane (Eisenhofer *et al*, 2004). DOPAL is a neurotoxin that selectively kills dopamine neurons (Burke *et al*, 2003; Mattammal *et al*, 1995; Panneton *et al*, 2010). Toxic DOPAL buildup due to insufficient sequestration by vesicular proteins has been hypothesized to be the precursor to dopamine cell death in PD pathogenesis (Goldstein *et al*, 2013, 2015). It is possible that L-dopa treatment in our PD patient population mediated the elevated DOPAL content.

However, while in the total patient population L-dopa dosage and DOPAL plasma concentration were associated ($r^2 = 0.365$), this correlation was absent when we restricted analysis to PD patients only. We were surprised to observe that DOPAL content differed between PD and control patients in the peripheral blood. The detection of DOPAL in plasma suggests that a test could be devised to measure the DOPAL:DA ratio as an indicator of vesicular dopamine function. The ability to measure DOPAL levels in plasma allows for the possibility of a future 'dopamine challenge' assay in humans, similar to a cortisol challenge for diagnosing depression. In such an assay, a patient suspected of PD would have their blood drawn before and after an injection of L-dopa. In non-PD patients, the DOPAL:DA ratio should stay relatively constant, as vesicular monoamine transporters store the L-dopa-induced dopamine into vesicles as quickly as it is synthesized. However, in PD patients, where vesicular inefficiency is a hallmark of the disease, the DOPAL:DA ratio would increase dramatically as a result of L-dopa. This assay would be more informative than a simple DOPAL:DA ratio without L-dopa, as the reduced dopamine content observed in PD patients would make the ratio artificially low. Since L-dopa is well-tolerated in non-PD patients and PD patients would not suffer severe deleterious consequences from a short-term L-dopa fast, this 'L-dopa challenge' paradigm could sidestep the ethical problem of taking PD patients off medication long-term in order to get cleaner metabolomics data while still providing information about PD pathology. It is important to note that this approach may face separate ethical challenges. Regardless, we see it as a potentially interesting avenue for future studies.

Conclusions. Our analysis shows that the presence of L-dopa widely influences the blood plasma metabolome in patients with PD. The influence of L-dopa may be more far-reaching than previously thought: our analysis shows that the effects of PD medications on the metabolome cannot simply be controlled for by removing direct metabolites of the medications. We caution other researchers to seek creative solutions when searching for potential diagnostic and/or prognostic biomarkers in future studies. Lastly, we highlight two metabolites of interest that were elevated in control versus PD serum, harmalol and the ganglioside metabolic pathway.

FIGURES

Characteristic	PD (n=21)	Control (n=13)	p-value
Sex			0.73
Male	10 (47.6%)	5 (38.5%)	
Female	11 (52.4%)	8 (61.5%)	
Age (mean ± sd)	61.7 ± 8.0	71.3 ± 5.4	0.001 **
Race			0.048 *
Caucasian	21 (100%)	10 (76.9%)	
African American	0 (0%)	3 (23.1%)	
Educational level			
Years of education	15.7	17.8	0.035 *
Less than high school	1 (4.8%)	0 (0%)	
High school	3 (14.3%)	1 (7.7%)	
Some college	3 (14.3%)	0 (0%)	
Associate/vocational	1 (4.8%)	0 (0%)	
Bachelor's	8 (38.1%)	5 (38.5%)	
Master's	5 (23.8%)	5 (38.5%)	
Doctorate	0 (0%)	2 (15.4%)	
PD characteristics			
UPDRS-III score	10.9 ± 6.5	2.6 ± 2.14	0.0001 ***
Disease duration	7.7 ± 3.4 years	N/A	0.35
L-dopa equivalent	817.8 ± 372.8	N/A	<0.0001 ***
MOCA score	27.6 ± 2.1	26.6 ± 3.7	
NMSQ score	3.7 ± 2.5	9.2 ± 3.8	

Table A2-1. Description of study participants. 21 PD patients and 13 aged controls were studied. Differences between groups were calculated by Fisher's exact test for Sex and Race, and t-test for all other categories.

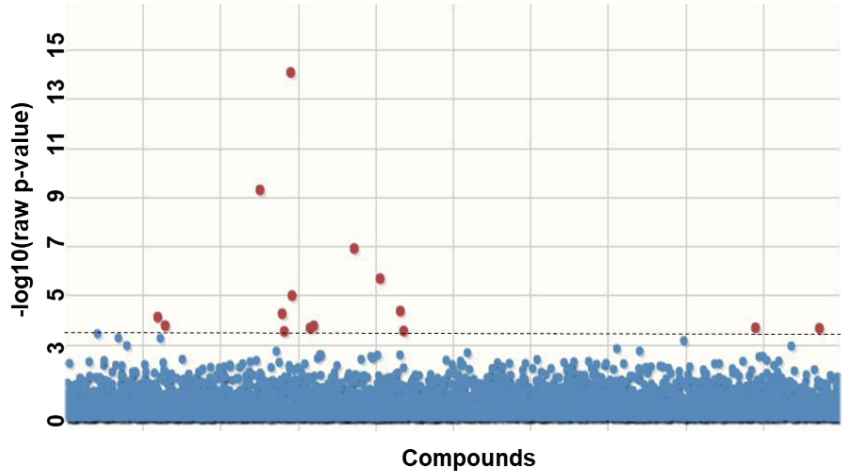

Figure A2-1. Manhattan plot for the untargeted MWAS. The x axis contains features arranged in order of *m/z*, and the y axis contains –log10 of the unadjusted p value.

m/z	RT (s)	Putative identity	Function	Higher in	p-value	FDR
212.092	71	3-methoxytyrosine	PD drug metabolite	PD	8.33E-15	7.56E-11
195.0653	71	3-methoxytyrosine	PD drug metabolite	PD	5.17E-10	2.34E-06
256.0555	66	3-methoxytyrosine	PD drug metabolite	PD	1.27E-07	0.000383
278.0327	142	DOPA sulfate	PD drug metabolite	PD	2.13E-06	0.004821
213.0951	73	3-methoxytyrosine	PD drug metabolite	PD	1.05E-05	0.019062
292.0489	143	Unknown	Unknown	PD	4.46E-05	0.067475
207.1104	69	Unknown	Unknown	Control	5.74E-05	0.074343
149.0599	74	Unknown	Unknown	PD	7.87E-05	0.089226
153.0548	76	DOPAL	DA metabolite	PD	0.000177	0.15867
225.0826	70	Unknown	Unknown	Control	0.000178	0.15867
916.6712	55	glycerophospolipids	Lipid membrane	PD	0.000215	0.15867
223.0846	69	Harmalol	Antioxidant	Control	0.000219	0.15867
1427.752	132	Ganglioside GM2	Lipid membrane	Control	0.000227	0.15867

294.846	64	gylcerophospholipids	Lipid membrane	Control	0.000292	0.18283
208.1141	69	Unknown	Unknown	Control	0.000302	0.18283

Table A2-2. 15 compounds resulted from the untargeted MWAS comparing features in PD patients against control patients. Using the Human Metabolome Database (HMDB), likely candidates for 10 of the 15 metabolic features were identified; the remaining 5 were provided no matches.

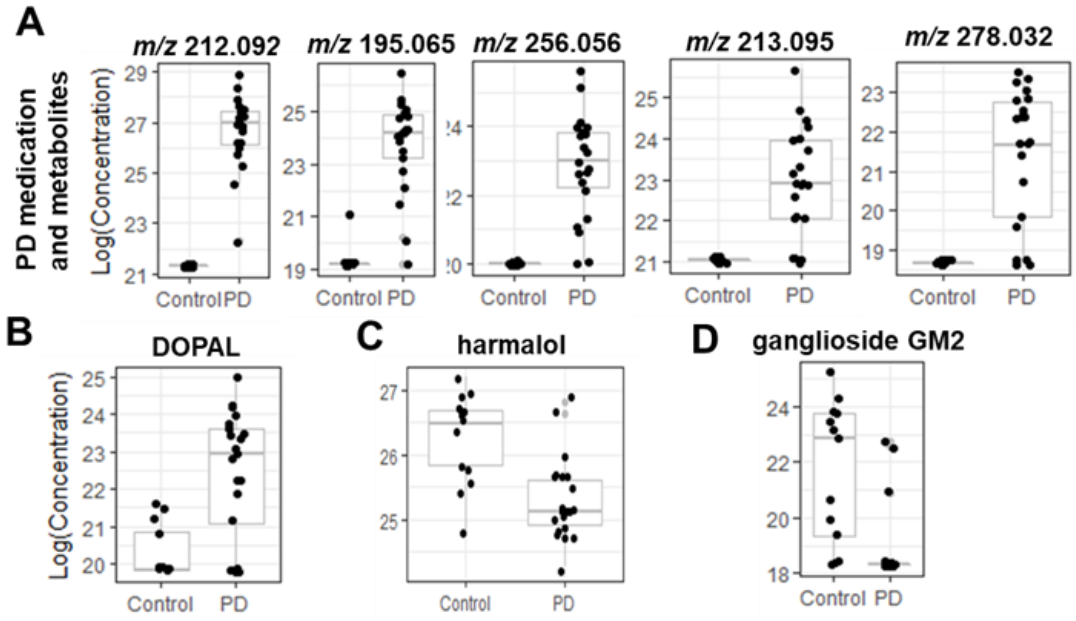

Figure A2-2. Boxplots for the 8 annotated compounds from the untargeted MWAS.

The x axis contains clinical status and the y axis contains Log10(Concentration).

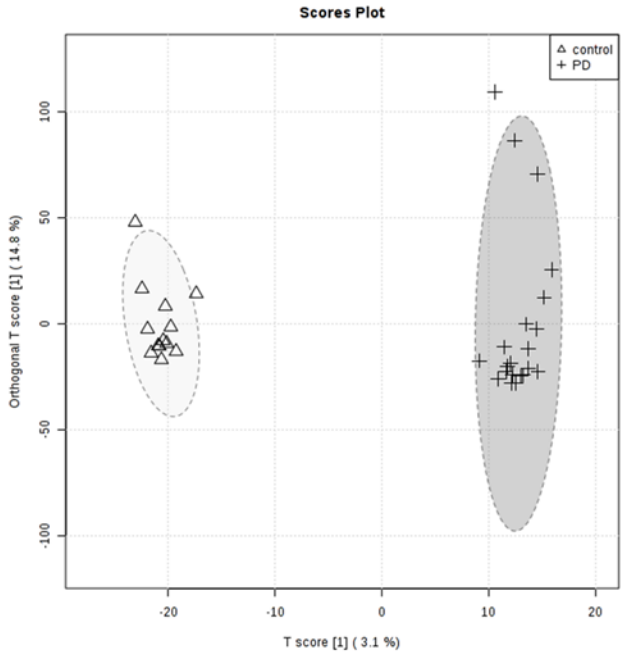

Figure A2-3. Orthogonal Partial Least Squares Discriminant Analysis (OPLS-DA).

Clear separation between the PD and Control group were visible.

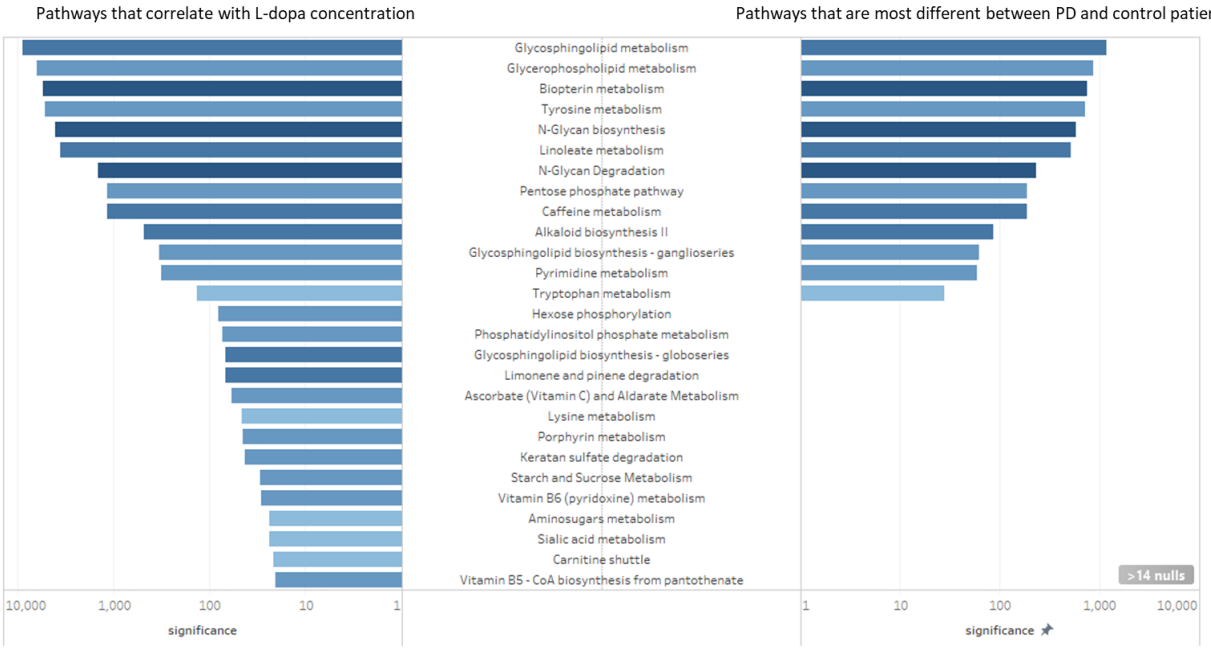

Figure A2-4. Altered metabolic pathways. Left, metabolic pathways that correlate with L-dopa concentration. Right, metabolic pathways that are most different between PD and control patients. The x-axis is degree of significance, calculated by log(1/adjusted-p-value). Metabolic pathways with adjusted p-values greater than 0.05 were excluded from visualization. Color corresponds with the extent that the network was affected, where dark blue denotes that a large proportion of metabolites within the network were affected, and a light blue denotes that a relatively small proportion of metabolites within a network were affected.

Metabolic Pathway	Metabolite Names
Glycosphingolipid metabolism	Choline phosphate; Phosphorylcholine; Phosphocholine; D-Glucose; Grape sugar; Sphinganine; Dihydrosphingosine; Psychosine; Galactosylsphingosine; N-Acetylneuraminate; N-Acetylneuraminic acid; 5-Acetamido-3,5-dideoxy-D-glycero-D-galacto-2-nonulosonic acid; CMP; Cytidine-5'-monophosphate; Sphingosine; Sphingenine; Sphingoid; 3-Dehydrosphinganine; beta-D-Galactose
Glycerophospholipid metabolism	Choline phosphate; Phosphorylcholine; Phosphocholine; Glycerol; Glycerin; 1,2,3-Trihydroxypropane; Acetylcholine; Sphinganine; Dihydrosphingosine; myo-Inositol; D-myo-Inositol; 1D-myo-Inositol; L-myo-Inositol; 1L-myo-Inositol; meso-Inositol; Inositol; Dambose; Cyclohexitol; Meat sugar; CTP; Cytidine 5'-triphosphate; Linoleate; Linoleic acid; (9Z,12Z)-Octadecadienoic acid; 9-cis,12-cis-Octadecadienoate; CMP; Cytidine-5'-monophosphate; (5Z,8Z,11Z,14Z)-Icosatetraenoic acid; Arachidonate; Arachidonic acid; Sphingosine; Sphingenine; Sphingoid; Inositol 1-phosphate; myo-Inositol 1-phosphate; 1D-myo-Inositol 1-phosphate; D-myo-Inositol 1-phosphate; 1D-myo-Inositol 1-monophosphate
Biopterin metabolism	L-Phenylalanine; L-Tyrosine; (S)-3-(p-Hydroxyphenyl)alanine; (S)-2-Amino-3-(p-hydroxyphenyl)propionic acid; Tetrahydrobiopterin; 5,6,7,8-Tetrahydrobiopterin; 6-Pyruvoyltetrahydropterin; 6-(1,2-Dioxopropyl)-5,6,7,8-tetrahydropterin; quinonoid dihydrobiopterin
Tyrosine metabolism	Phenethylamine; Tetrahydrobiopterin; 5,6,7,8-Tetrahydrobiopterin; L-Phenylalanine; Ascorbate; Ascorbic acid; L-Ascorbate; L-Ascorbic acid; L-Tyrosine; (S)-3-(p-Hydroxyphenyl)alanine; (S)-2-Amino-3-(p-hydroxyphenyl)propionic acid; Dopamine; 4-(2-Aminoethyl)-1,2-benzenediol; 4-(2-Aminoethyl)benzene-1,2-diol; 3,4-Dihydroxyphenylacetaldehyde; 3-O-methyldopa
N-Glycan biosynthesis	D-Mannose; Mannose; Seminose; CMP; Cytidine-5'-monophosphate; CTP; Cytidine 5'-triphosphate; Dolichyl phosphate D-mannose; D-Glucose; Grape sugar; Dextrose
Linoleate metabolism	Ascorbate; Ascorbic acid; L-Ascorbate; L-Ascorbic acid; Linoleate; Linoleic acid; (9Z,12Z)-Octadecadienoic acid; 9-cis,12-cis-Octadecadienoate; 9(S)-HPODE; 9(S)-HPOD; (9Z,11E)-(13S)-13-Hydroperoxyoctadeca-9,11-dienoic acid; (9Z,11E)-(13S)-13-Hydroperoxyoctadeca-9,11-dienoate; 13(S)-HPODE; 13S-Hydroperoxy-9Z,11E-octadecadienoic acid
N-Glycan Degradation	D-Mannose; Mannose; Seminose; N-Acetylneuraminate; N-Acetylneuraminic acid; 5-Acetamido-3,5-dideoxy-D-glycero-D-galacto-2-nonulosonic acid; D-Galactose
Pentose phosphate pathway	D-Sedoheptulose 1,7-bisphosphate; Deoxyribose; 2-Deoxy-D-erythro-pentose; Thyminose; D-Fructose 6-phosphate; D-Fructose 6-phosphoric acid; Sedoheptulose 1-phosphate; Sedoheptulose 7-phosphate; D-Glucose 6-phosphate; Glucose 6-phosphate; D-Sedoheptulose 7-phosphate; beta-D-Fructose 6-phosphate
Caffeine metabolism	1,7-Dimethylxanthine; 1-Methylxanthine

Alkaloid biosynthesis II	Benzoate; Benzoic acid; Benzenecarboxylic acid; Phenylformic acid; N-Methylputrescine
Glycosphingolipid biosynthesis - ganglioseries	CMP; Cytidine-5'-monophosphate; Chondroitin; Galactose
Pyrimidine metabolism	Deoxyribose; 2-Deoxy-D-erythro-pentose; Thyminose; dTMP; Thymidine 5'-phosphate; Deoxythymidine 5'-phosphate; Thymidylic acid; 5'-Thymidylic acid; Thymidine monophosphate; Deoxythymidylic acid; dUMP; Deoxyuridylic acid; Deoxyuridine monophosphate; D-Glucose 1-phosphate; alpha-D-Glucose 1-phosphate; Cori ester; 5,6-Dihydrouracil; 2,4(1H,3H)-Pyrimidinedione, dihydro-; Dihydrouracile; Dihydrouracil; 5,6-Dihydro-2,4-dihydroxypyrimidine; Dihydrofolate; Dihydrofolic acid; 7,8-Dihydrofolate; 7,8-Dihydrofolic acid; CTP; Cytidine 5'-triphosphate; CMP; Cytidine-5'-monophosphate; 2-Deoxy-D-ribose 1-phosphate; dGTP; 2'-Deoxyguanosine 5'-triphosphate; Deoxyguanosine 5'-triphosphate; dUDP; 2'-Deoxyuridine 5'-diphosphate
Tryptophan metabolism	L-Tryptophan; Tryptophan; Indole-3-acetaldehyde; 2-(Indol-3-yl)acetaldehyde; 3-Hydroxyanthranilate; Indolepyruvate; Indolepyruvic acid; (Indol-3-yl)pyruvate; Indole-3-pyruvate; Tetrahydrobiopterin; 5,6,7,8-Tetrahydrobiopterin; 4,6-Dihydroxyquinoline; Quinoline-4,6-diol

Table A2-3. 13 metabolic pathways identified as significantly different between PD patients and control patients. Mummichog software identified metabolic pathways that are most likely to be different between the PD and control patients. Identities of

Metabolic Pathway	Metabolite Names
Glycosphingolipid metabolism	Choline phosphate; Phosphorylcholine; Phosphocholine; D-Glucose; Grape sugar; Sphinganine; Dihydrosphingosine; Psychosine; Galactosylsphingosine; N-Acetylneuraminate; N-Acetylneuraminic acid; 5-Acetamido-3,5-dideoxy-D-glycero-D-galacto-2-nonulosonic acid; CMP; Cytidine-5'-monophosphate; Sphingosine; Sphingenine; Sphingoid; 3-Dehydrosphinganine; beta-D-Galactose
Glycerophospholipid metabolism	Choline phosphate; Phosphorylcholine; Phosphocholine; Glycerol; Glycerin; 1,2,3-Trihydroxypropane; Acetylcholine; Sphinganine; Dihydrosphingosine; myo-Inositol; D-myo-Inositol; 1D-myo-Inositol; L-myo-Inositol; 1L-myo-Inositol; meso-Inositol; Inositol; Dambose; Cyclohexitol; Meat sugar; CTP; Cytidine 5'-triphosphate; Linoleate; Linoleic acid; (9Z,12Z)-Octadecadienoic acid; 9-cis,12-cis-Octadecadienoate; CMP; Cytidine-5'-monophosphate; (5Z,8Z,11Z,14Z)-Icosatetraenoic acid; Arachidonate; Arachidonic acid; Sphingosine; Sphingenine; Sphingoid; Inositol 1-phosphate; myo-Inositol 1-phosphate; 1D-myo-Inositol 1-phosphate; D-myo-Inositol 1-phosphate; 1D-myo-Inositol 1-monophosphate
Biopterin metabolism	L-Phenylalanine; L-Tyrosine; (S)-3-(p-Hydroxyphenyl)alanine; (S)-2-Amino-3-(p-hydroxyphenyl)propionic acid; Tetrahydrobiopterin; 5,6,7,8-Tetrahydrobiopterin; 6-Pyruvoyltetrahydropterin; 6-(1,2-Dioxopropyl)-5,6,7,8-tetrahydropterin; quinonoid dihydrobiopterin
Tyrosine metabolism	Phenethylamine; Tetrahydrobiopterin; 5,6,7,8-Tetrahydrobiopterin; L-Phenylalanine; Ascorbate; Ascorbic acid; L-Ascorbate; L-Ascorbic acid; L-Tyrosine; (S)-3-(p-Hydroxyphenyl)alanine; (S)-2-Amino-3-(p-hydroxyphenyl)propionic acid; Dopamine; 4-(2-Aminoethyl)-1,2-benzenediol; 4-(2-Aminoethyl)benzene-1,2-diol; 3,4-Dihydroxyphenylacetaldehyde; 3-O-methyldopa
N-Glycan biosynthesis	D-Mannose; Mannose; Seminose; CMP; Cytidine-5'-monophosphate; CTP; Cytidine 5'-triphosphate; Dolichyl phosphate D-mannose; D-Glucose; Grape sugar; Dextrose
Linoleate metabolism	Ascorbate; Ascorbic acid; L-Ascorbate; L-Ascorbic acid; Linoleate; Linoleic acid; (9Z,12Z)-Octadecadienoic acid; 9-cis,12-cis-Octadecadienoate; 9(S)-HPODE; 9(S)-HPOD; (9Z,11E)-(13S)-13-Hydroperoxyoctadeca-9,11-dienoic acid; (9Z,11E)-(13S)-13-Hydroperoxyoctadeca-9,11-dienoate; 13(S)-HPODE; 13S-Hydroperoxy-9Z,11E-octadecadienoic acid
N-Glycan Degradation	D-Mannose; Mannose; Seminose; N-Acetylneuraminate; N-Acetylneuraminic acid; 5-Acetamido-3,5-dideoxy-D-glycero-D-galacto-2-nonulosonic acid; D-Galactose
Pentose phosphate pathway	D-Sedoheptulose 1,7-bisphosphate; Deoxyribose; 2-Deoxy-D-erythro-pentose; Thyminose; D-Fructose 6-phosphate; D-Fructose 6-phosphoric acid; Sedoheptulose 1-phosphate; Sedoheptulose 7-phosphate; D-Glucose 6-phosphate; Glucose 6-phosphate; D-Sedoheptulose 7-phosphate; beta-D-Fructose 6-phosphate
Caffeine metabolism	1,7-Dimethylxanthine; 1-Methylxanthine

Alkaloid biosynthesis II	Benzoate; Benzoic acid; Benzenecarboxylic acid; Phenylformic acid; N-Methylputrescine
Glycosphingolipid biosynthesis - ganglioseries	CMP; Cytidine-5'-monophosphate; Chondroitin; Galactose
Pyrimidine metabolism	Deoxyribose; 2-Deoxy-D-erythro-pentose; Thyminose; dTMP; Thymidine 5'-phosphate; Deoxythymidine 5'-phosphate; Thymidylic acid; 5'-Thymidylic acid; Thymidine monophosphate; Deoxythymidylic acid; dUMP; Deoxyuridylic acid; Deoxyuridine monophosphate; Deoxyuridine 5'-phosphate; D-Glucose 1-phosphate; alpha-D-Glucose 1-phosphate; Cori ester; 5,6-Dihydrouracil; 2,4(1H,3H)-Pyrimidinedione, dihydro-; Dihydrouracile; Dihydrouracil; 5,6-Dihydro-2,4-dihydroxypyrimidine; Dihydrofolate; Dihydrofolic acid; 7,8-Dihydrofolate; 7,8-Dihydrofolic acid; CTP; Cytidine 5'-triphosphate; CMP; Cytidine-5'-monophosphate; 2-Deoxy-D-ribose 1-phosphate; dGTP; 2'-Deoxyguanosine 5'-triphosphate; Deoxyguanosine 5'-triphosphate; dUDP; 2'-Deoxyuridine 5'-diphosphate
Tryptophan metabolism	L-Tryptophan; Tryptophan; Indole-3-acetaldehyde; 2-(Indol-3-yl)acetaldehyde; 3-Hydroxyanthranilate; Indolepyruvate; Indolepyruvic acid; (Indol-3-yl)pyruvate; Tetrahydrobiopterin; 4,8-Dihydroxyquinoline; 4,6-Dihydroxyquinoline; Quinoline-4,6-diol
Hexose phosphorylation	D-Mannose; Mannose; Seminose; cis-beta-D-Glucosyl-2-hydroxycinnamate; -Fructose 6-phosphate; D-Fructose 6-phosphoric acid; D-Glucose; Grape sugar; D-Glucose 6-phosphate; Glucose 6-phosphate; D-Fructose; Levulose; Fruit sugar; D-arabino-Hexulose
Phosphatidylinositol phosphate metabolism	Glycerol; Glycerin; 1,2,3-Trihydroxypropane; Dolichyl phosphate D-mannose; myo-Inositol; D-myo-Inositol; 1D-myo-Inositol; L-myo-Inositol; 1L-myo-Inositol; meso-Inositol; Inositol; Dambose; Cyclohexitol; Meat sugar; Inositol 1-phosphate; myo-Inositol 1-phosphate; 1D-myo-Inositol 1-phosphate; D-myo-Inositol 1-phosphate; CMP; Cytidine-5'-monophosphate; D-myo-Inositol 1,4,5-trisphosphate; 1D-myo-Inositol 1,4,5-trisphosphate; Inositol 1,4,5-trisphosphate; 1D-myo-Inositol 1,3,4-trisphosphate; D-myo-Inositol 1,3,4-trisphosphate; myo-Inositol 4-phosphate; D-myo-Inositol 4-phosphate; 1D-myo-Inositol 4-phosphate; 1D-myo-Inositol 4-monophosphate; D-Glucose 6-phosphate; Glucose 6-phosphate; 1D-myo-Inositol 3-phosphate; D-myo-Inositol 3-phosphate; myo-Inositol 3-phosphate; Inositol 3-phosphate; 1D-myo-Inositol 3-monophosphate; D-myo-Inositol 3-monophosphate; myo-Inositol 3-monophosphate; Inositol 3-monophosphate; 1L-myo-Inositol 1-phosphate; L-myo-Inositol 1-phosphate
Limonene and pinene degradation	Perillyl alcohol; (-)-Perillyl alcohol; p-Mentha-1,8-dien-7-ol; Perillyl aldehyde; Perillaldehyde

Glycosphingolipid biosynthesis - globoseries	CMP; Cytidine-5'-monophosphate; alpha-D-Galactose
Ascorbate (Vitamin C) and Aldarate Metabolism	D-Glucarate; D-Glucaric acid; L-Gularic acid; d-Saccharic acid; Ascorbate; Ascorbic acid; L-Ascorbate; L-Ascorbic acid; D-glucurono-6,3-lactone
Lysine metabolism	L-Pipecolate; Pipecolinic acid; Pipecolic acid; Dihydrolipoamide; L-2-Aminoadipate; L-alpha-Aminoadipate; L-alpha-Aminoadipic acid; L-2-Aminoadipic acid; L-2-Aminohexanedioate
Porphyrin metabolism	Ascorbate; Ascorbic acid; L-Ascorbate; L-Ascorbic acid; 5-Aminolevulinate; 5-Amino-4-oxopentanoate; 2-Amino-3-oxoadipate; 2-Amino-3-oxohexanedioic acid
Keratan sulfate degradation	N-Acetylneuraminate; N-Acetylneuraminic acid; 5-Acetamido-3,5-dideoxy-D-glycero-D-galacto-2-nonulosonic acid; D-Galactose
Starch and Sucrose Metabolism	D-Glucose 1-phosphate; alpha-D-Glucose 1-phosphate; Cori ester; D-Glucose; Grape sugar; Dextrose
Vitamin B6 (pyridoxine) metabolism	Pyridoxine phosphate; Pyridoxine 5-phosphate; Pyridoxine 5'-phosphate
Aminosugars metabolism	D-Fructose 6-phosphate; D-Fructose 6-phosphoric acid; Cytidine 5'-triphosphate; N-Acetylneuraminate; N-Acetylneuraminic acid; 5-Acetamido-3,5-dideoxy-D-glycero-D-galacto-2-nonulosonic acid; CMP; Cytidine-5'-monophosphate; N-Glycoloyl-neuraminate; N-Glycolylneuraminate; NeuNGc
Sialic acid metabolism	Glycerol; Glycerin; 1,2,3-Trihydroxypropane; myo-Inositol; D-myo-Inositol; 1D-myo-Inositol; L-myo-Inositol; 1L-myo-Inositol; meso-Inositol; Inositol; Dambose; Cyclohexitol; Meat sugar; N-Acetylneuraminate; N-Acetylneuraminic acid; 5-Acetamido-3,5-dideoxy-D-glycero-D-galacto-2-nonulosonic acid; CMP; Cytidine-5'-monophosphate; 1D-myo-Inositol 3-phosphate; D-myo-Inositol 3-phosphate; myo-Inositol 3-phosphate; Inositol 3-phosphate; 1D-myo-Inositol 3-monophosphate; D-myo-Inositol 3-monophosphate; myo-Inositol 3-monophosphate; Inositol 3-monophosphate; 1L-myo-Inositol 1-phosphate; myo-Inositol 4-phosphate; D-myo-Inositol 4-phosphate; 1D-myo-Inositol 4-phosphate; 1D-myo-Inositol 4-monophosphate; Inositol 1-phosphate; myo-Inositol 1-phosphate; 1D-myo-Inositol 1-phosphate; D-myo-Inositol 1-phosphate; 1D-myo-Inositol 1-monophosphate
Carnitine shuttle	octadecenoyl carnitine
Vitamin B5 - CoA biosynthesis from pantothenate	CTP; Cytidine 5'-triphosphate; Pantetheine; (R)-Pantetheine

Table A2-4. 27 metabolic pathways identified as correlated with L-DOPA. Mummichog software identified metabolic pathways that are strongly associated with the presence of L-DOPA. Identities of compounds found within these pathways are also listed.

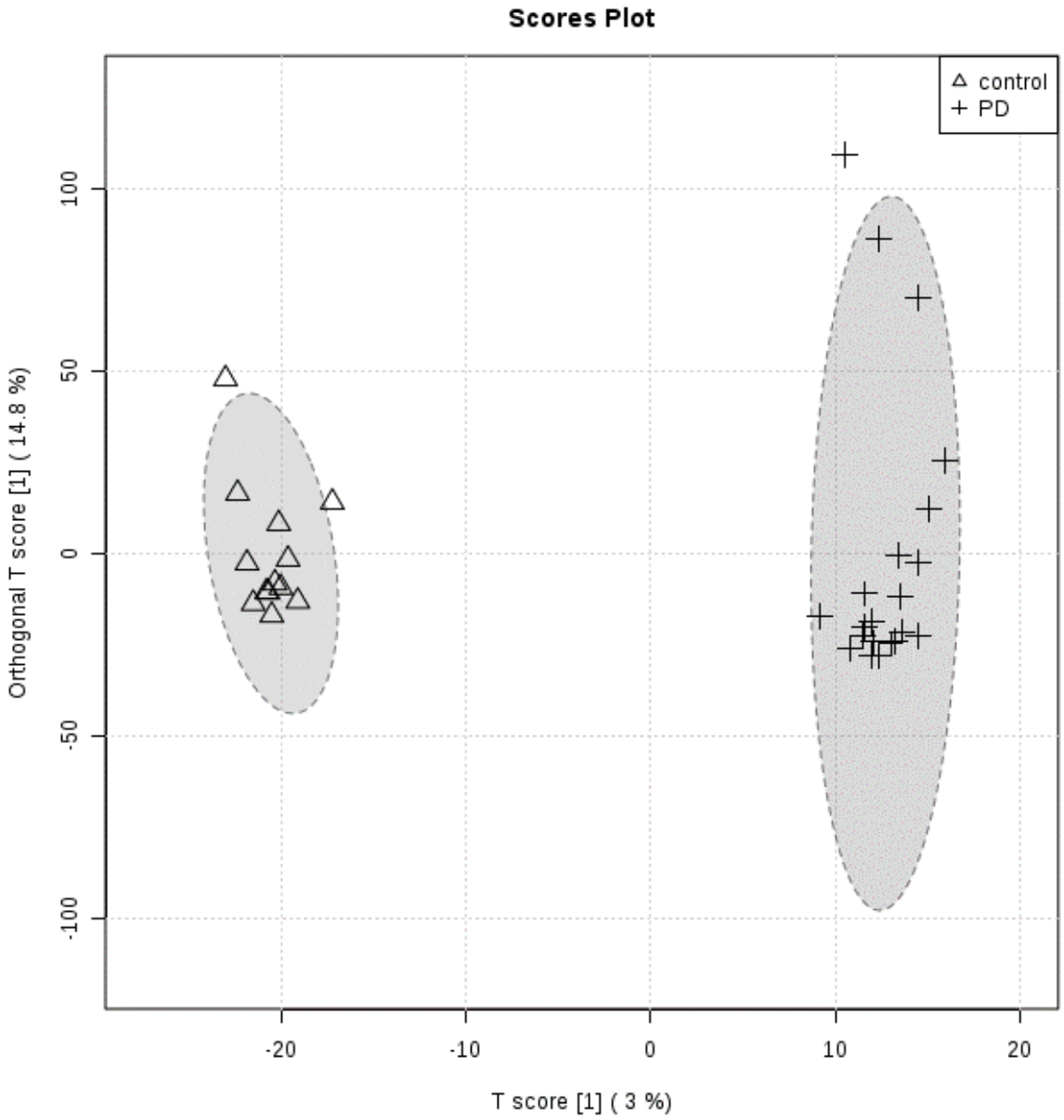

Figure A2-5. OPLS-DA between PD and control metabolomes with PD drug metabolites manually removed.

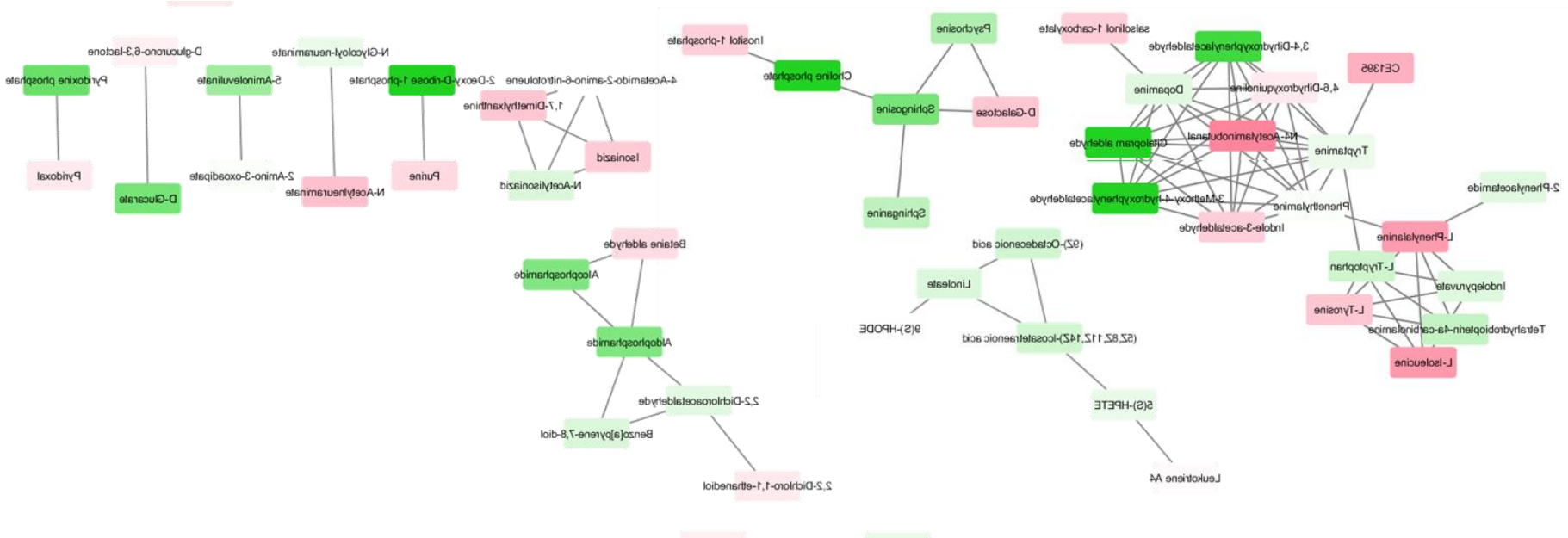
Pyridoxine phosphate
Pyridoxal
D-glucurono-6,3-lactone
D-Glucarate
5-Aminolevulinate
2-Amino-3-oxoadipate
N-Glycolyl-neuraminate
N-Acetylneuraminate
2-Deoxy-D-ribose 1-phosphate
Purine
4-Acetamido-2-amino-6-nitrotoluene
1,7-Dimethylxanthine
Isoniazid
N-Acetylisoniazid
Inositol 1-phosphate
Choline phosphate
Sphingosine
Psychosine
D-Galactose
Sphinganine
Betaine aldehyde
Alkosphosphamide
Aldophosphamide
2,2-Dichloroacetaldehyde
Benzo[a]pyrene-7,8-diol
2,2-Dichloro-1,1-ethanediol
Salicylinol 1-carboxylate
3,4-Dihydroxyphenylacetaldehyde
CE1395
Dopamine
4,6-Dihydroxyquinoline
Cytaldopam aldehyde
N4-Acetylaminobutanal
Tryptamine
3-Methoxy-4-hydroxyphenylacetaldehyde
Phenethylamine
Indole-3-acetaldehyde
2-Phenylacetamide
L-Phenylalanine
L-Tryptophan
Indolepyruvate
L-Tyrosine
Tetrahydrobiopterin-4a-carbinolamine
L-Isoleucine
(9Z)-Octadecenoic acid
Linoleate
9(S)-HPODE
(5Z,8Z,11Z,14Z)-Icosatetraenoic acid
5(S)-HPETE
Leukotriene A4

Figure A2-6. Network analysis of PD plasma analytes that correlate with l-dopa (rotated 90 degrees for legibility). Spearman correlation between each *m/z* and L-dopa was calculated among PD patients. Darker shades of green correspond to stronger positive Spearman correlations; darker shades of red correspond to stronger negative Spearmen correlations.

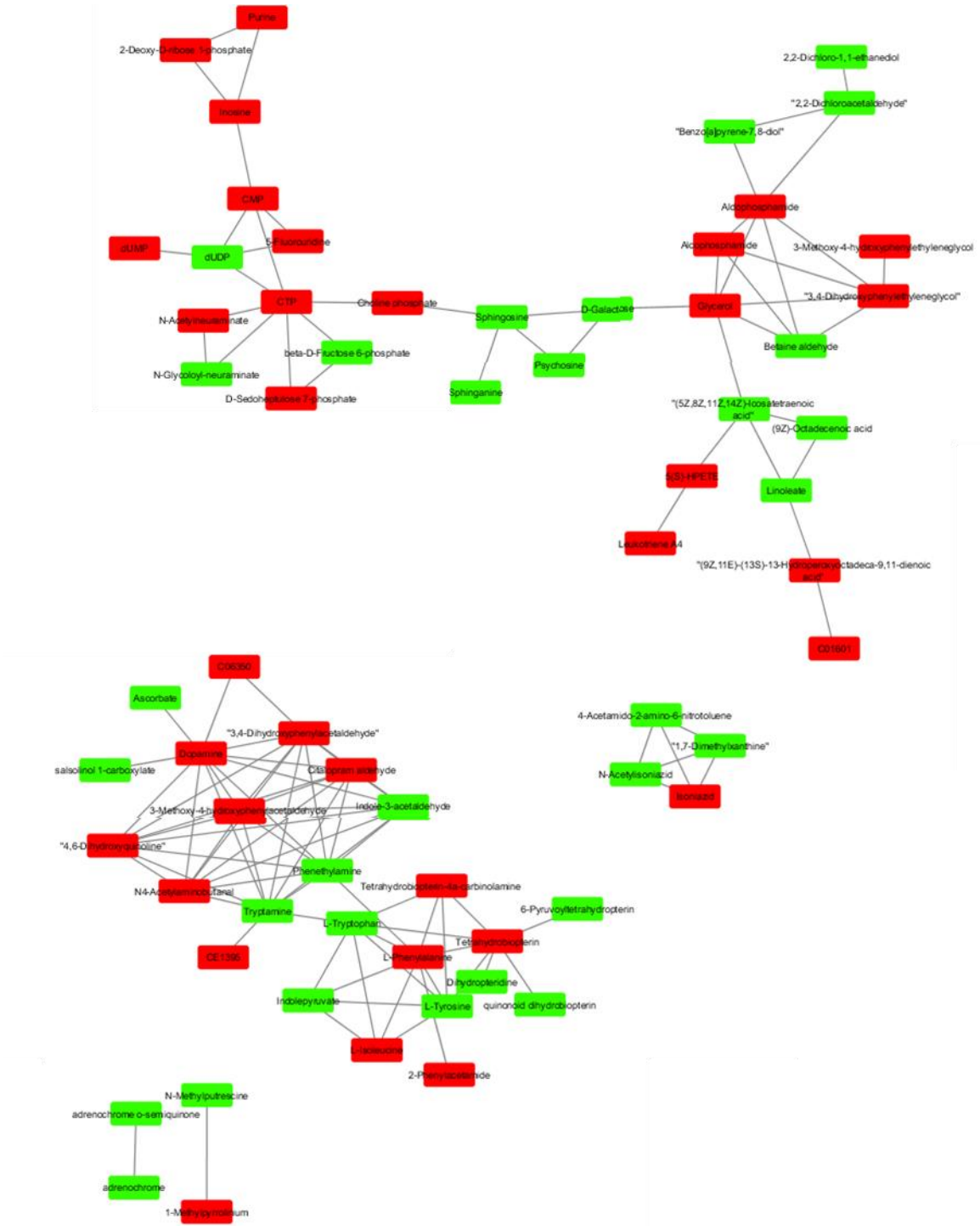
Purine
2-Deoxy-D-ribose 1-phosphate
Inosine
CMP
dUMP
dUDP
5-Fluorouridine
CTP
Choline phosphate
N-Acetylneuraminate
beta-D-Fructose 6-phosphate
N-Glycoloyl-neuraminate
D-Sedoheptulose 7-phosphate
Sphingosine
D-Galactose
Psychosine
Sphinganine
2,2-Dichloro-1,1-ethanediol
"2,2-Dichloroacetaldehyde"
"Benzo(a)pyrene-7,8-diol"
Aldophosphamide
Aldophosphamide
3-Methoxy-4-hydroxyphenylethyleneglycol
Glycerol
"3,4-Dihydroxyphanylethyleneglycol"
Betaine aldehyde
"(5Z,8Z,11Z,14Z)-Icosatetraenoic acid"
(9Z)-Octadecenoic acid
5(S)-HPETE
Linoleate
Leukotriene A4
"(9Z,11E)-(13S)-13-Hydroperoxyoctadeca-9,11-dienoic acid"
C01601
C06350
Ascorbate
"3,4-Dihydroxyphenylacetaldehyde"
Dopamine
salsolinol 1-carboxylate
Citalopram aldehyde
3-Methoxy-4-hydroxyphenylacetaldehyde
Indole-3-acetaldehyde
"4,6-Dihydroxyquinoline"
Phenethylamine
N4-Acetylaminobutanal
Tetrahydrobiopterin-4a-carbinolamine
Tryptamine
6-Pyruvoyltetrahydropterin
L-Tryptophan
Tetrahydrobiopterin
C01395
L-Phenylalanine
Dihydropteridine
Indolepyruvate
L-Tyrosine
quinonoid dihydrobiopterin
L-Isoleucine
2-Phenylacetamide
4-Acetamido-2-amino-6-nitrotoluene
"1,7-Dimethylxanthine"
N-Acetylisoniazid
Isoniazid
N-Methylputrescine
adrenochrome o-semiquinone
adrenochrome
1-Methylpyrrolinium

Figure A2-7. Network analysis of the metabolites that are most different between PD and control patients. Red nodes correspond to metabolites elevated in PD patients compared to controls, while green nodes correspond to metabolites lower in PD patients compared to controls.

IX. References

Abraini JH, Fechtali T, Rostain JC (1994). Lasting effects of dopamine receptor agonists upon striatal dopamine release in free-moving rats: an in vivo voltammetric study. *Brain Res* **642**: 199–205.

Ahmed SS, Santosh W, Kumar S, Christlet HTT (2009). Metabolic profiling of Parkinson's disease: evidence of biomarker from gene expression analysis and rapid neural network detection. *J Biomed Sci* **16**: 63.

Airaksinen MM, Kari I (1981). Beta-carbolines, psychoactive compounds in the mammalian body. Part I: Occurrence, origin and metabolism. *Med Biol* **59**: 21–34.

Alonso A, Marsal S, Julià A (2015). Analytical methods in untargeted metabolomics: state of the art in 2015. *Front Bioeng Biotechnol* **3**: 23.

Alter SP, Lenzi GM, Bernstein AI, Miller GW (2013). Vesicular Integrity in Parkinson's Disease. *Curr Neurol Neurosci Rep* **13**: 362.

Alter SP, Stout KA, Lohr KM, Taylor TN, Shepherd KR, Wang M, *et al* (2016). Reduced vesicular monoamine transport disrupts serotonin signaling but does not cause serotonergic degeneration. *Exp Neurol* **275 Pt 1**: 17–24.

American Psychiatric Association (American Psychiatric Association: 1952). *Diagnostic and Statistical Manual of Mental Disorders*. doi:10.1176/appi.books.9780890425596.

American Psychiatric Association (2013). Diagnostic and Statistical Manual of Mental

Disorders, 5th Edition (DSM-5). *Diagnostic Stat Man Ment Disord 4th Ed TR* 280doi:10.1176/appi.books.9780890425596.744053.

Anderson RE, Hruska B, Boros AP, Richardson CJ, Delahanty DL (2018). Patterns of co-occurring addictions, posttraumatic stress disorder, and major depressive disorder in detoxification treatment seekers: Implications for improving detoxification treatment outcomes. *J Subst Abuse Treat* **86**: 45–51.

Andersson JL, Marcus M, Nomikos GG, Svensson TH (1994). Prazosin modulates the changes in firing pattern and transmitter release induced by raclopride in the mesolimbic, but not in the nigrostriatal dopaminergic system. *Naunyn Schmiedebergs Arch Pharmacol* **349**: 236–43.

Andreasen NC (2010). Posttraumatic stress disorder: a history and a critique. *Ann N Y Acad Sci* **1208**: 67–71.

Andrews B, Brewin CR, Philpott R, Stewart L (2007). Delayed-Onset Posttraumatic Stress Disorder: A Systematic Review of the Evidence. *Am J Psychiatry* **164**: 1319–1326.

Anlauf M, Eissele R, Schäfer MK-H, Eiden LE, Arnold R, Pauser U, *et al* (2003). Expression of the two isoforms of the vesicular monoamine transporter (VMAT1 and VMAT2) in the endocrine pancreas and pancreatic endocrine tumors. *J Histochem Cytochem* **51**: 1027–40.

Anlauf M, Schafer MK-H, Depboylu C, Hartschuh W, Eiden LE, Kloppel G, *et al* (2004). The vesicular monoamine transporter 2 (VMAT2) is expressed by normal and tumor cutaneous mast cells and Langerhans cells of the skin but is absent from Langerhans

cell histiocytosis. *J Histochem Cytochem* **52**: 779–88.

Anlauf M, Schäfer MK-H, Schwark T, Wurmb-Schwark N von, Brand V, Sipos B, *et al* (2006). Vesicular monoamine transporter 2 (VMAT2) expression in hematopoietic cells and in patients with systemic mastocytosis. *J Histochem Cytochem Off J Histochem Soc* **54**: 201–13.

Araújo AX, Berger W, Coutinho ES., Marques-Portella C, Luz MP, Cabizuca M, *et al* (2014). Comorbid depressive symptoms in treatment-seeking PTSD outpatients affect multiple domains of quality of life. *Compr Psychiatry* **55**: 56–63.

Bajor LA, Lai Z, Goodrich DE, Miller CJ, Penfold RB, Myra Kim H, *et al* (2013). Posttraumatic stress disorder, depression, and health-related quality of life in patients with bipolar disorder: review and new data from a multi-site community clinic sample. *J Affect Disord* **145**: 232–9.

Bauer EP (2015). Serotonin in fear conditioning processes. *Behav Brain Res* **277**: 68–77.

Bauer MR, Ruef AM, Pineles SL, Japuntich SJ, Macklin ML, Lasko NB, *et al* (2013). Psychophysiological assessment of PTSD: a potential research domain criteria construct. *Psychol Assess* **25**: 1037–43.

Baumann A, Moreira CG, Morawska MM, Masneuf S, Baumann CR, Noain D (2016). Preliminary Evidence of Apathetic-Like Behavior in Aged Vesicular Monoamine Transporter 2 Deficient Mice. *Front Hum Neurosci* **10**: 587.

Beitz JM (2014). Parkinson's disease: a review. *Front Biosci (Schol Ed)* **6**: 65–74.

Berg RA van den, Hoefsloot HC, Westerhuis JA, Smilde AK, Werf MJ van der (2006).

Centering, scaling, and transformations: improving the biological information content of metabolomics data. *BMC Genomics* **7**: 142.

Berger M, Gray JA, Roth BL (2009). The Expanded Biology of Serotonin. *Annu Rev Med* **60**: 355–366.

Bernal M, Haro JM, Bernert S, Brugha T, Graaf R de, Bruffaerts R, *et al* (2007). Risk factors for suicidality in Europe: results from the ESEMED study. *J Affect Disord* **101**: 27–34.

Bernardy NC, Lund BC, Alexander B, Friedman MJ (2012). Prescribing Trends in Veterans With Posttraumatic Stress Disorder. *J Clin Psychiatry* **73**: 297–303.

Bernstein DP, Fink L, Handelsman L, Foote J, Lovejoy M, Wenzel K, *et al* (1994). Initial reliability and validity of a new retrospective measure of child abuse and neglect. *Am J Psychiatry* **151**: 1132–1136.

Bharadwaj RA, Jaffe AE, Chen Q, Deep-Soboslay A, Goldman AL, Mighdoll MI, *et al* (2016). Genetic risk mechanisms of posttraumatic stress disorder in the human brain. *J Neurosci Res* doi:10.1002/jnr.23957.

Binder EB (2009). The role of FKBP5, a co-chaperone of the glucocorticoid receptor in the pathogenesis and therapy of affective and anxiety disorders. *Psychoneuroendocrinology* **34 Suppl 1**: S186-95.

Binder EB, Bradley RG, Liu W, Epstein MP, Deveau TC, Mercer KB, *et al* (2008). Association of FKBP5 polymorphisms and childhood abuse with risk of posttraumatic stress disorder symptoms in adults. *JAMA* **299**: 1291–305.

Birkmayer W, Hornykiewicz O (1962). The L-dihydroxyphenylalanine (L-DOPA) effect in Parkinson's syndrome in man: On the pathogenesis and treatment of Parkinson akinesias. *Arch Psychiatr Nervenkr Z Gesamte Neurol Psychiatr* **203**: 560–74.

Bisel B, Pavone FS, Calamai M (2014). GM1 and GM2 gangliosides: recent developments. *Biomol Concepts* **5**: 87–93.

Blake DD, Weathers FW, Nagy LM, Kaloupek DG, Gusman FD, Charney DS, *et al* (1995). The development of a Clinician-Administered PTSD Scale. *J Trauma Stress* **8**: 75–90.

Blanco C, Xu Y, Brady K, Pérez-Fuentes G, Okuda M, Wang S (2013). Comorbidity of posttraumatic stress disorder with alcohol dependence among US adults: Results from National Epidemiological Survey on Alcohol and Related Conditions. *Drug Alcohol Depend* **132**: 630–638.

Bobak MJ, Weber MW, Doellman MA, Schuweiler DR, Athens JM, Juliano SA, *et al* (2016). Modafinil Activates Phasic Dopamine Signaling in Dorsal and Ventral Striata. *J Pharmacol Exp Ther* **359**: 460–470.

Bocchio M, McHugh SB, Bannerman DM, Sharp T, Capogna M (2016). Serotonin, Amygdala and Fear: Assembling the Puzzle. *Front Neural Circuits* **10**: 24.

Bogdanov M, Matson WR, Wang L, Matson T, Saunders-Pullman R, Bressman SS, *et al* (2008). Metabolomic profiling to develop blood biomarkers for Parkinson's disease. *Brain* **131**: 389–396.

Boscarino JA, Erlich PM, Hoffman SN, Rukstalis M, Stewart WF (2011). Association of

FKBP5, COMT and CHRNA5 polymorphisms with PTSD among outpatients at risk for PTSD. *Psychiatry Res* **188**: 173–174.

Bourgault S, Chatenet D, Wurtz O, Doan ND, Leprince J, Vaudry H, *et al* (2011). Strategies to convert PACAP from a hypophysiotropic neurohormone into a neuroprotective drug. *Curr Pharm Des* **17**: 1002–24.

Bowery BJ, Razzaque Z, Emms F, Patel S, Freedman S, Bristow L, *et al* (1996). Antagonism of the effects of (+)-PD 128907 on midbrain dopamine neurones in rat brain slices by a selective D2 receptor antagonist L-741,626. *Br J Pharmacol* **119**: 1491–7.

Braak H, Braak E (1991). Neuropathological stageing of Alzheimer-related changes. *Acta Neuropathol* **82**: 239–59.

Bremner JD, Southwick SM, Darnell A, Charney DS (1996). Chronic PTSD in Vietnam combat veterans: course of illness and substance abuse. *Am J Psychiatry* **153**: 369–375.

Breslau N, Chilcoat HD, Kessler RC, Peterson EL, Lucia VC (1999). Vulnerability to assaultive violence: further specification of the sex difference in post-traumatic stress disorder. *Psychol Med* **29**: 813–21.

Briscione MA, Jovanovic T, Norrholm SD (2014). Conditioned fear associated phenotypes as robust, translational indices of trauma-, stressor-, and anxiety-related behaviors. *Front psychiatry* **5**: 88.

Briscione MA, Michopoulos V, Jovanovic T, Norrholm SD (2017). Neuroendocrine

Underpinnings of Increased Risk for Posttraumatic Stress Disorder in Women. *Vitam Horm* **103**: 53–83.

Brown JM, Hanson GR, Fleckenstein AE (2001). Regulation of the vesicular monoamine transporter-2: a novel mechanism for cocaine and other psychostimulants. *J Pharmacol Exp Ther* **296**: 762–7.

Burke WJ, Li SW, Williams EA, Nonneman R, Zahm DS (2003). 3,4-Dihydroxyphenylacetaldehyde is the toxic dopamine metabolite in vivo: implications for Parkinson's disease pathogenesis. *Brain Res* **989**: 205–13.

Careaga MBL, Girardi CEN, Suchecki D (2016). Understanding posttraumatic stress disorder through fear conditioning, extinction and reconsolidation. *Neurosci Biobehav Rev* **71**: 48–57.

Carvalho CM, Coimbra BM, Ota VK, Mello MF, Belangero SI (2017). Single-nucleotide polymorphisms in genes related to the hypothalamic-pituitary-adrenal axis as risk factors for posttraumatic stress disorder. *Am J Med Genet Part B Neuropsychiatr Genet* **174**: 671–682.

Caudle WM, Colebrooke RE, Emson PC, Miller GW (2008). Altered vesicular dopamine storage in Parkinson's disease: a premature demise. *Trends Neurosci* **31**: 303–308.

Caudle WM, Richardson JR, Wang MZ, Taylor TN, Guillot TS, McCormack AL, *et al* (2007). Reduced vesicular storage of dopamine causes progressive nigrostriatal neurodegeneration. *J Neurosci* **27**: 8138–8148.

Chang K-H, Cheng M-L, Tang H-Y, Huang C-Y, Wu Y-R, Chen C-M (2018).

Alternations of Metabolic Profile and Kynurenine Metabolism in the Plasma of Parkinson's Disease. *Mol Neurobiol* 1–10doi:10.1007/s12035-017-0845-3.

Charney DS (2004). Psychobiological Mechanisms of Resilience and Vulnerability: Implications for Successful Adaptation to Extreme Stress. *Am J Psychiatry* **161**: 195–216.

Chaudhry FA, Edwards RH, Fonnum F (2008). Vesicular neurotransmitter transporters as targets for endogenous and exogenous toxic substances. *Annu Rev Pharmacol Toxicol* **48**: 277–301.

Chaudhuri KR, Martinez-Martin P, Schapira AHV, Stocchi F, Sethi K, Odin P, *et al* (2006). International multicenter pilot study of the first comprehensive self-completed nonmotor symptoms questionnaire for Parkinson's disease: The NMSQuest study. *Mov Disord* **21**: 916–923.

Cheshire WP (2016). Thermoregulatory disorders and illness related to heat and cold stress. *Auton Neurosci* **196**: 91–104.

Chiara G Di, Imperato A (1988). Drugs abused by humans preferentially increase synaptic dopamine concentrations in the mesolimbic system of freely moving rats. *Proc Natl Acad Sci U S A* **85**: 5274–8.

Choi KR, Seng JS, Briggs EC, Munro-Kramer ML, Graham-Bermann SA, Lee RC, *et al* (2017). The Dissociative Subtype of Posttraumatic Stress Disorder (PTSD) Among Adolescents: Co-Occurring PTSD, Depersonalization/Derealization, and Other Dissociation Symptoms. *J Am Acad Child Adolesc Psychiatry* **56**: 1062–1072.

Ciliax BJ, Heilman C, Demchyshyn LL, Pristupa ZB, Ince E, Hersch SM, *et al* (1995). The dopamine transporter: immunochemical characterization and localization in brain. *J Neurosci* **15**: 1714–23.

Cipriani A, Williams T, Nikolakopoulou A, Salanti G, Chaimani A, Ipser J, *et al* (2017). Comparative efficacy and acceptability of pharmacological treatments for post-traumatic stress disorder in adults: a network meta-analysis. *Psychol Med* 1–10doi:10.1017/S003329171700349X.

Cliburn RA, Dunn AR, Stout KA, Hoffman CA, Lohr KM, Bernstein AI, *et al* (2016). Immunochemical localization of vesicular monoamine transporter 2 (VMAT2) in mouse brain. *J Chem Neuroanat* doi:10.1016/j.jchemneu.2016.11.003.

Cobuzzi RJ, Neafsey EJ, Collins MA (1994). Differential cytotoxicities of N-methyl-beta-carbolinium analogues of MPP+ in PC12 cells: insights into potential neurotoxicants in Parkinson's disease. *J Neurochem* **62**: 1503–10.

Congestri F, Formenti F, Sonntag V, Hdou G, Crespi F (2008). Selective D3 Receptor Antagonist SB-277011-A Potentiates the Effect of Cocaine on Extracellular Dopamine in the Nucleus Accumbens: a Dual Core-Shell Voltammetry Study in Anesthetized Rats. *Sensors* **8**: 6936–6951.

Cooper AA, Clifton EG, Feeny NC (2017). An empirical review of potential mediators and mechanisms of prolonged exposure therapy. *Clin Psychol Rev* **56**: 106–121.

Cooper HA, Gunn JA (1931). Harmalol in the treatment of Parkinsonism. *Lancet* **218**: 901–903.

Coppen A (1967). The biochemistry of affective disorders. *Br J Psychiatry* **113**: 1237–64.

Creese I, Burt DR, Snyder SH (1996). Dopamine receptor binding predicts clinical and pharmacological potencies of antischizophrenic drugs. *J Neuropsychiatry Clin Neurosci* **8**: 223–226.

Cruz-Muros I, Afonso-Oramas D, Abreu P, Rodríguez M, González MC, González-Hernández T (2008). Deglycosylation and subcellular redistribution of VMAT2 in the mesostriatal system during normal aging. *Neurobiol Aging* **29**: 1702–11.

Curry DW, Young MB, Tran AN, Daoud GE, Howell LL (2018). Separating the agony from ecstasy: R (–)-3,4-methylenedioxymethamphetamine has prosocial and therapeutic-like effects without signs of neurotoxicity in mice. *Neuropharmacology* **128**: 196–206.

Dale E, Pehrson AL, Jeyarajah T, Li Y, Leiser SC, Smagin G, *et al* (2016). Effects of serotonin in the hippocampus: how SSRIs and multimodal antidepressants might regulate pyramidal cell function. *CNS Spectr* **21**: 143–61.

Dauer W, Przedborski S (2003). Parkinson's disease: mechanisms and models. *Neuron* **39**: 889–909.

Davis M (1992). The Role of the Amygdala in Fear and Anxiety. *Annu Rev Neurosci* **15**: 353–375.

Davis TA, Jovanovic T, Norrholm SD, Glover EM, Swanson M, Spann S, *et al* (2013). Substance Use Attenuates Physiological Responses Associated With PTSD among

Individuals with Co-Morbid PTSD and SUDS. *J Psychol Psychother* **Suppl 7**: .

Debell F, Fear NT, Head M, Batt-Rawden S, Greenberg N, Wessely S, *et al* (2014). A systematic review of the comorbidity between PTSD and alcohol misuse. *Soc Psychiatry Psychiatr Epidemiol* **49**: 1401–25.

Diana M (2011). The dopamine hypothesis of drug addiction and its potential therapeutic value. *Front psychiatry* **2**: 64.

Driessen M, Schulte S, Luedecke C, Schaefer I, Sutmann F, Ohlmeier M, *et al* (2008). Trauma and PTSD in Patients With Alcohol, Drug, or Dual Dependence: A Multi-Center Study. *Alcohol Clin Exp Res* **32**: 481–488.

Dunn AR, Stout KA, Ozawa M, Lohr KM, Hoffman CA, Bernstein AI, *et al* (2017). Synaptic vesicle glycoprotein 2C (SV2C) modulates dopamine release and is disrupted in Parkinson disease. *Proc Natl Acad Sci* **114**: E2253–E2262.

Eiden LE, Schäfer MK-H, Weihe E, Schütz B (2004). The vesicular amine transporter family (SLC18): amine/proton antiporters required for vesicular accumulation and regulated exocytotic secretion of monoamines and acetylcholine. *Pflugers Arch* **447**: 636–40.

Eiden LE, Weihe E (2011). VMAT2: a dynamic regulator of brain monoaminergic neuronal function interacting with drugs of abuse. *Ann N Y Acad Sci* **1216**: 86–98.

Eisenberg J, Asnis GM, Praag HM Van, Vela RM (1988). Effect of tyrosine on attention deficit disorder with hyperactivity. *J Clin Psychiatry* **49**: 193–195.

Eisenhofer G, Kopin IJ, Goldstein DS (2004). Catecholamine Metabolism: A

Contemporary View with Implications for Physiology and Medicine. *Pharmacol Rev* **56**: 331–349.

El-Solh AA, Riaz U, Roberts J (2018). Sleep Disorders in Patients with Post-Traumatic Stress Disorder. *Chest* doi:10.1016/j.chest.2018.04.007.

Erickson, J.D.; Eiden, L.E.; Schafer, M.K.; Weihe E (1995). Reserpine- and tetrabenazine-sensitive transport of (3)H-histamine by the neuronal isoform of the vesicular monoamine transporter. - PubMed - NCBI. *J Mol Neurosci* **6**: 277–87.

Erickson J, Schafer M, Bonner T, Eiden L, Weihe E (1996a). Distinct pharmacological properties and distribution in neurons and endocrine cells of two isoforms of the human vesicular monoamine transporter. *Proc Natl Acad Sci USA 93* **93**: 5166–5171.

Erickson JD, Eiden LE, Hoffman BJ (1992). Expression cloning of a reserpine-sensitive vesicular monoamine transporter. *Proc Natl Acad Sci U S A* **89**: 10993–7.

Erickson JD, Schafer MK, Bonner TI, Eiden LE, Weihe E (1996b). Distinct pharmacological properties and distribution in neurons and endocrine cells of two isoforms of the human vesicular monoamine transporter. *Neurobiology* **93**: 5166–5171.

Estrada VB, Matsubara NK, Gomes MV, Corrêa FMA, Pelosi GG (2016). Noradrenaline microinjected into the dorsal periaqueductal gray matter causes anxiolytic-like effects in rats tested in the elevated T-maze. *Life Sci* **152**: 94–98.

Fanselow MS, LeDoux JE (1999). Why we think plasticity underlying Pavlovian fear

conditioning occurs in the basolateral amygdala. *Neuron* **23**: 229–32.

Fitoussi A, Dellu-Hagedorn F, Deurwaerdère P De (2013). Monoamines tissue content analysis reveals restricted and site-specific correlations in brain regions involved in cognition. *Neuroscience* **255**: 233–245.

Fitzgerald PJ, Giustino TF, Seemann JR, Maren S (2015). Noradrenergic blockade stabilizes prefrontal activity and enables fear extinction under stress. *Proc Natl Acad Sci* **112**: E3729–E3737.

Flandreau E, Risbrough V, Lu A, Ableitner M, Geyer MA, Holsboer F, *et al* (2015). Cell type-specific modifications of corticotropin-releasing factor (CRF) and its type 1 receptor (CRF1) on startle behavior and sensorimotor gating. *Psychoneuroendocrinology* **53**: 16–28.

Flandreau EI, Toth M (2017). Animal Models of PTSD: A Critical Review. *Curr Top Behav Neurosci* doi:10.1007/7854_2016_65.

Foa EB, Hembree EA, Cahill SP, Rauch SAM, Riggs DS, Feeny NC, *et al* (2005). Randomized trial of prolonged exposure for posttraumatic stress disorder with and without cognitive restructuring: Outcome at academic and community clinics. *J Consult Clin Psychol* **73**: 953–964.

Fon EA, Pothos EN, Sun B-CC, Killeen N, Sulzer D, Edwards RH (1997). Vesicular transport regulates monoamine storage and release but is not essential for amphetamine action. *Neuron* **19**: 1271–1283.

Fox AS, Shackman AJ (2017). The central extended amygdala in fear and anxiety:

Closing the gap between mechanistic and neuroimaging research. *Neurosci Lett* doi:10.1016/j.neulet.2017.11.056.

Freis ED (1954). Mental depression in hypertensive patients treated for long periods with large doses of reserpine. *N Engl J Med* **251**: 1006–8.

Fujiwara K, Masuyama Y, Yagisawa S, Tanabe T, Yabuuchi M, Tsuru D (1999). Histamine monoclonal antibody for brain immunocytochemistry. *J Biochem* **126**: 503–9.

Fukui M, Rodriguiz RM, Zhou J, Jiang SX, Phillips LE, Caron MG, *et al* (2007). Vmat2 heterozygous mutant mice display a depressive-like phenotype. *J Neurosci* **27**: 10520–10529.

Gainetdinov RR, Fumagalli F, Wang YM, Jones SR, Levey AI, Miller GW, *et al* (1998). Increased MPTP neurotoxicity in vesicular monoamine transporter 2 heterozygote knockout mice. *J Neurochem* **70**: 1973–1978.

Garza K, Jovanovic T (2017). Impact of Gender on Child and Adolescent PTSD. *Curr Psychiatry Rep* **19**: 87.

Gilbert DB, Millar J, Cooper SJ (1995). The putative dopamine D3 agonist, 7-OH-DPAT, reduces dopamine release in the nucleus accumbens and electrical self-stimulation to the ventral tegmentum. *Brain Res* **681**: 1–7.

Gillespie CF, Bradley B, Mercer K, Smith AK, Conneely K, Gapen M, *et al* (2009). Trauma exposure and stress-related disorders in inner city primary care patients. *Gen Hosp Psychiatry* **31**: 505–14.

Giustino TF, Maren S (2018). Noradrenergic Modulation of Fear Conditioning and Extinction. *Front Behav Neurosci* **12**: 43.

Glover E, Mercer K, Norrholm S, Davis M, Duncan E, Bradley B, *et al* (2013). Inhibition of fear is differentially associated with cycling estrogen levels in women. *J Psychiatry Neurosci* **38**: 341–348.

Goetz CG, Fahn S, Martinez-Martin P, Poewe W, Sampaio C, Stebbins GT, *et al* (2007). Movement Disorder Society-sponsored revision of the Unified Parkinson's Disease Rating Scale (MDS-UPDRS): Process, format, and clinimetric testing plan. *Mov Disord* **22**: 41–47.

Goldstein DS, Holmes C, Sullivan P, Mash DC, Sidransky E, Stefani A, *et al* (2015). Deficient vesicular storage: A common theme in catecholaminergic neurodegeneration. *Parkinsonism Relat Disord* **21**: 1013–1022.

Goldstein DS, Sullivan P, Holmes C, Miller GW, Alter S, Strong R, *et al* (2013). Determinants of buildup of the toxic dopamine metabolite DOPAL in Parkinson's disease. *J Neurochem* **126**: 591–603.

Goldstein LE, Rasmusson AM, Bunney BS, Roth RH (1996). Role of the amygdala in the coordination of behavioral, neuroendocrine, and prefrontal cortical monoamine responses to psychological stress in the rat. *J Neurosci* **16**: 4787–98.

Gourley SL, Swanson AM, Koleske AJ (2013). Corticosteroid-induced neural remodeling predicts behavioral vulnerability and resilience. *J Neurosci* **33**: 3107–3112.

Gourley SL, Wu FJ, Taylor JR (2008). Corticosterone Regulates pERK1/2 Map Kinase in

a Chronic Depression Model. *Ann N Y Acad Sci* **1148**: 509–514.

Gowda GAN, Zhang S, Gu H, Asiago V, Shanaiah N, Raftery D (2008). Metabolomics-based methods for early disease diagnostics. *Expert Rev Mol Diagn* **8**: 617–33.

Grillon C, Morgan CA, Southwick SM, Davis M, Charney DS (1996). Baseline startle amplitude and prepulse inhibition in Vietnam veterans with posttraumatic stress disorder. *Psychiatry Res* **64**: 169–78.

Grimmer T, Riemenschneider M, Förstl H, Henriksen G, Klunk WE, Mathis CA, *et al* (2009). Beta Amyloid in Alzheimer's Disease: Increased Deposition in Brain Is Reflected in Reduced Concentration in Cerebrospinal Fluid. *Biol Psychiatry* **65**: 927–934.

Guillot TS, Miller GW (2009). Protective actions of the vesicular monoamine transporter 2 (VMAT2) in monoaminergic neurons. *Mol Neurobiol* **39**: 149–70.

Guillot TS, Richardson JR, Wang MZ, Li YJ, Taylor TN, Ciliax BJ, *et al* (2008a). PACAP38 increases vesicular monoamine transporter 2 (VMAT2) expression and attenuates methamphetamine toxicity. *Neuropeptides* **42**: 423–34.

Guillot TS, Shepherd KR, Richardson JR, Wang MZ, Li Y, Emson PC, *et al* (2008b). Reduced vesicular storage of dopamine exacerbates methamphetamine-induced neurodegeneration and astrogliosis. *J Neurochem* **106**: 2205–2217.

Guina J, Nahhas RW, Sutton P, Farnsworth S (2018). The Influence of Trauma Type and Timing on PTSD Symptoms. *J Nerv Ment Dis* **206**: 72–76.

Guthrie RM, Bryant RA (2006). Extinction Learning Before Trauma and Subsequent

Posttraumatic Stress. *Psychosom Med* **68**: 307–311.

Han Y-S, Kim J-M, Cho J-S, Lee CS, Kim D-E (2005). Comparison of the Protective Effect of Indole beta-carbolines and R-(-)-deprenyl Against Nitrogen Species-Induced Cell Death in Experimental Culture Model of Parkinson's Disease. *J Clin Neurol* **1**: 81–91.

Harris RA, Bajo M, Bell RL, Blednov YA, Varodayan FP, Truitt JM, *et al* (2017). Genetic and Pharmacologic Manipulation of TLR4 Has Minimal Impact on Ethanol Consumption in Rodents. *J Neurosci* **37**: 1139–1155.

Hatano T, Saiki S, Okuzumi A, Mohney RP, Hattori N (2016). Identification of novel biomarkers for Parkinson's disease by metabolomic technologies. *J Neurol Neurosurg Psychiatry* **87**: 295–301.

Heal DJ, Gosden J, Smith SL (2014). Dopamine reuptake transporter (DAT) "inverse agonism"--a novel hypothesis to explain the enigmatic pharmacology of cocaine. *Neuropharmacology* **87**: 19–40.

Henry JP, Botton D, Sagne C, Isambert MF, Desnos C, Blanchard V, *et al* (1994). Biochemistry and molecular biology of the vesicular monoamine transporter from chromaffin granules. *J Exp Biol* **196**: 251–62.

Highland KB, Costanzo ME, Jovanovic T, Norrholm SD, Ndiongue RB, Reinhardt BJ, *et al* (2015). Catecholamine responses to virtual combat: implications for post-traumatic stress and dimensions of functioning. *Front Psychol* **6**: 256.

Hitzemann R, Oberbeck D, Iancu O, Darakjian P, McWeeney S, Spence S, *et al* (2017).

Alignment of the transcriptome with individual variation in animals selectively bred for High Drinking-In-the-Dark (HDID). *Alcohol* **60**: 115–120.

Hoge CW, Castro CA, Messer SC, McGurk D, Cotting DI, Koffman RL (2004). Combat Duty in Iraq and Afghanistan, Mental Health Problems, and Barriers to Care. *N Engl J Med* **351**: 13–22.

Holmstedt B, Lindgren J (1967). Chemical constituents and pharmacology of South American snuffs. *Psychopharmacol Bull* **4**: 16.

Hopper JW, Pitman RK, Su Z, Heyman GM, Lasko NB, Macklin ML, *et al* (2008). Probing reward function in posttraumatic stress disorder: expectancy and satisfaction with monetary gains and losses. *J Psychiatr Res* **42**: 802–7.

Hornykiewicz O (1970). The metabolism of brain dopamine in human parkinsonism. *Riv Patol Nerv Ment* **91**: 281–6.

Hornykiewicz O (1998). Biochemical aspects of Parkinson's disease. *Neurology* **51**: S2-9.

Hornykiewicz O (2017). L-DOPA. *J Parkinsons Dis* **7**: S3–S10.

Hoskins M, Pearce J, Bethell A, Dankova L, Barbui C, Tol WA, *et al* (2015). Pharmacotherapy for post-traumatic stress disorder: Systematic review and meta-analysis. *Br J Psychiatry* **206**: 93–100.

Ipser JC, Wilson D, Akindipe TO, Sager C, Stein DJ (2015). Pharmacotherapy for anxiety and comorbid alcohol use disorders. *Cochrane Database Syst Rev* **1**: CD007505.

Iritani S, Sekiguchi H, Habuchi C, Hikita T, Taya S, Kaibuchi K, *et al* (2010). Immunohistochemical study of vesicle monoamine transporter 2 in the hippocampal region of genetic animal model of schizophrenia. *Synapse* **64**: 948–953.

Isbister GK, Bowe SJ, Dawson A, Whyte IM (2004). Relative toxicity of selective serotonin reuptake inhibitors (SSRIs) in overdose. *J Toxicol Clin Toxicol* **42**: 277–85.

Ishiwata T, Hasegawa H, Greenwood BN (2017). Involvement of serotonin in the ventral tegmental area in thermoregulation of freely moving rats. *Neurosci Lett* **653**: 71–77.

Isingrini E, Perret L, Rainer Q, Sagueby S, Moquin L, Gratton A, *et al* (2016). Selective genetic disruption of dopaminergic, serotonergic and noradrenergic neurotransmission: insights into motor, emotional and addictive behaviour. *J Psychiatry Neurosci* **41**: 169–81.

Jacobsen LK, Southwick SM, Kosten TR (2001). Substance use disorders in patients with posttraumatic stress disorder: a review of the literature. *Am J Psychiatry* **158**: 1184–90.

Janak PH, Tye KM (2015). From circuits to behaviour in the amygdala. *Nature* **517**: 284–92.

Johansen KK, Wang L, Aasly JO, White LR, Matson WR, Henchcliffe C, *et al* (2009). Metabolomic Profiling in LRRK2-Related Parkinson's Disease. *PLoS One* **4**: e7551.

Johnson PL, Molosh A, Fitz SD, Arendt D, Deehan GA, Federici LM, *et al* (2015). Pharmacological depletion of serotonin in the basolateral amygdala complex reduces

anxiety and disrupts fear conditioning. *Pharmacol Biochem Behav* **138**: 174–179.

Jovanovic P, Spasojevic N, Stefanovic B, Bozovic N, Jasnic N, Djordjevic J, *et al* (2014). Peripheral oxytocin treatment affects the rat adreno-medullary catecholamine content modulating expression of vesicular monoamine transporter 2. *Peptides* **51**: 110–114.

Jovanovic T, Ely T, Fani N, Glover EM, Gutman D, Tone EB, *et al* (2013). Reduced neural activation during an inhibition task is associated with impaired fear inhibition in a traumatized civilian sample. *Cortex* **49**: 1884–91.

Jovanovic T, Kazama A, Bachevalier J, Davis M (2012). Impaired safety signal learning may be a biomarker of PTSD. *Neuropharmacology* **62**: 695–704.

Jovanovic T, Keyes M, Fiallos A, Myers KM, Davis M, Duncan EJ (2005). Fear potentiation and fear inhibition in a human fear-potentiated startle paradigm. *Biol Psychiatry* **57**: 1559–64.

Jovanovic T, Norrholm SD (2011). Neural Mechanisms of Impaired Fear Inhibition in Posttraumatic Stress Disorder. *Front Behav Neurosci* **5**: 8.

Jovanovic T, Norrholm SD, Blanding NQ, Davis M, Duncan E, Bradley B, *et al* (2010). Impaired fear inhibition is a biomarker of PTSD but not depression. *Depress Anxiety* **27**: 244–51.

Jovanovic T, Rauch SA, Rothbaum AO, Rothbaum BO (2017). Using experimental methodologies to assess posttraumatic stress. *Curr Opin Psychol* **14**: 23–28.

Jovanovic T, Ressler KJ (2010). How the neurocircuitry and genetics of fear inhibition

may inform our understanding of PTSD. *Am J Psychiatry* **167**: 648–62.

Kaczkurkin AN, Burton PC, Chazin SM, Manbeck AB, Espensen-Sturges T, Cooper SE, *et al* (2017). Neural Substrates of Overgeneralized Conditioned Fear in PTSD. *Am J Psychiatry* **174**: 125–134.

Kane MJ, Angoa-Peréz M, Briggs DI, Sykes CE, Francescutti DM, Rosenberg DR, *et al* (2012). Mice genetically depleted of brain serotonin display social impairments, communication deficits and repetitive behaviors: possible relevance to autism. *PLoS One* **7**: e48975.

Kao C-Y, Stalla G, Stalla J, Wotjak CT, Anderzhanova E (2015). Norepinephrine and corticosterone in the medial prefrontal cortex and hippocampus predict PTSD-like symptoms in mice. *Eur J Neurosci* **41**: 1139–1148.

Keane TM, Kolb LC, Kaloupek DG, Orr SP, Blanchard EB, Thomas RG, *et al* (1998). Utility of psychophysiological measurement in the diagnosis of posttraumatic stress disorder: results from a Department of Veterans Affairs Cooperative Study. *J Consult Clin Psychol* **66**: 914–23.

Keane TM, Marx BP, Sloan DM (2009). Post-Traumatic Stress Disorder: Definition, Prevalence, and Risk Factors. *Post-Traumatic Stress Disord* 1–19doi:10.1007/978-1-60327-329-9_1.

Keeshin BR, Ding Q, Presson AP, Berkowitz SJ, Strawn JR (2017). Use of Prazosin for Pediatric PTSD-Associated Nightmares and Sleep Disturbances: A Retrospective Chart Review. *Neurol Ther* **6**: 247–257.

Keller RW, Maisonneuve IM, Carlson JN, Glick SD (1992). Within-subject sensitization of striatal dopamine release after a single injection of cocaine: an in vivo microdialysis study. *Synapse* **11**: 28–34.

Kelmendi B, Adams TG, Yarnell S, Southwick S, Abdallah CG, Krystal JH (2016). PTSD: from neurobiology to pharmacological treatments. *Eur J Psychotraumatol* **7**: 31858.

Kessler RC, Aguilar-Gaxiola S, Alonso J, Bromet EJ, Gureje O, Karam EG, *et al* (2017). The associations of earlier trauma exposures and history of mental disorders with PTSD after subsequent traumas. *Mol Psychiatry* doi:10.1038/mp.2017.194.

Kessler RC, Berglund P, Demler O, Jin R, Merikangas KR, Walters EE (2005). Lifetime Prevalence and Age-of-Onset Distributions of DSM-IV Disorders in the National Comorbidity Survey Replication. *Arch Gen Psychiatry* **62**: 593.

Kessler RC, Crum RM, Warner LA, Nelson CB, Schulenberg J, Anthony JC (1997). Lifetime co-occurrence of DSM-III-R alcohol abuse and dependence with other psychiatric disorders in the National Comorbidity Survey. *Arch Gen Psychiatry* **54**: 313–21.

Kessler RC, Sonnega A, Bromet E, Hughes M, Nelson CB (1995). Posttraumatic stress disorder in the National Comorbidity Survey. *Arch Gen Psychiatry* **52**: 1048–60.

Kim DH, Jang YY, Han ES, Lee CS (2001). Protective effect of harmaline and harmalol against dopamine- and 6-hydroxydopamine-induced oxidative damage of brain mitochondria and synaptosomes, and viability loss of PC12 cells. *Eur J Neurosci* **13**: 1861–72.

Klawans HL, Goodman RM, Paulson GW, Barbeau A (1972). Levodopa in the presymptomatic diagnosis of Huntington's chorea. *Lancet (London, England)* **2**: 49.

Koen N, Fourie J, Terburg D, Stoop R, Morgan B, Stein DJ, *et al* (2016). Translational neuroscience of basolateral amygdala lesions: Studies of urbach-wiethe disease. *J Neurosci Res* **94**: 504–512.

Koenen KC, Lyons MJ, Goldberg J, Simpson J, Williams WM, Toomey R, *et al* (2003). A High Risk Twin Study of Combat-Related PTSD Comorbidity. *Twin Res* **6**: 218–226.

Kolassa I-T, Kolassa S, Ertl V, Papassotiropoulos A, Quervain DJ-F De (2010). The risk of posttraumatic stress disorder after trauma depends on traumatic load and the catechol-o-methyltransferase Val(158)Met polymorphism. *Biol Psychiatry* **67**: 304–8.

Kolk B van der, Najavits LM (2013). Interview: What is PTSD Really? Surprises, Twists of History, and the Politics of Diagnosis and Treatment. *J Clin Psychol* **69**: 516–522.

Kolter T (2012). Ganglioside Biochemistry. *ISRN Biochem* **2012**: 1–36.

Krabbe S, Gründemann J, Lüthi A (2018). Amygdala Inhibitory Circuits Regulate Associative Fear Conditioning. *Biol Psychiatry* **83**: 800–809.

Kuhn W, Müller T, Groβe H, Rommelspacher H (1996). Elevated levels of harman and norharman in cerebrospinal fluid of Parkinsonian patients. *J Neural Transm* **103**: 1435–1440.

Kulka RA, Schlenger WE, Fairbank JA, Hough RL, Jordan BK, Marmar CR, *et al*

(1988). *Contractual Report of Findings from the National Vietnam Veterans Readjustment Study*. .

Lachman HM, Papolos DF, Saito T, Yu YM, Szumlanski CL, Weinshilboum RM (1996). Human catechol-O-methyltransferase pharmacogenetics: description of a functional polymorphism and its potential application to neuropsychiatric disorders. *Pharmacogenetics* **6**: 243–50.

Lacivita E, Perrone R, Margari L, Leopoldo M (2017). Targets for Drug Therapy for Autism Spectrum Disorder: Challenges and Future Directions. *J Med Chem* **60**: 9114–9141.

Lai HMX, Cleary M, Sitharthan T, Hunt GE (2015). Prevalence of comorbid substance use, anxiety and mood disorders in epidemiological surveys, 1990-2014: A systematic review and meta-analysis. *Drug Alcohol Depend* **154**: 1–13.

Lee DJ, Schnitzlein CW, Wolf JP, Vythilingam M, Rasmusson AM, Hoge CW (2016). Psychotherapy versus pharmacotherapy for posttraumatic stress disorder systemic review and meta-analyses to determine first-line treatments. *Depress Anxiety* **33**: 792–806.

Lee JH, Kim J-H (2016). Dopamine-dependent synaptic plasticity in an amygdala inhibitory circuit controls fear memory expression. *BMB Rep* **49**: 1–2.

Lee JH, Lee S, Kim J-H (2017). Amygdala Circuits for Fear Memory: A Key Role for Dopamine Regulation. *Neurosci* **23**: 542–553.

Lee Gregory M, Burton VJ, Shapiro BK (2015). Developmental Disabilities and

Metabolic Disorders. *Neurobiol Brain Disord* 18–41doi:10.1016/B978-0-12-398270-4.00003-3.

Levant B (1998). Differential distribution of D3 dopamine receptors in the brains of several mammalian species. *Brain Res* **800**: 269–74.

Levy-Gigi E, Szabo C, Richter-Levin G, Kéri S (2015). Reduced hippocampal volume is associated with overgeneralization of negative context in individuals with PTSD. *Neuropsychology* **29**: 151–161.

Li L, Bao Y, He S, Wang G, Guan Y, Ma D, *et al* (2016). The Association Between Genetic Variants in the Dopaminergic System and Posttraumatic Stress Disorder: A Meta-Analysis. *Medicine (Baltimore)* **95**: e3074.

Li S, Park Y, Duraisingham S, Strobel FH, Khan N, Soltow QA, *et al* (2013). Predicting Network Activity from High Throughput Metabolomics. *PLoS Comput Biol* **9**: e1003123.

Lin C-C, Tung C-S, Lin P-H, Huang C-L, Liu Y-P (2016). Traumatic stress causes distinctive effects on fear circuit catecholamines and the fear extinction profile in a rodent model of posttraumatic stress disorder. *Eur Neuropsychopharmacol* doi:10.1016/j.euroneuro.2016.06.004.

Little KY, Krolewski DM, Zhang L, Cassin BJ (2003). Loss of striatal vesicular monoamine transporter protein (VMAT2) in human cocaine users. *Am J Psychiatry* **160**: 47–55.

Liu Y, Peter D, Roghani A, Schuldiner S, Privé GG, Eisenberg D, *et al* (1992). A cDNA

that suppresses MPP+ toxicity encodes a vesicular amine transporter. *Cell* **70**: 539–51.

Lohoff FW (2010). Genetic Variants in the Vesicular Monoamine Transporter 1 (VMAT1/SLC18A1) and Neuropsychiatric Disorders. *Methods Mol Biol* **637**: 165–180.

Lohoff FW, Dahl JP, Ferraro TN, Arnold SE, Gallinat J, Sander T, *et al* (2006). Variations in the vesicular monoamine transporter 1 gene (VMAT1/SLC18A1) are associated with bipolar i disorder. *Neuropsychopharmacology* **31**: 2739–47.

Lohr KM, Bernstein AI, Stout KA, Dunn AR, Lazo CR, Alter SP, *et al* (2014). Increased vesicular monoamine transporter enhances dopamine release and opposes Parkinson disease-related neurodegeneration in vivo. *Proc Natl Acad Sci U S A* **111**: 9977–9982.

Lohr KM, Chen M, Hoffman CA, McDaniel MJ, Stout KA, Dunn AR, *et al* (2016). Vesicular monoamine transporter 2 (VMAT2) level regulates MPTP vulnerability and clearance of excess dopamine in mouse striatal terminals. *Toxicol Sci* **153**: 79–88.

Lohr KM, Miller GW (2014). VMAT2 and Parkinson's disease: harnessing the dopamine vesicle. *Expert Rev Neurother* **14**: 1115–7.

Lohr KM, Stout KA, Dunn AR, Wang M, Salahpour A, Guillot TS, *et al* (2015). Increased Vesicular Monoamine Transporter 2 (VMAT2; Slc18a2) Protects against Methamphetamine Toxicity. *ACS Chem Neurosci* **6**: 790–9.

Luan H, Liu L-F, Meng N, Tang Z, Chua K-K, Chen L-L, *et al* (2015a). LC–MS-Based Urinary Metabolite Signatures in Idiopathic Parkinson's Disease. *J Proteome Res* **14**: 467–478.

Luan H, Liu L-F, Tang Z, Zhang M, Chua K-K, Song J-X, *et al* (2015b). Comprehensive urinary metabolomic profiling and identification of potential noninvasive marker for idiopathic Parkinson's disease. *Sci Rep* **5**: 13888.

Luchins DJ, Goldman MB, Lieb M, Hanrahan P (1992). Repetitive behaviors in chronically institutionalized schizophrenic patients. *Schizophr Res* **8**: 119–23.

Maina FK, Khalid M, Apawu AK, Mathews TA (2012). Presynaptic dopamine dynamics in striatal brain slices with fast-scan cyclic voltammetry. *J Vis Exp* doi:10.3791/3464.

Maina FK, Mathews TA (2010). A functional fast scan cyclic voltammetry assay to characterize dopamine D2 and D3 autoreceptors in the mouse striatum. *ACS Chem Neurosci* **1**: 450–462.

Manning M, Misicka A, Olma A, Bankowski K, Stoev S, Chini B, *et al* (2012). Oxytocin and Vasopressin Agonists and Antagonists as Research Tools and Potential Therapeutics. *J Neuroendocrinol* **24**: 609–628.

Martenyi F, Brown EB, Zhang H, Prakash A, Koke SC (2002). Fluoxetine versus placebo in posttraumatic stress disorder. *J Clin Psychiatry* **63**: 199–206.

Martinez Z, Zhu M, Han S, Fink AL (2007). GM1 specifically interacts with alpha-synuclein and inhibits fibrillation. *Biochemistry* **46**: 1868–77.

Masoud ST, Vecchio LM, Bergeron Y, Hossain MM, Nguyen LT, Bermejo MK, *et al* (2015). Increased expression of the dopamine transporter leads to loss of dopamine neurons, oxidative stress and l-DOPA reversible motor deficits. *Neurobiol Dis* **74**: 66–75.

Matsubara K, Kobayashi S, Kobayashi Y, Yamashita K, Koide H, Hatta M, *et al* (1995). beta-Carbolinium cations, endogenous MPP+ analogs, in the lumbar cerebrospinal fluid of patients with Parkinson's disease. *Neurology* **45**: 2240–5.

Mattammal MB, Haring JH, Chung HD, Raghu G, Strong R (1995). An endogenous dopaminergic neurotoxin: implication for Parkinson's disease. *Neurodegeneration* **4**: 271–81.

Mazzoni IE, Jaffe E, Cuello AC (1991). Production and immunocytochemical application of a highly sensitive and specific monoclonal antibody against rat dopamine-beta-hydroxylase. *Histochemistry* **96**: 45–50.

McGinnis MM, Siciliano CA, Jones SR (2016). Dopamine D3 autoreceptor inhibition enhances cocaine potency at the dopamine transporter. *J Neurochem* **138**: 821–9.

McHugh SB, Barkus C, Lima J, Glover LR, Sharp T, Bannerman DM (2015). SERT and uncertainty: serotonin transporter expression influences information processing biases for ambiguous aversive cues in mice. *Genes Brain Behav* **14**: 330–6.

Mefford I, Oke A, Adams RN, Jonsson G (1977). Epinephrine localization in human brain stem. *Neurosci Lett* **5**: 141–5.

Meletti S, Cantalupo G, Santoro F, Benuzzi F, Marliani AF, Tassinari CA, *et al* (2014).

Temporal lobe epilepsy and emotion recognition without amygdala: a case study of Urbach-Wiethe disease and review of the literature. *Epileptic Disord* **16**: 518–27.

Milad MR, Pitman RK, Ellis CB, Gold AL, Shin LM, Lasko NB, *et al* (2009). Neurobiological basis of failure to recall extinction memory in posttraumatic stress disorder. *Biol Psychiatry* **66**: 1075–82.

Miller GW, Erickson JD, Perez JT, Penland SN, Mash DC, Rye DB, *et al* (1999). Immunochemical analysis of vesicular monoamine transporter (VMAT2) protein in Parkinson's disease. *Exp Neurol* **156**: 138–48.

Mitchell HA, Weinshenker D (2010). Good night and good luck: Norepinephrine in sleep pharmacology. *Biochem Pharmacol* **79**: 801–809.

Mithoefer MC, Wagner MT, Mithoefer AT, Jerome L, Doblin R (2011). The safety and efficacy of {+/-}3,4-methylenedioxymethamphetamine-assisted psychotherapy in subjects with chronic, treatment-resistant posttraumatic stress disorder: the first randomized controlled pilot study. *J Psychopharmacol* **25**: 439–52.

Modlin HC (1967). The postaccident anxiety syndrome: psychosocial aspects. *Am J Psychiatry* **123**: 1008–1012.

Mohammad-Zadeh LF, Moses L, Gwaltney-Brant SM (2008). Serotonin: a review. *J Vet Pharmacol Ther* **31**: 187–199.

Moita MAP, Rosis S, Zhou Y, LeDoux JE, Blair HT (2003). Hippocampal place cells acquire location-specific responses to the conditioned stimulus during auditory fear conditioning. *Neuron* **37**: 485–97.

Moloudizargari M, Mikaili P, Aghajanshakeri S, Asghari MH, Shayegh J (2013). Pharmacological and therapeutic effects of Peganum harmala and its main alkaloids. *Pharmacogn Rev* **7**: 199–212.

Montoya A, Bruins R, Katzman M, Blier P (2016). The noradrenergic paradox: implications in the management of depression and anxiety. *Neuropsychiatr Dis Treat* **12**: 541.

Morey RA, Dunsmoor JE, Haswell CC, Brown VM, Vora A, Weiner J, *et al* (2015a). Fear learning circuitry is biased toward generalization of fear associations in posttraumatic stress disorder. *Transl Psychiatry* **5**: e700.

Morey RA, Dunsmoor JE, Haswell CC, Brown VM, Vora A, Weiner J, *et al* (2015b). Fear learning circuitry is biased toward generalization of fear associations in posttraumatic stress disorder. *Transl Psychiatry* **5**: e700–e700.

Narboux-Nême N, Sagné C, Doly S, Diaz SL, Martin CBP, Angenard G, *et al* (2011). Severe serotonin depletion after conditional deletion of the vesicular monoamine transporter 2 gene in serotonin neurons: neural and behavioral consequences. *Neuropsychopharmacology* **36**: 2538–50.

Nasreddine ZS, Phillips NA, BÃ©dirian V, Charbonneau S, Whitehead V, Collin I, *et al* (2005). The Montreal Cognitive Assessment, MoCA: A Brief Screening Tool For Mild Cognitive Impairment. *J Am Geriatr Soc* **53**: 695–699.

Naß J, Efferth T (2017). Pharmacogenetics and Pharmacotherapy of Military Personnel Suffering from Post-traumatic Stress Disorder. *Curr Neuropharmacol* **15**: 831–860.

Newman AH, Blaylock BL, Nader MA, Bergman J, Sibley DR, Skolnick P (2012). Medication discovery for addiction: translating the dopamine D3 receptor hypothesis. *Biochem Pharmacol* **84**: 882–90.

Newman AH, Grundt P, Nader MA (2005). Dopamine D3 Receptor Partial Agonists and Antagonists as Potential Drug Abuse Therapeutic Agents. *J Med Chem* **48**: 3663–3679.

Nirenberg MJ, Liu Y, Peter D, Edwards RH, Pickel VM (1995). The vesicular monoamine transporter 2 is present in small synaptic vesicles and preferentially localizes to large dense core vesicles in rat solitary tract nuclei. *Proc Natl Acad Sci U S A* **92**: 8773–7.

Norrholm SD, Glover EM, Stevens JS, Fani N, Galatzer-Levy IR, Bradley B, *et al* (2015a). Fear load: The psychophysiological over-expression of fear as an intermediate phenotype associated with trauma reactions. *Int J Psychophysiol* **98**: 270–5.

Norrholm SD, Glover EM, Stevens JS, Fani N, Galatzer-Levy IR, Bradley B, *et al* (2015b). Fear load: The psychophysiological over-expression of fear as an intermediate phenotype associated with trauma reactions. *Int J Psychophysiol* **98**: 270–275.

Norrholm SD, Jovanovic T (2010). Tailoring therapeutic strategies for treating posttraumatic stress disorder symptom clusters. *Neuropsychiatr Dis Treat* **6**: 517–32.

Norrholm SD, Jovanovic T, Olin IW, Sands LA, Karapanou I, Bradley B, *et al* (2011).

Fear extinction in traumatized civilians with posttraumatic stress disorder: relation to symptom severity. *Biol Psychiatry* **69**: 556–63.

Norrholm SD, Ressler KJ (2009). Genetics of anxiety and trauma-related disorders. *Neuroscience* **164**: 272–287.

O'Connell LA, Hofmann HA (2011). The Vertebrate mesolimbic reward system and social behavior network: A comparative synthesis. *J Comp Neurol* **519**: 3599–3639.

O'Donnell T, Hegadoren KM, Coupland NC (2004). Noradrenergic Mechanisms in the Pathophysiology of Post-Traumatic Stress Disorder. *Neuropsychobiology* **50**: 273–283.

O'Hearn E, Molliver ME (1993). Degeneration of Purkinje cells in parasagittal zones of the cerebellar vermis after treatment with ibogaine or harmaline. *Neuroscience* **55**: 303–10.

O'Neill C, Evers-Donnelly A, Nicholson D, O'Boyle KM, O'Connor JJ (2009). D2 receptor-mediated inhibition of dopamine release in the rat striatum in vitro is modulated by CB1 receptors: studies using fast cyclic voltammetry. *J Neurochem* **108**: 545–51.

Okamura N, Villemagne VL, Drago J, Pejoska S, Dhamija RK, Mulligan RS, *et al* (2010). In vivo measurement of vesicular monoamine transporter type 2 density in Parkinson disease with (18)F-AV-133. *J Nucl Med* **51**: 223–8.

Ordway GA, Schwartz MA, Frazer A (Cambridge University Press: 2007). *Brain Norepinephrine: Neurobiology and Therapeutics - Google Books*. .

Orr SP, Metzger LJ, Lasko NB, Macklin ML, Peri T, Pitman RK (2000). De novo conditioning in trauma-exposed individuals with and without posttraumatic stress disorder. *J Abnorm Psychol* **109**: 290–298.

Orsini CA, Maren S (2012). Neural and cellular mechanisms of fear and extinction memory formation. *Neurosci Biobehav Rev* **36**: 1773–1802.

Otis JM, Werner CT, Mueller D (2015). Noradrenergic Regulation of Fear and Drug-Associated Memory Reconsolidation. *Neuropsychopharmacology* **40**: 793–803.

Ozer EJ, Best SR, Lipsey TL, Weiss DS (2003). Predictors of posttraumatic stress disorder and symptoms in adults: A meta-analysis. *Psychol Bull* **129**: 52–73.

Panneton WM, Kumar VB, Gan Q, Burke WJ, Galvin JE (2010). The neurotoxicity of DOPAL: behavioral and stereological evidence for its role in Parkinson disease pathogenesis. *PLoS One* **5**: e15251.

Pari K, Sundari CS, Chandani S, Balasubramanian D (2000). beta-carbolines that accumulate in human tissues may serve a protective role against oxidative stress. *J Biol Chem* **275**: 2455–62.

Park TH, Kwon OS, Park SY, Han ES, Lee CS (2003). N-methylated beta-carbolines protect PC12 cells from cytotoxic effect of MPP+ by attenuation of mitochondrial membrane permeability change. *Neurosci Res* **46**: 349–58.

Peri T, Ben-Shakhar G, Orr SP, Shalev AY (2000). Psychophysiologic assessment of aversive conditioning in posttraumatic stress disorder. *Biol Psychiatry* **47**: 512–9.

Peskin M, Wyka K, Cukor J, Olden M, Altemus M, Lee FS, *et al* (2018). The relationship

between posttraumatic and depressive symptoms during virtual reality exposure therapy with a cognitive enhancer. *J Anxiety Disord* doi:10.1016/j.janxdis.2018.03.001.

Peter D, Liu Y, Brecha N, Edwards RH (1995a). The transport of neurotransmitters into synaptic vesicles. *Prog Brain Res* **105**: 273–81.

Peter D, Liu Y, Sternini C, Giorgio R de, Brecha N, Edwards RH (1995b). Differential expression of two vesicular monoamine transporters. *J Neurosci* **15**: 6179–88.

Phelps EA, O'Connor KJ, Gatenby JC, Gore JC, Grillon C, Davis M (2001). Activation of the left amygdala to a cognitive representation of fear. *Nat Neurosci* **4**: 437–41.

Pietrzak RH, Goldstein RB, Southwick SM, Grant BF (2011). Prevalence and Axis I comorbidity of full and partial posttraumatic stress disorder in the United States: Results from Wave 2 of the National Epidemiologic Survey on Alcohol and Related Conditions. *J Anxiety Disord* **25**: 456–465.

Pifl C, Rajput A, Reither H, Blesa J, Cavada C, Obeso JA, *et al* (2014). Is Parkinson's disease a vesicular dopamine storage disorder? Evidence from a study in isolated synaptic vesicles of human and nonhuman primate striatum. *J Neurosci* **34**: 8210–8.

Pitman RK, Orr SP, Forgue DF, Jong JB de, Claiborn JM (1987). Psychophysiologic assessment of posttraumatic stress disorder imagery in Vietnam combat veterans. *Arch Gen Psychiatry* **44**: 970–5.

Pittig A, Treanor M, LeBeau RT, Craske MG (2018). The role of associative fear and avoidance learning in anxiety disorders: Gaps and directions for future research.

Neurosci Biobehav Rev **88**: 117–140.

Pitts EG, Minerva AR, Chandler EB, Kohn JN, Logun MT, Sulima A, *et al* (2017). 3,4-Methylenedioxymethamphetamine Increases Affiliative Behaviors in Squirrel Monkeys in a Serotonin 2A Receptor-Dependent Manner. *Neuropsychopharmacology* **42**: 1962–1971.

Polanski W, Enzensperger C, Reichmann H, Gille G (2010). The exceptional properties of 9-methyl-β-carboline: stimulation, protection and regeneration of dopaminergic neurons coupled with anti-inflammatory effects. *J Neurochem* **113**: no-no.

Pole N (2007). The psychophysiology of posttraumatic stress disorder: A meta-analysis. *Psychol Bull* **133**: 725–746.

Porter-Stransky KA, Wescott SA, Hershman M, Badrinarayan A, Weele CM Vander, Lovic V, *et al* (2011). Cocaine must enter the brain to evoke unconditioned dopamine release within the nucleus accumbens shell. *Neurosci Lett* **504**: 13–7.

Post LM, Feeny NC, Zoellner LA, Connell AM (2016). Post-traumatic stress disorder and depression co-occurrence: Structural relations among disorder constructs and trait and symptom dimensions. *Psychol Psychother Theory, Res Pract* **89**: 418–434.

Raskind MA, Peskind ER, Chow B, Harris C, Davis-Karim A, Holmes HA, *et al* (2018). Trial of Prazosin for Post-Traumatic Stress Disorder in Military Veterans. *N Engl J Med* **378**: 507–517.

Rauch SL, Whalen PJ, Shin LM, McInerney SC, Macklin ML, Lasko NB, *et al* (2000). Exaggerated amygdala response to masked facial stimuli in posttraumatic stress

disorder: a functional MRI study. *Biol Psychiatry* **47**: 769–76.

Rayport S, Sulzer D, Shi WX, Sawasdikosol S, Monaco J, Batson D, *et al* (1992). Identified postnatal mesolimbic dopamine neurons in culture: morphology and electrophysiology. *J Neurosci* **12**: 4264 LP-4280.

Ressler KJ, Mercer KB, Bradley B, Jovanovic T, Mahan A, Kerley K, *et al* (2011). Post-traumatic stress disorder is associated with PACAP and the PAC1 receptor. *Nature* **470**: 492–497.

Reveron ME, Savelieva K V, Tillerson JL, McCormack AL, Monte DA Di, Miller GW (2002). L-DOPA does not cause neurotoxicity in VMAT2 heterozygote knockout mice. *Neurotoxicology* **23**: 611–9.

Rhodes JS, Best K, Belknap JK, Finn DA, Crabbe JC (2005). Evaluation of a simple model of ethanol drinking to intoxication in C57BL/6J mice. *Physiol Behav* **84**: 53–63.

Rhodes JS, Ford MM, Yu C-H, Brown LL, Finn DA, Garland T, *et al* (2007). Mouse inbred strain differences in ethanol drinking to intoxication. *Genes, Brain Behav* **6**: 1–18.

Richardson JR, Caudle WM, Wang M, Dean ED, Pennell KD, Miller GW (2006). Developmental exposure to the pesticide dieldrin alters the dopamine system and increases neurotoxicity in an animal model of Parkinson's disease. *FASEB J* **20**: 1695–7.

Rilstone JJ, Alkhater RA, Minassian BA (2013). Brain Dopamine–Serotonin Vesicular

Transport Disease and Its Treatment. *N Engl J Med* **368**: 543–550.

Ritz MC, Lamb RJ, Goldberg SR, Kuhar MJ (1988). Cocaine self-administration appears to be mediated by dopamine uptake inhibition. *Prog Neuropsychopharmacol Biol Psychiatry* **12**: 233–9.

Roberts C, Cummins R, Gnoffo Z, Kew JNC (2006). Dopamine D3 receptor modulation of dopamine efflux in the rat nucleus accumbens. *Eur J Pharmacol* **534**: 108–114.

Robinson JD, Howard CD, Pastuzyn ED, Byers DL, Keefe KA, Garris PA (2014). Methamphetamine-induced neurotoxicity disrupts pharmacologically evoked dopamine transients in the dorsomedial and dorsolateral striatum. *Neurotox Res* **26**: 152–67.

Roede JR, Uppal K, Park Y, Lee K, Tran V, Walker D, *et al* (2013). Serum metabolomics of slow vs. rapid motor progression Parkinson's disease: a pilot study. *PLoS One* **8**: e77629.

Rojas SM, Bujarski S, Babson KA, Dutton CE, Feldner MT (2014). Understanding PTSD comorbidity and suicidal behavior: associations among histories of alcohol dependence, major depressive disorder, and suicidal ideation and attempts. *J Anxiety Disord* **28**: 318–25.

Rooij SJH van, Stevens JS, Ely TD, Fani N, Smith AK, Kerley KA, *et al* (2016). Childhood Trauma and COMT Genotype Interact to Increase Hippocampal Activation in Resilient Individuals. *Front psychiatry* **7**: 156.

Rosen ZB, Cheung S, Siegelbaum SA (2015). Midbrain dopamine neurons

bidirectionally regulate CA3-CA1 synaptic drive. *Nat Neurosci* **18**: 1763–1771.

Sareen J, Cox BJ, Stein MB, Afifi TO, Fleet C, Asmundson GJG (2007). Physical and mental comorbidity, disability, and suicidal behavior associated with posttraumatic stress disorder in a large community sample. *Psychosom Med* **69**: 242–8.

Savelieva K V, Caudle WM, Miller GW (2006). Altered ethanol-associated behaviors in vesicular monoamine transporter heterozygote knockout mice. *Alcohol* **40**: 87–94.

Schäfer I, Najavits LM (2007). Clinical challenges in the treatment of patients with posttraumatic stress disorder and substance abuse. *Curr Opin Psychiatry* **20**: 614–618.

Scher CD, Stein MB, Asmundson GJ, McCreary DR, Forde DR (2001). The childhood trauma questionnaire in a community sample: psychometric properties and normative data. *J Trauma Stress* **14**: 843–57.

Schmitz Y, Lee CJ, Schmauss C, Gonon F, Sulzer D (2001). Amphetamine distorts stimulation-dependent dopamine overflow: effects on D2 autoreceptors, transporters, and synaptic vesicle stores. *J Neurosci* **21**: 5916–24.

Schneider JS, Cambi F, Gollomp SM, Kuwabara H, Brašić JR, Leiby B, *et al* (2015). GM1 ganglioside in Parkinson's disease: Pilot study of effects on dopamine transporter binding. *J Neurol Sci* **356**: 118–23.

Schuldiner S, Shirvan A, Linial M (1995). Vesicular neurotransmitter transporters: from bacteria to humans. *Physiol Rev* **75**: 369–92.

Schwartz K, Yadid G, Weizman A, Rehavi M (2003). Decreased limbic vesicular

monoamine transporter 2 in a genetic rat model of depression. *Brain Res* **965**: 174–179.

Schymanski EL, Jeon J, Gulde R, Fenner K, Ruff M, Singer HP, *et al* Identifying Small Molecules via High Resolution Mass Spectrometry: Communicating Confidence. doi:10.1021/es5002105.

Shannon P, Markiel A, Ozier O, Baliga NS, Wang JT, Ramage D, *et al* (2003). Cytoscape: a software environment for integrated models of biomolecular interaction networks. *Genome Res* **13**: 2498–504.

Shay J (1991). Learning about combat stress from Homer's Iliad. *J Trauma Stress* **4**: 561–579.

Shin E-J, Duong CX, Nguyen X-KT, Li Z, Bing G, Bach J-H, *et al* (2012). Role of oxidative stress in methamphetamine-induced dopaminergic toxicity mediated by protein kinase Cδ. *Behav Brain Res* **232**: 98–113.

Shin LM, Rauch SL, Pitman RK (2006). Amygdala, medial prefrontal cortex, and hippocampal function in PTSD. *Ann N Y Acad Sci* **1071**: 67–79.

Shiromani P, Keane T, LeDoux J (Humana Press: 2009). *Post-traumatic stress disorder: basic science and clinical practice*. .

Shorter D, Hsieh J, Kosten TR (2015). Pharmacologic management of comorbid post-traumatic stress disorder and addictions. *Am J Addict* **24**: 705–712.

Singer BF, Bryan MA, Popov P, Robinson TE, Aragona BJ (2017). Rapid induction of dopamine sensitization in the nucleus accumbens shell induced by a single injection

of cocaine. *Behav Brain Res* **324**: 66–70.

Sirek A, Sirek O V (1970). Serotonin: a review. *Can Med Assoc J* **102**: 846–9.

Smith HR, Porrino LJ (2008). The comparative distributions of the monoamine transporters in the rodent, monkey, and human amygdala. *Brain Struct Funct* **213**: 73–91.

Solovieff N, Roberts AL, Ratanatharathorn A, Haloosim M, Vivo I De, King AP, *et al* (2014). Genetic association analysis of 300 genes identifies a risk haplotype in SLC18A2 for post-traumatic stress disorder in two independent samples. *Neuropsychopharmacology* **39**: 1872–1879.

Song C-HH, Fan X, Exeter CJ, Hess EJ, Jinnah HA (2012). Functional analysis of dopaminergic systems in a DYT1 knock-in mouse model of dystonia. *Neurobiol Dis* **48**: 66–78.

Soto-Otero R, Méndez-Alvarez E, Riguera-Vega R, Quiñoá-Cabana E, Sánchez-Sellero I, López-Rivadulla Lamas M (1998). Studies on the interaction between 1,2,3,4-tetrahydro-beta-carboline and cigarette smoke: a potential mechanism of neuroprotection for Parkinson's disease. *Brain Res* **802**: 155–62.

Spinhoven P, Penninx BW, Hemert AM van, Rooij M de, Elzinga BM (2014). Comorbidity of PTSD in anxiety and depressive disorders: Prevalence and shared risk factors. *Child Abuse Negl* **38**: 1320–1330.

Spitzer EG, Zuromski KL, Davis MT, Witte TK, Weathers F (2018). Posttraumatic Stress Disorder Symptom Clusters and Acquired Capability for Suicide: A Reexamination

Using *DSM*- 5 Criteria. *Suicide Life-Threatening Behav* **48**: 105–115.

Stamford JA, Kruk ZL, Millar J (1988). Actions of dopamine antagonists on stimulated striatal and limbic dopamine release: an in vivo voltammetric study. *Br J Pharmacol* **94**: 924–32.

Steenkamp MM, Schlenger WE, Corry N, Henn-Haase C, Qian M, Li M, *et al* (2017). Predictors of PTSD 40 years after combat: Findings from the National Vietnam Veterans longitudinal study. *Depress Anxiety* doi:10.1002/da.22628.

Stevens JS, Jovanovic T, Fani N, Ely TD, Glover EM, Bradley B, *et al* (2013). Disrupted amygdala-prefrontal functional connectivity in civilian women with posttraumatic stress disorder. *J Psychiatr Res* **47**: 1469–1478.

Stevens JS, Kim YJ, Galatzer-Levy IR, Reddy R, Ely TD, Nemeroff CB, *et al* (2017). Amygdala Reactivity and Anterior Cingulate Habituation Predict Posttraumatic Stress Disorder Symptom Maintenance After Acute Civilian Trauma. *Biol Psychiatry* **81**: 1023–1029.

Storch A, Hwang Y-I, Gearhart DA, Beach JW, Neafsey EJ, Collins MA, *et al* (2004). Dopamine transporter-mediated cytotoxicity of beta-carbolinium derivatives related to Parkinson's disease: relationship to transporter-dependent uptake. *J Neurochem* **89**: 685–94.

Stout KA, Dunn AR, Lohr KM, Alter SP, Cliburn RA, Guillot TS, *et al* (2016). Selective enhancement of dopamine release in the ventral pallidum of methamphetamine-sensitized mice. *ACS Chem Neurosci* **7**: 1364–1373.

Sulzer D, Zecca L (2000). Intraneuronal dopamine-quinone synthesis: a review. *Neurotox Res* **1**: 181–95.

Susskind O, Ruzek JI, Friedman MJ (2012). The VA/DOD Clinical Practice Guideline for Management of Post-Traumatic Stress (update 2010): development and methodology. *J Rehabil Res Dev* **49**: xvii–xxviii.

Swanson LW (1982). The projections of the ventral tegmental area and adjacent regions: a combined fluorescent retrograde tracer and immunofluorescence study in the rat. *Brain Res Bull* **9**: 321–53.

Takahashi N, Miner LL, Sora I, Ujike H, Revay RS, Kostic V, *et al* (1997). VMAT2 knockout mice: heterozygotes display reduced amphetamine-conditioned reward, enhanced amphetamine locomotion, and enhanced MPTP toxicity. *Proc Natl Acad Sci U S A* **94**: 9938–9943.

Tanabe M, Kanehisa M (2012). Using the KEGG Database Resource. *Curr Protoc Bioinforma* **Chapter 1**: Unit1.12.

Taylor TN, Alter SP, Wang M, Goldstein DS, Miller GW (2014). Reduced vesicular storage of catecholamines causes progressive degeneration in the locus ceruleus. *Neuropharmacology* **76**: 97–105.

Taylor TN, Caudle WM, Miller GW (2011). VMAT2-deficient mice display nigral and extranigral pathology and motor and nonmotor symptoms of Parkinson's disease. *Park Dis* **2011**: 124165.

Taylor TN, Caudle WM, Shepherd KR, Noorian A, Jackson CR, Iuvone PM, *et al* (2009).

Nonmotor symptoms of Parkinson's disease revealed in an animal model with reduced monoamine storage capacity. *J Neurosci* **29**: 8103–8113.

Temple W, Mendelsohn L, Kim GE, Nekritz E, Gustafson WC, Lin L, *et al* (2016). Vesicular monoamine transporter protein expression correlates with clinical features, tumor biology, and MIBG avidity in neuroblastoma: a report from the Children's Oncology Group. *Eur J Nucl Med Mol Imaging* **43**: 474–481.

Thal SB, Lommen MJJ (2018). Current Perspective on MDMA-Assisted Psychotherapy for Posttraumatic Stress Disorder. *J Contemp Psychother* **48**: 99–108.

Thiele TE, Crabbe JC, Boehm SL (2014). "Drinking in the Dark" (DID): A Simple Mouse Model of Binge-Like Alcohol Intake. *Curr Protoc Neurosci* **68**: 9.49.1-9.49.12.

Tillinger A, Sollas A, Serova LI, Kvetnansky R, Sabban EL (2010). Vesicular monoamine transporters (VMATs) in adrenal chromaffin cells: stress-triggered induction of VMAT2 and expression in epinephrine synthesizing cells. *Cell Mol Neurobiol* **30**: 1459–65.

Trupp M, Jonsson P, Ohrfelt A, Zetterberg H, Obudulu O, Malm L, *et al* (2014). Metabolite and peptide levels in plasma and CSF differentiating healthy controls from patients with newly diagnosed Parkinson's disease. *J Parkinsons Dis* **4**: 549–60.

Uppal K, Soltow QA, Strobel FH, Pittard WS, Gernert KM, Yu T, *et al* (2013). xMSanalyzer: automated pipeline for improved feature detection and downstream analysis of large-scale, non-targeted metabolomics data. *BMC Bioinformatics* **14**:

15.

Uppal K, Walker DI, Liu K, Li S, Go Y-M, Jones DP (2016). Computational Metabolomics: A Framework for the Million Metabolome. *Chem Res Toxicol* **29**: 1956–1975.

Vaht M, Kiive E, Veidebaum T, Harro J (2016). A Functional Vesicular Monoamine Transporter 1 (VMAT1) Gene Variant Is Associated with Affect and the Prevalence of Anxiety, Affective, and Alcohol Use Disorders in a Longitudinal Population-Representative Birth Cohort Study. *Int J Neuropsychopharmacol* **19**: .

Veenstra-VanderWeele J, Muller CL, Iwamoto H, Sauer JE, Owens WA, Shah CR, *et al* (2012). Autism gene variant causes hyperserotonemia, serotonin receptor hypersensitivity, social impairment and repetitive behavior. *Proc Natl Acad Sci U S A* **109**: 5469–74.

Venton BJ, Seipel AT, Phillips PEM, Wetsel WC, Gitler D, Greengard P, *et al* (2006). Cocaine increases dopamine release by mobilization of a synapsin-dependent reserve pool. *J Neurosci* **26**: 3206–9.

Vinaixa M, Samino S, Saez I, Duran J, Guinovart JJ, Yanes O (2012). A Guideline to Univariate Statistical Analysis for LC/MS-Based Untargeted Metabolomics-Derived Data. *Metabolites* **2**: 775–95.

Vujanovic AA, Wardle MC, Smith LJ, Berenz EC (2017). Reward functioning in posttraumatic stress and substance use disorders. *Curr Opin Psychol* **14**: 49–55.

Walker DI, Pennell KD, Uppal K, Xia X, Hopke PK, Utell MJ, *et al* (2016). Pilot

Metabolome-Wide Association Study of Benzo(a)pyrene in Serum From Military Personnel. *J Occup Environ Med* **58**: S44-52.

Wang Y, Li S, Liu W, Wang F, Hu L-F, Zhong Z, *et al* (2016). *Vesicular monoamine transporter 2 (Vmat2) knockdown elicits anxiety-like behavior in zebrafish*. *Biochem Biophys Res Commun* **470**: .

Wang YM, Gainetdinov RR, Fumagalli F, Xu F, Jones SR, Bock CB, *et al* (1997). Knockout of the vesicular monoamine transporter 2 gene results in neonatal death and supersensitivity to cocaine and amphetamine. *Neuron* **19**: 1285–1296.

Watts B V., Shiner B, Zubkoff L, Carpenter-Song E, Ronconi JM, Coldwell CM (2014). Implementation of Evidence-Based Psychotherapies for Posttraumatic Stress Disorder in VA Specialty Clinics. *Psychiatr Serv* **65**: 648–653.

Weihe E, Schafer MK, Erickson JD, Eiden LE. (1994). Localization of vesicular monoamine transporter isoforms (VMAT1 and VMAT2) to endocrine cells and neurons in rat. *J Mol Neurosci* **5**: 149–64.

Weitemier AZ, McHugh TJ (2017). Noradrenergic modulation of evoked dopamine release and pH shift in the mouse dorsal hippocampus and ventral striatum. *Brain Res* **1657**: 74–86.

Wernicke C, Hellmann J, Zieba B, Kuter K, Ossowska K, Frenzel M, *et al* 9-Methyl-beta-carboline has restorative effects in an animal model of Parkinson's disease. *Pharmacol Rep* **62**: 35–53.

Wicking M, Steiger F, Nees F, Diener SJ, Grimm O, Ruttorf M, *et al* (2016). Deficient

fear extinction memory in posttraumatic stress disorder. *Neurobiol Learn Mem* **136**: 116–126.

Wiklund S, Johannson E, Sjostrom L, Mellerowicz E, Edlund U, Shockcor J, *et al* (2008). Visualization of GC/TOF-MS-based metabolomics data for identification of biochemically interesting compounds using OPLS class models. *Anal Chem* 115–122.

Wilk JE, Bliese PD, Kim PY, Thomas JL, McGurk D, Hoge CW (2010). Relationship of combat experiences to alcohol misuse among U.S. soldiers returning from the Iraq war. *Drug Alcohol Depend* **108**: 115–121.

Wimalasena K (2011). Vesicular monoamine transporters: structure-function, pharmacology, and medicinal chemistry. *Med Res Rev* **31**: 483–519.

Wingenfeld K, Whooley MA, Neylan TC, Otte C, Cohen BE (2015). Effect of current and lifetime posttraumatic stress disorder on 24-h urinary catecholamines and cortisol: results from the Mind Your Heart Study. *Psychoneuroendocrinology* **52**: 83–91.

Wise RA (1980). Action of drugs of abuse on brain reward systems. *Pharmacol Biochem Behav* **13 Suppl 1**: 213–23.

Wise RA (1987). The role of reward pathways in the development of drug dependence. *Pharmacol Ther* **35**: 227–63.

Wishart DS, Jewison T, Guo AC, Wilson M, Knox C, Liu Y, *et al* (2012). HMDB 3.0—The Human Metabolome Database in 2013. *Nucleic Acids Res* **41**: D801–D807.

Wolpe J, Plaud JJ (1997). Pavlov's contributions to behavior therapy. The obvious and not so obvious. *Am Psychol* **52**: 966–72.

Wu G, Lu Z-H, Kulkarni N, Amin R, Ledeen RW (2011). Mice lacking major brain gangliosides develop parkinsonism. *Neurochem Res* **36**: 1706–14.

Wu Q, Reith MEA, Walker QD, Kuhn CM, Carroll FI, Garris PA (2002). Concurrent autoreceptor-mediated control of dopamine release and uptake during neurotransmission: an in vivo voltammetric study. *J Neurosci* **22**: 6272–81.

Xia J, Wishart DS, Xia J, Wishart DS (2016). Using MetaboAnalyst 3.0 for Comprehensive Metabolomics Data Analysis. *Curr Protoc Bioinforma* 14.10.1-14.10.91doi:10.1002/cpbi.11.

Xian H, Chantarujikapong SI, Scherrer JF, Eisen SA, Lyons MJ, Goldberg J, *et al* (2000). Genetic and environmental influences on posttraumatic stress disorder, alcohol and drug dependence in twin pairs. *Drug Alcohol Depend* **61**: 95–102.

Xiao C, Liu Y, Xu J, Gan X, Xiao Z (2018). Septal and Hippocampal Neurons Contribute to Auditory Relay and Fear Conditioning. *Front Cell Neurosci* **12**: 102.

Yang M, Crawley JN (2009). Simple behavioral assessment of mouse olfaction. *Curr Protoc Neurosci* **Chapter 8**: Unit 8 24.

Yang Z, Oathes DJ, Linn KA, Bruce SE, Satterthwaite TD, Cook PA, *et al* (2018). Cognitive Behavioral Therapy Is Associated With Enhanced Cognitive Control Network Activity in Major Depression and Posttraumatic Stress Disorder. *Biol psychiatry Cogn Neurosci neuroimaging* **3**: 311–319.

Yehuda R, Boisoneau D, Lowy MT, Giller EL (1995). Dose-response changes in plasma cortisol and lymphocyte glucocorticoid receptors following dexamethasone administration in combat veterans with and without posttraumatic stress disorder. *Arch Gen Psychiatry* **52**: 583–93.

Yehuda R, Morris A, Labinsky E, Zemelman S, Schmeidler J (2007). Ten-year follow-up study of cortisol levels in aging holocaust survivors with and without PTSD. *J Trauma Stress* **20**: 757–61.

Yehuda R, Schmeidler J, Giller EL, Siever LJ, Binder-Brynes K (1998). Relationship between posttraumatic stress disorder characteristics of Holocaust survivors and their adult offspring. *Am J Psychiatry* **155**: 841–3.

Yehuda R, Yang R-K, Buchsbaum MS, Golier JA (2006). Alterations in cortisol negative feedback inhibition as examined using the ACTH response to cortisol administration in PTSD. *Psychoneuroendocrinology* **31**: 447–51.

Young KA, Gobrogge KL, Wang Z (2011). The role of mesocorticolimbic dopamine in regulating interactions between drugs of abuse and social behavior. *Neurosci Biobehav Rev* **35**: 498–515.

Young MB, Andero R, Ressler KJ, Howell LL (2015). 3,4-Methylenedioxymethamphetamine facilitates fear extinction learning. *Transl Psychiatry* **5**: e634–e634.

Young MB, Norrholm SD, Khoury LM, Jovanovic T, Rauch SAM, Reiff CM, *et al* (2017). Inhibition of serotonin transporters disrupts the enhancement of fear memory extinction by 3,4-methylenedioxymethamphetamine (MDMA).

Psychopharmacology (Berl) **234**: 2883–2895.

Yu T, Park Y, Li S, Jones DP (2013). Hybrid Feature Detection and Information Accumulation Using High-Resolution LC–MS Metabolomics Data. *J Proteome Res* **12**: 1419–1427.

Zaba M, Kirmeier T, Ionescu IA, Wollweber B, Buell DR, Gall-Kleebach DJ, *et al* (2015). Identification and characterization of HPA-axis reactivity endophenotypes in a cohort of female PTSD patients. *Psychoneuroendocrinology* **55**: 102–115.

Zapata A, Shippenberg TS (2002). D(3) receptor ligands modulate extracellular dopamine clearance in the nucleus accumbens. *J Neurochem* **81**: 1035–42.

Zhang J, Kravtsov V, Amarnath V, Picklo MJ, Graham DG, Montine TJ (2000). Enhancement of dopaminergic neurotoxicity by the mercapturate of dopamine: relevance to Parkinson's disease. *J Neurochem* **74**: 970–8.

Zhang S, Qi J, Li X, Wang H-L, Britt JP, Hoffman AF, *et al* (2015). Dopaminergic and glutamatergic microdomains in a subset of rodent mesoaccumbens axons. *Nat Neurosci* **18**: 386–92.

Zhou FC, Xu Y, Bledsoe S, Lin R, Kelley MR (1996). Serotonin transporter antibodies: production, characterization, and localization in the brain. *Brain Res Mol Brain Res* **43**: 267–78.

Zubieta JK, Taylor SF, Huguelet P, Koeppe RA, Kilbourn MR, Frey KA (2001). Vesicular monoamine transporter concentrations in bipolar disorder type I, schizophrenia, and healthy subjects. *Biol Psychiatry* **49**: 110–116.

Zucker M, Aviv A, Shelef A, Weizman A, Rehavi M (2002). Elevated platelet vesicular monoamine transporter density in untreated patients diagnosed with major depression. *Psychiatry Res* **112**: 251–6.